The influence of thyroid hormone and temperature on the transcriptomic response of *Rana [Lithobates] catesbeiana* tadpole cultured back skin

By

Ellis Evans

A Thesis Submitted in Partial Fulfillment of the Requirements for the Degree of

MASTER OF SCIENCE

in the Department of Biochemistry and Microbiology

We acknowledge and respect the lək^{w}əŋən peoples on whose traditional territory the university stands and the Songhees, Esquimalt and W̱SÁNEĆ peoples whose historical relationships with the land continue to this day.

Supervisory Committee

The influence of thyroid hormone and temperature on the transcriptomic response of *Rana [Lithobates] catesbeiana* tadpole cultured back skin

By

Ellis Evans

Supervisory Committee

Dr. Caren C. Helbing
Supervisor, Department of Biochemistry and Microbiology

Dr. Chris Nelson
Departmental Member, Department of Biochemistry and Microbiology

Dr. Leigh Anne Swayne
Outside Member, Division of Medical Sciences

Abstract

Thyroid hormones (THs) are essential signalling molecules for the postembryonic development of all vertebrates. THs are capable of initiating a diverse set of developmental programs across multiple tissues. The role of TH in regulating gene expression is well-known, but the initiation of TH signalling is still not fully understood. In amphibians, THs are the sole hormones required for the metamorphosis from tadpole to juvenile froglet. Amphibians are a useful model for studying TH signalling, as they undergo extensive, tissue-specific response programs in response to exogenous TH.

The metamorphosis of the American bullfrog, *Rana [Lithobates] catesbeiana* is temperature sensitive. *R. catesbeiana* tadpoles do not undergo metamorphosis at cold temperatures (4-5 °C) even in the presence of THs that should otherwise prompt it. However, tadpoles undergo metamorphosis at an accelerated rate when returned to warm temperatures (24-25 °C) forty days after their initial TH exposure. *R. catesbeiana* tadpoles possess a "molecular memory" of TH exposure which establishes the TH signal at cold temperatures and prompts accelerated metamorphosis after a return to warmer temperatures.

The mechanisms of the molecular memory which allow it to uncouple the initiation of TH signalling from the execution of the TH response program are not fully understood. Previous research has established that transcripts encoding transcription factors are a substantial component of the TH-dependent transcriptomic response of cultured tailfin (C-Fin) at cold temperatures. However, not all of these putative transcripts encoding transcription factors required active transcription and translation for their induction, which suggests that the initiation of a TH signal involves mechanisms other than regulating gene expression.

Herein, we used quantitative polymerase chain reaction (qPCR) and RNA-Sequencing (RNA-Seq) to investigate the TH-dependent transcriptomic response of the back skin, a tissue that undergoes extensive remodelling during metamorphosis. Cultured back skin (C-Skin) was TH-responsive in warm, cold and temperature shift conditions. Forty-four transcripts underwent significant changes in abundance in response to TH in cold temperatures under which the molecular memory is established. Seven of these transcripts encoded putative transcription factors. Surprisingly, the only TH-responsive transcript significantly changed at 4 °C in both the C-Skin and the previously studied C-Fin was *thyroid hormone-induced basic leucine zipper-containing protein (thibz)*. *Thibz* has been found to be TH-responsive at cold temperatures in the liver, lung, liver, brain, tailfin and back skin of whole animals, which suggests it may be an important regulator of initiating TH signalling. The lack of overlap in the transcriptomic responses of C-Skin and C-Fin may suggest that even the early initiation of TH signalling has tissue-specificity.

Alternately, the molecular memory may include mechanisms that do not require active transcription and translation. Transcripts associated with epigenetic modifications and post-transcriptional changes to mRNA stability were also significantly expressed at 4 °C within the C-Skin. Previous investigation of the putative transcription factors in C-Fin revealed that active transcription and translation was not always required for changes in transcript abundance.

Multiple mechanisms may be at play in the TH response at different temperatures. In cold temperatures, TH may modulate mRNA stability to influence transcript abundance as a part of initiating TH signalling without executing metamorphosis. Further research is needed to explore potential alternative mechanisms of establishing the molecular memory and the accelerated metamorphic response. The temperature sensitivity of *R. catesbeiana's* TH response is incredibly valuable in investigating mechanisms of early TH signalling during postembryonic vertebrate development.

Table of Contents

List of Tables

List of Figures

Acknowledgements

I would like to thank my supervisor, Dr. Caren Helbing, for her guidance and support throughout my project.

I would also like to thank my supervisory committee, Dr. Chris Nelson and Dr. Leigh Anne Swayne for their advice and input throughout my project.

I am incredibly grateful to all the members of the Helbing Lab, past and present.

To Emily, who provided a tremendous amount of support for my project without which my project would not have been possible.

To Lauren, who was instrumental in helping me learn the ins and outs of the lab and was incredibly supportive during the many trials and tribulations that followed.

To Jacob, whose knowledge and patience made my bioinformatics work possible.

To my fellow graduate students Lorissa, Haley, Michael, and Neha. Their companionship and enthusiasm for science was a bright spot throughout my project.

To Vanessa and Anita, for all their insight throughout my program.

To Elliot, who has persistently supported me throughout this long journey.

To my family, for all their lovely help along the way.

Dedication

In memory of Grace, a dear friend often thought of and sorely missed.

List of Abbreviations

Abbreviated genes and transcripts are italicized and capitalized following the nomenclature as set by http://www.xenbase.org/gene/static/geneNomenclature.jsp for Amphibia and http://www.informatics.jax.org/mgihome/nomen/gene.shtml for Mammalia as demonstrated below:

	Gene	Transcript Protein
Amphibia	*thra*	Thra
Mammalia	*Thra*	Thra

3'-UTR 3' untranslated region

5'-UTR 5' untranslated region

ABCA2 ATP binding cassette subfamily A member 2

ATP Adenosine triphosphate

bp Base pair

cDNA Complimentary DNA

cebp1 CCAAT/enhancer binding protein 1

C-Fin Cultured tail fin

CHX Cyclohexamide

c-Jun Transcription factor Jun

CNBP CCHC-type zinc finger nucleic acid binding protein

CREB3L4 cAMP responsive element binding protein 3 like 4

CRF Corticotropin-releasing factor

C-Skin Cultured back skin

Ct Cycle threshold

ddH_2O Double-distilled water

DDX21 DEAD-box helicase 21, nucleolar RNA helicase 2A

DE Differentially expressed

Dio2 Type II iodothyronine deiodinase, deiodinase 2

Dio3 Type III iodothyronine deiodinase, deiodinase 3

DIT Diiodotyrosine

DNA Deoxyribonucleic acid

dNTP Deoxynucleotide triphosphate

eef1a Eukaryotic translation elongation factor 1

EP400 E1A binding protein p400

ER Estrogen receptor

FC Fold change

FCRL Fc receptor-like

FCRL6 Fc receptor-like 6

FDR False discovery rate

GO Gene ontology

G-quadruplex Guanine quadruplex

hnRNP Heterogenous nuclear ribonucleoprotein

HNRNPL Heterogenous nuclear riboprotein L

HPT Hypothalamus-pituitary-thyroid

klf Krueppel-like factor

klf9 Krueppel-like factor 9

klfX Krueppel-like factor X

L-15 Leibovitz-15 media

MAD Median absolute deviation

MAPK Mitogen-activated protein kinase

MCT8 Monocarboxylate transporter 8

MED1 Mediator complex subunit 1

MFM Magnesium-Free Media

MIT Monoiodotyrosine

mRNA Messenger ribonucleic acid

NaOH Sodium Hydroxide

NCoR1 Nuclear Receptor Corepressor 1

OATP1C1 Organic anion-transporting polypeptide 1C1

PCA Principal component analysis

PI3K Phosphatidylinositol 3-kinase

PPAR Peroxisome proliferator-activated receptor

qPCR Quantitative polymerase chain reaction

RIN RNA Integrity Number

rlk1 *Rana* larval keratin 1

RNA Ribonucleic acid

RNA-Seq RNA-Sequencing

rpl8 Ribosomal protein L8

rps10 Ribosomal protein S10

rRNA Ribosomal ribonucleic acid

rT_3 reverse triiodothyronine

RXR Retinoid X receptor

SIPA1L2 Signal induced proliferation associated 1 like 2

SMAD4 Mothers against decapentaplegic 4-like

SMRT Silencing Mediator of Retinoic Acid and Thyroid Hormone Receptor

snoRNA small nucleolar RNA

snRNP Small nuclear ribonucleoprotein

T_2 Diiodothyronine

T_3 3,5,3'-triiodothyronine

T_4 Thyroxine

TH Thyroid hormone

thibz Thyroid hormone-induced basic leucine zipper-containing protein

thra Thyroid hormone receptor α mRNA

thrb Thyroid hormone receptor β mRNA

TK Taylor and Kollros

TR Thyroid hormone receptor

TRE Thyroid hormone responsive element

TRH Thyrotropin-releasing hormone

TRα Thyroid hormone receptor α

TRβ Thyroid hormone receptor β

TSH Thyroid-stimulating hormone

tshb Thyroid stimulating hormone subunit beta

VWA8 Von Willebrand Domain-containing Protein 8

ZZEF1 Zinc finger ZZ-type and EF-hand domain containing 1

1 Introduction

1.1 Role of Thyroid Hormones in Vertebrate Development

Thyroid hormones (THs) are crucial for the health, growth, and development of all vertebrates. THs are most familiar for their role in modulating carbohydrate and lipid metabolism in adult humans (Mullur et al., 2014). In addition, THs are essential signalling molecules in the postembryonic development of all vertebrates. The synthesis, transport, and metabolism of TH signalling molecules is carefully coordinated throughout the perinatal period in mammals. Deficiencies in maternal or endogenous THs *in utero* lead to a variety of neurological and physiological impairments (Burrow et al., 1994). Further studies have established a key role for TH in organ, skeletal, and neurological development and maturation (Gilbert et al., 2012; Kim and Mohan, 2013; Sirakov and Plateroti, 2011)

THs also play a part in the postembryonic development of many vertebrates which transition from a larval to juvenile form. THs regulate flatfish, lamprey, and amphibian metamorphosis (Gilbert, 2013; Manzon and Manzon, 2017; Schreiber and Specker, 1998). In amphibians of the order Anura, THs are both necessary and sufficient to prompt metamorphosis from tadpole to juvenile froglet (Shi, 2000). Tadpoles undergo a diverse set of drastic biochemical and physiological changes during metamorphosis, all of which are initiated by a single set of hormones. TH signalling prompts complex cascades of gene expression that orchestrate various postembryonic developmental responses, including tissue remodelling, apoptosis, and *de novo* limb formation (Gilbert et al., 1996; Ishizuya-Oka et al., 2010; Tata, 1999). This TH-driven metamorphic program must be carefully coordinated both spatially and temporally to ensure a successful transition from tadpole to froglet.

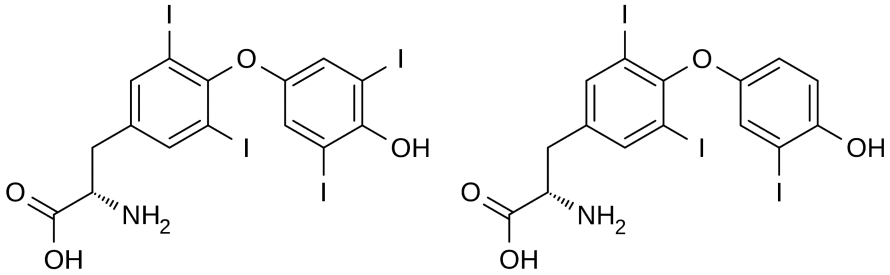

Figure 1. Examples of thyroid hormones

Amphibians have enjoyed prominence as a model organism for studying how TH signalling controls a crucial developmental period which is conserved amongst vertebrates. Perinatal mammals and amphibians undergo a similar increase in TH that peaks either at birth or metamorphic climax, respectively (Buchholz, 2015). Both tadpoles and perinatal mammals undergo postembryonic development in preparation for a transition from an aquatic to terrestrial environment. TH prompts skin keratinization, lung maturation, intestinal remodelling, the production of urea cycle enzymes in the liver, and the proliferation of neurons in the central nervous system, among other shared changes (Buchholz, 2015; Tata, 1993). The

molecular mechanisms of TH signalling, as well as the developmental changes prompted by THs, are similarly conserved among amphibians and mammals. Both share similar nuclear thyroid hormone receptors (TRs), co-repressors, co-activators, and thyroid hormone responsive elements (TREs) on TH-responsive target genes (Sachs and Buchholz, 2017).

Amphibians offer an additional advantage as a model organism for studying TH-driven development. Perinatal mammals are exposed to maternal hormones *in utero* as a cofounding factor but otherwise chemically or physically ablating the thyroid gland produces a disease state (Buchholz, 2015; Forhead and Fowden, 2014). Tadpoles are free-swimming larvae that are not exposed to maternal hormones. Furthermore, premetamorphic tadpoles are functionally athyroid, naturally lacking detectable levels of circulating TH prior to metamorphosis (Shi, 2000). Metamorphosis is triggered by exposure to exogenous THs in water or through injection, allowing TH-driven development to be studied more easily in amphibians. Amphibians have been previously used as model organisms to identify TH-responsive genes, TH-associated chromatin modifications, and the potential effects of TH-mimicking environmental pollutants on vertebrate species (Corrie et al., 2021; Das et al., 2009; Grimaldi et al., 2013).

TH signalling is complex, with multiple regulatory processes occurring across different tissues. THs regulate comparable developmental events through comparable mechanisms in both amphibians and mammals. Metamorphosis can therefore be used to model how TH regulates and coordinates a diverse set of response programs in a conserved period of postembryonic development. As THs are essential to early development, greater understanding of the initiation of TH signalling in vertebrates is incredibly valuable.

1.2 Thyroid Hormone Synthesis and Transport

The hypothalamus-pituitary-thyroid (HPT) endocrine axis controls the initial synthesis of TH (Figure 2). Environmental cues prompt the hypothalamus to produce thyrotropin-releasing hormone (TRH) in mammals or corticotropin-releasing factor (CRF) in amphibians (Okada et al., 2007; Zoeller et al., 2007). In turn, this stimulates the anterior pituitary to produce thyroid-stimulating hormone (TSH). TSH then stimulates the thyroid gland to produce THs (Denver, 2013). TSH stimulates TSH receptors on follicular cells within the thyroid gland. TSH modulates multiple processes during TH production, including enhancing iodide uptake, thyroglobulin production and peroxidase enzyme activity (Rousset et al., 2000). Sodium-iodide symporters transport iodide into thyroid hormone follicular cells against a concentration gradient. Thyroglobulin, a tyrosine-rich protein, is synthesized within the follicular cells. Iodide is oxidized to iodine by peroxidases (Nussey and Whitehead, 2001). Peroxidases then causes iodine to bind to the tyrosine residues on thyroglobulin at either position 3 or position 5, to produce monoiodotyrosine (MIT) or diiodotyrosine (DIT), respectively. DIT coupling with MIT produces 3,5,3'-triiodothyronine (T_3), and DIT coupling with another DIT produces a thyroxine (T_4) molecule (Rousset et al., 2000).

THs are released from iodinated thyroglobulin by proteolysis and secreted out of follicular cells into the plasma. T_4 is released from the thyroid gland at a greater magnitude than T_3 though both are produced by the thyroid gland (Nussey and Whitehead, 2001). Circulating

THs bind to transporter proteins such as transthyretin and are transported into peripheral tissues. THs are then actively transported across the plasma membrane into cells. Known TH transporters include monocarboxylate transporter 8 (Mct8) and organic anion-transporting polypeptide 1C1 (Oatp1c1) (Visser et al., 2011). The release of TH molecules into circulation creates a negative feedback loop which inhibits the production of TRH and TSH, and in turn regulates the production of THs (Denver, 2013). The HPT axis thus influences development by controlling TH synthesis and the concentration of available THs.

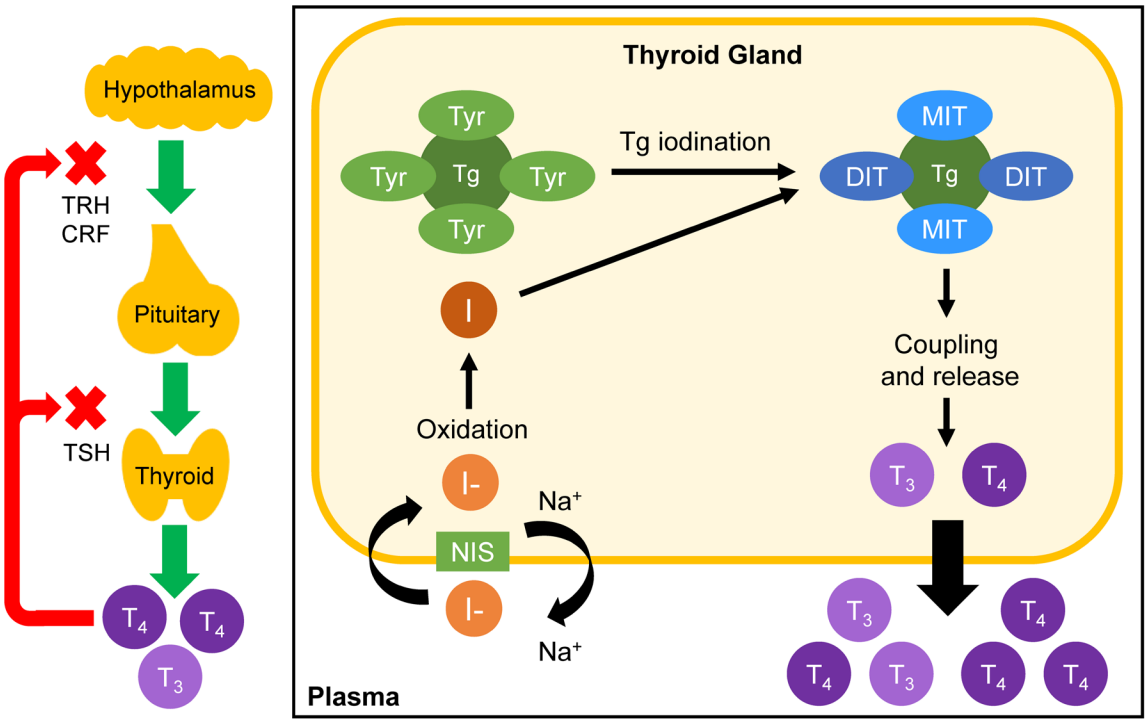

Figure 2. Control of thyroid hormone synthesis by the HPT axis
The hypothalamus-pituitary-thyroid (HPT) endocrine axis controls the production of THs. Environmental cues prompt the hypothalamus to produce thyrotropin-releasing hormone (TRH) in mammals or corticotropin-releasing factor (CRF) in amphibians. This signals the pituitary to produce TSH, which stimulates the synthesis of THs. Sodium-iodide (NIS) symporters transport iodide (I-) into thyroid hormone follicular cells against a concentration gradient. Iodide is oxidized to iodine (I) by peroxidases. Thyroglobulin (Tg) is synthesized within the follicular cells. Peroxidases then cause iodine to bind to the tyrosine residues (Tyr) on the thyroglobulin at either position 3 or position 5, to produce monoiodotyrosine (MIT) or diiodotyrosine (DIT), respectively. DIT coupling with MIT produces 3,5,3'-triiodothyronine (T_3), and DIT coupling with another DIT produces a thyroxine (T_4) molecule. Production of TH creates a feedback loop which negatively regulates the production of TRH/CRF and TSH. Adapted from (Thambirajah et al., 2019) and (Thanas et al., 2020).

1.3 Deiodinase-Mediated Conversion of T_4 to T_3

The availability of TH is also controlled after transport into the peripheral tissues. Deiodinase enzymes in the cytoplasm catalyze multiple types of TH conversion (Mullur et al., 2014). Deiodinase 2 (Dio2) converts T_4 to T_3 by outer ring deiodination (Bianco et al., 2002). Deiodinase 3 (Dio3) converts T_3 to diiodothyronine (T_2) by inner ring deiodination as well as converting T_4 to reverse triiodothyronine (rT_3), which are unable to bind nuclear hormone receptors (Bianco and Kim, 2006). Deiodinases, consequently, can regulate the availability of different TH isoforms at a local level (Figure 3).

Both Dio2 and Dio3 are known to regulate developmental timing during amphibian metamorphosis (Brown, 2005). In the tadpole tailfin, *dio3* is expressed throughout metamorphosis ensuring low levels of bioactive TH and stalling tail regression. At metamorphic climax, *dio3* is downregulated and *dio2* upregulated. Together, these events ensure tail regression only occurs once peak levels of T_3 are present at metamorphic climax (Berry et al., 1998; Wang and Brown, 1993). *Dio2* is similarly upregulated in the intestine directly preceding its remodeling to ensure maximal levels of T_3 (Ishizuya-Oka, 2011). T_3 and T_4 have distinct binding affinities to nuclear hormone receptors and other cofactors; both nuclear hormone receptors bind T_3 with a 5-fold higher affinity than T_4 (Maher et al., 2016; Schroeder et al., 2014). The expression of the deiodinases in a time- and tissue-specific manner can influence the availability of certain THs, which can subsequently influence TH signaling. The expression of the deiodinases corresponds to the ability of peripheral tissues to respond to TH during metamorphosis (Cai and Brown, 2004).

The conventional dogma of TH action describes T_4 as the circulating prohormone which must be converted to T_3 in the target tissues to become bioactive. However, some tadpole tissues lack Dio2 and are unable to convert T_4 to T_3. The gills do not express *dio2* and are reliant on high levels of T_3 circulating in bloodstream to induce reabsorption at metamorphic climax (Cai and Brown, 2004). Current research also suggests that T_4 may act directly in the tadpole liver without conversion to T_3 as a subset of transcripts within this tissue responded in a manner consistent with T_4 binding to TRs (Maher et al., 2016). Differences in deiodinase activity and T_3- and T_4-mediated gene expression may aid in coordinating the unique developmental outcomes of different tissues during metamorphosis.

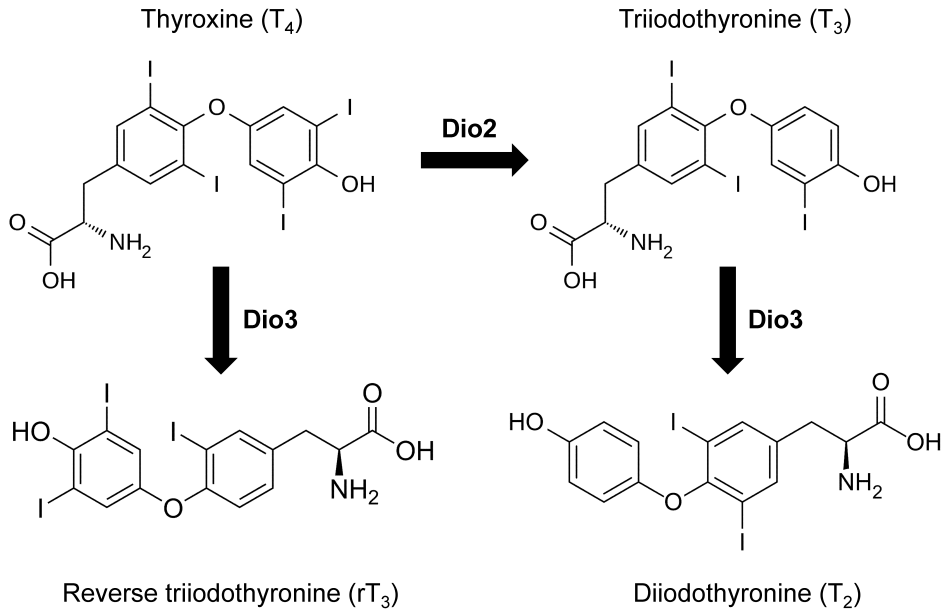

Figure 3. Deiodinase-mediated conversion of thyroid hormones
Deiodinase 2 (Dio2) converts thyroxine (T_4) to triiodothyronine (T_3) by outer ring deiodination. Deiodinase 3 (Dio3) converts T_3 to diiodothyronine (T_2) by inner ring deiodination as well as converting T_4 to reverse triiodothyronine (rT_3). Adapted from Bianco et al., 2002.

1.4 Thyroid Hormone Signalling

The most common form of TH action is genomic signalling through the thyroid hormone nuclear receptors (TRs), TRα and TRβ. TRs are part of the nuclear receptor superfamily, which includes the estrogen receptors (ERs) and peroxisome proliferator-activated receptors (PPARs) (Mangelsdorf et al., 1995). TRs form heterodimers with retinoid X receptors (RXRs) to bind to thyroid hormone responsive elements (TREs) in the genome typically in close proximity to the promoters of TH-responsive genes (Lee and Privalsky, 2005).

In the dual function model proposed by Shi and Buchholz, TRs negatively regulate gene expression in the absence of TH and positively regulate gene expression in the presence of TH (Buchholz et al., 2006). Unliganded TR heterodimers form corepressor complexes with proteins like Nuclear Receptor Corepressor 1 (NCoR1) and Silencing Mediator of Retinoic Acid and Thyroid Hormone Receptor (SMRT) (Tomita et al., 2004). Corepressors bind to TREs in a transcriptionally inactive state to regulate gene expression. In addition, corepressor complexes often include histone deacetylases, suggesting that chromatin modifications also aid in repressing TH-associated gene expression. TH binding to TRs displaces corepressors and recruits coactivators including acetyl transferases, arginine methyl transferases, and ATP-dependent chromatin remodelers (Buchholz et al., 2006; Matsuda et al., 2009; Paul et al., 2007). Histone modifications in response to T_3 binding TRs *in vivo* occur during intestinal remodelling in *Xenopus* metamorphosis (Sun et al., 2014). Together, corepressors/coactivators and epigenetic modifications play a role in TH signalling (Shi et al., 2012).

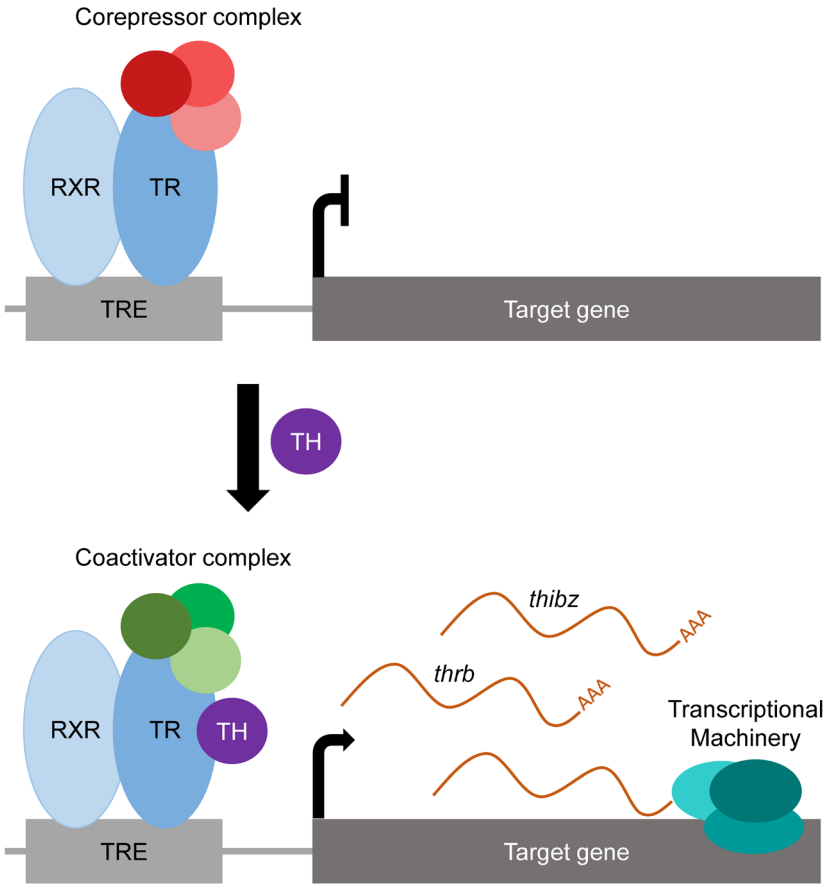

Figure 4. The dual function model of thyroid hormone signalling.
Shi and Buccholz's dual function model describes how gene expression is either repressed or induced in the absence or presence of TH. When TH is absent, corepressors bind to the TH receptors (TRs) to repress transcription of TH-responsive target genes. In the presence of TH, corepressors are replaced with coactivators, and the expression of TH-responsive genes such as thyroid hormone receptor beta (*thrb*) and thyroid hormone-induced basic leucine zipper-containing protein *(thibz)* are induced. Adapted from Koide et al., 2022.

Further studies of TR knockout *Xenopus* have provided further evidence for the dual function model. TRα knockouts led to earlier initiation of hind limb development as genes associated with limb growth during metamorphosis were no longer repressed by unliganded receptors (Wen and Shi, 2015). However, this was also coupled with lower expression of TH-responsive genes after exposure to exogenous TH in multiple studies, as the knockout led to a reduction in coactivators binding to TREs (Choi et al., 2015; Wen and Shi, 2016). TRβ knockouts likewise led to early induction and diminished expression of several TH-responsive genes in the tadpole intestine (Shibata et al., 2020). TRα and TRβ knockouts had different effects on developmental timing across different tissues. For example, TRα knockouts have no effect on the rate of tail regression in the presence of TH, but TRβ knockouts experience a delay in TH-induced tail regression at metamorphic climax. However, TRβ knockouts do not display changes in TH-dependent eruption of forelimbs. TRα knockouts cause *Xenopus* to advance through

premetamorphosis at a quicker rate, but the TH-dependent eruption of their forelimbs is delayed (Shi, 2021). TR expression can play a role in determining sensitivity (level of circulating TH at which the tissue responds) and responsivity (rate at which transcriptomic and phenotypic changes occur) of specific tissues throughout metamorphosis (Shi, 2021).

The dual function model describes how TRs negatively regulate gene expression in the absence of TH, and positively regulate gene expression in the presence of TH (Shi, 2009). However, the dual function model does not account for those genes which are repressed by TH. The release of TH molecules into circulation inhibits the production of TSH in a negative feedback loop, which is how the HPT axis regulates the production of TH (Wu and Koenig, 2000). The mechanism of TH-dependent gene repression is not fully understood. Interactions between unliganded TRs and corepressors in the absence of TH may induce the expression of *thyroid stimulating hormone subunit alpha (tsha*), as overexpression of the co-repressors SMRT and NCor leads to increased *tsha* expression (Tagami et al., 1997). Curiously, co-activators enhanced the suppression of the *tsha* gene, which may suggest that both co-activators and co-repressors are needed for the negative regulation of TH-responsive genes (Tagami et al., 1999). For *thyroid stimulating hormone subunit beta* (*tshb*), research suggests that liganded TR binds the GATA-binding factor 2 transcription factor via protein-protein interactions, which aids in repressing the transactivation of *tshb* (Hirahara et al., 2020; Sasaki et al., 2018). Different target genes may employ different mechanisms for TH-mediated repression, not all of which require direct TR-DNA interactions (Sasaki et al., 2018; Wu and Koenig, 2000).

TH is also able to signal "non-genomically" outside of binding to the nuclear TRs. TH can bind to extranuclear TRs or cellular membrane receptors. T_3 can bind to TRβ1 in the cytoplasm to mediate the transcription of glycolytic genes through the phosphatidylinositol 3-kinase (PI3K) pathway (Moeller et al., 2006; Moeller et al., 2005). As previously mentioned, T_4 has different affinity for the nuclear TRs than T_3 and has been found to interact differently with specific nuclear co-regulators (Schroeder et al., 2014). T_4 can also bind to membrane receptor integrin αVβ3 with greater affinity than T_3 in initiating the mitogen-activated protein kinase (MAPK) signaling cascade (Davis et al., 2008). In turn, T_4 can cause MAPK to phosphorylate, relocate to the nucleus and associate with TRβ1, influencing the transcription of specific genes (Davis et al., 2000). Genomic and non-genomic signalling may therefore both facilitate time- and tissue-specific developmental programs in response to TH.

1.5 Thyroid Hormones and Amphibian Metamorphosis

The remarkable ability of THs to control amphibian metamorphosis was first seen in 1912, when tadpoles given extracts from the thyroid gland in their rearing water promptly became frogs (Gudernatsch, 1912). Physical ablation of the thyroid gland and ensuing inhibition of metamorphosis further confirmed the importance of thyroid hormones in amphibian metamorphosis (Allen, 1925). THs are the only hormones necessary to prompt amphibian metamorphosis from tadpole to juvenile froglet (Brown and Cai, 2007).

As previously stated, premetamorphic tadpoles do not have a functional thyroid gland and have undetectable levels of circulating TH. TRα is expressed in premetamorphic tadpoles, which provides competence to respond to either endogenous or exogenous TH (Yaoita and Brown, 1990). As the thyroid gland develops, TH levels rise and prometamorphosis begins. Expression of TRβ also rises in response to the TH signal during metamorphosis (Yaoita and Brown, 1990). TH triggers a carefully coordinated set of developmental changes which alter the structure and function of virtually all tissues. TH triggers changes as varied as *de novo* limb formation, tissue remodelling, and coordinated apoptosis (Gilbert et al., 1996; Tata, 1999). Peak levels of TH coincide with metamorphic climax, where reabsorption of the larval tissues is synchronized with the development of juvenile froglet tissues. For example, the tail is retained until metamorphic climax, then rapidly reabsorbed once TH levels are at their peak and all four limbs are developed (Berry et al., 1998; Wang and Brown, 1993). Developmental changes during metamorphosis must be carefully timed for a successful life stage transition from an aquatic herbivore to an amphibious carnivore. Exposure to exogenous TH in water or through injection prompts physiological and transcriptomic changes associated with the metamorphic program in premetamorphic tadpoles. Experimental induction of metamorphosis has allowed the study of TH signalling during metamorphosis in greater depth.

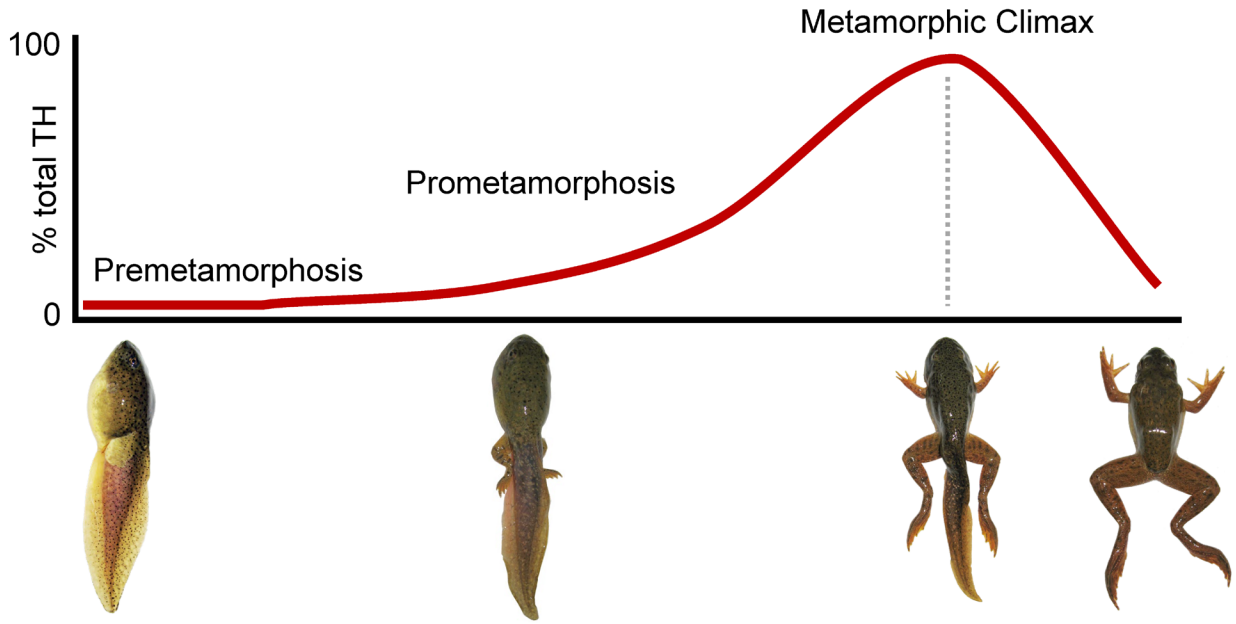

Figure 5. Thyroid hormone levels during amphibian metamorphosis
Premetamorphic tadpoles have virtually undetectable levels of endogenous TH. As the thyroid gland develops and circulating levels of TH rise, tadpoles undergo phenotypic changes required for the transition from an aquatic herbivore to a semi-terrestrial carnivore, including limb development and tail regression. Adapted from (White and Nicoll, 1981).

Subsequent research has elucidated that the TH response in amphibians is biphasic, consisting of an induction and execution phase. The induction phase involves a distinct group of early TH-response transcripts including the TRβ-encoding mRNA, *TH receptor beta (thrb)* and *thyroid hormone-induced B/Zip (thibz)* which respond within the first 8 h across multiple tissues

(Shi and Brown, 1993; Wang and Brown, 1993). In the execution phase, a secondary set of TH-responsive transcripts is later expressed downstream. Transcripts expressed in the execution phase vary between tissues, which is consistent with TH acting to produce tissue-specific changes during development. Tail regression in tadpoles exposed to exogenous T_3 is blocked by transcriptional and translational inhibitors within the first 24 h of TH exposure (Ji et al., 2007). Initiation of the TH-dependent metamorphic program passes the commitment point within 48 h of TH exposure after which the program cannot be halted by protein synthesis inhibitors (Gilbert et al., 1996; Wang and Brown, 1993).The protein synthesis inhibitor cycloheximide (CHX) was used to differentiate between TH-responsive transcripts that require *de novo* protein synthesis and those that do not (Das et al., 2009). Transcripts that did not require *de novo* protein synthesis were likely expressed as a result of TH interacting with direct response genes, early during the induction phase. Transcripts that required *de novo* protein synthesis, on the other hand, were likely part of the later execution phase. CHX-susceptible transcripts would rely on prior translation of proteins from direct TH-responsive genes to induce their expression after the metamorphic program had begun.

In *X. laevis*, 188 TH-responsive genes were upregulated and 249 downregulated in the presence of the protein synthesis inhibitor CHX (Das et al., 2009). This study also found these genes contained TREs capable of binding to TR heterodimers *in vitro*, further suggesting that the expression of direct response genes is important in transducing the TH signal. Direct response genes associated with transcriptional regulation were strongly represented, indicating that transcriptomic changes during the induction phase are important in initiating the early TH response. Genes encoding the *thrb* and *thibz* transcripts were part of the CHX-resistant group. CHX-susceptible genes were largely related to apoptosis and the later stages of DNA replication. Whilst not directly responsive to TH, these secondary transcripts are required for the gene expression cascades associated with developmental changes during the execution phase.

Notably, not all of the TH-responsive transcripts identified in the presence of protein inhibitors were marked as TH-responsive in the absence of protein inhibitors (Das et al., 2009). There are several explanations possible. Cycloheximide inhibits mRNA decapping and can prevent mRNA decay (Santos et al., 2019). Some TH-responsive genes may have low transcript abundance levels that are not consistently detected by microarray, and upon stabilization by CHX, produce a more robust signal that allows them to be identified (Das et al., 2009). In addition, several early TH-response transcripts are upregulated transiently in response to T_3, and transcript abundance decreases to untreated levels by later timepoints (Wang and Brown, 1993). The greater number of TH-responsive transcripts in the presence of CHX may be due to the stabilization of transcripts that would otherwise only undergo transient increases in abundance during the induction phase (Das et al., 2009).

In summary, TH initiates transcriptomic changes which execute tissue-specific cascades of gene expression during metamorphic development. There is evidence that the early expression of direct TH-response genes such as *thrb* and *thibz* plays a role in induction of the TH signal across multiple tissues. It is thought that *thrb* and *thibz*, as well as other transcripts related to transcriptional regulation, may play a key role initiating the TH response. Regulating

gene expression may also contribute to how TH coordinates various developmental outcomes during amphibian metamorphosis.

1.6 Tissue-Specific, TH-Dependent Responses in the Skin during Amphibian Metamorphosis

TH triggers a variety of developmental changes in amphibians that are remarkably specific to both cell type and location (Brown and Cai, 2007). The skin undergoes drastic remodelling from a larval to adult type during amphibian metamorphosis (Brown and Cai, 2007). Tadpole skin has no dermis, and three layers separated from the underlying muscle tissue by collagen. The epidermis consists of an outermost layer of apical cells analogous to the mammal periderm, the skein cells, and an innermost basal layer (Furlow et al., 1997; Robinson and Heintzelman, 1987). All three layers of tadpole skin undergo cell replication, as does the mammalian periderm (Brown and Cai, 2007). TH prompts cell-specific changes in tadpole skin. Apical and skein cells undergo apoptosis and are not found in froglets. Basal cells are progenitors for adult germinative cells (Yoshizato, 1992). Fully developed froglet skin has skin glands, a dermis, and an epidermis containing spinous, granular and cornified cells like other terrestrial vertebrates (Brown and Cai, 2007; Furlow et al., 1997). TH can induce tadpole skin to undergo apoptosis and keratinization autonomously in cell culture (Nishikawa et al., 1989; Nishikawa and Yoshizato, 1986). Studies of *X. laevis* show that the larval epidermis is directly targeted by TH to undergo apoptosis (Schreiber and Brown, 2003). Transcripts expressing larval and adult keratin are also expressed in a cell-specific manner in response to TH (Suzuki et al., 2001; Watanabe et al., 2001). Furthermore, TH prompts changes in tadpole skin in a region-specific manner. Transcripts expressing four extracellular glycoproteins in the apical cell layer are downregulated after exposure to TH in a coordinated manner across the tadpole epidermis (Furlow et al., 1997). On the other hand, adult keratin expression only occurs later and unevenly in the reabsorbing tail (Furlow et al., 1997). There is a sharp delineation between the two tissue regions, where adult dermis only forms fully on the body skin (Berry et al., 1998; Brown and Cai, 2007).

TH can produce vastly different responses even among similar tissues in different locations, such as the tail and the back skin. The back skin undergoes remodelling as previously described to prepare for a transition from an aquatic to semi-terrestrial lifestyle. Contrastingly, the tail undergoes an extensive apoptotic program and is wholly reabsorbed. Multiple tissue types, including notochord, muscle, and epidermis undergo histolysis at the climax of metamorphosis (Shi, 2000). In the tailfin, apoptosis proceeds from the epidermal cells inwards to the mesenchymal cells. The TH response in tailfin is similarly autonomous and tissue-specific. Exposure to exogenous TH prompts a similar apoptotic program in cultured tail tips and tailfin biopsies as in whole animals (Hinther et al., 2010; Skirrow et al., 2008).

1.7 Temperature Sensitivity of Amphibian Metamorphosis

Temperature is another important regulator of development in both invertebrates and vertebrates. Temperature influences the rate of growth in insects across multiple life stages

(Mirth et al., 2021). In turtles and crocodilians, temperature as well as endocrine cues influence sex determination (Ramsey and Crews, 2009; Rice et al., 2017). *R. catesbeiana* is an amphibian that inhabits a temperate climate with a larval stage lasting 2-3 years (Cecil and Just, 1979). *R. catesbeiana* typically overwinters as a tadpole before later undergoing metamorphosis. In order to avoid undergoing an energetically costly metamorphosis during unfavourable winter conditions*, R. catesbeiana* relies on both temperature and TH signalling to time its development (Hammond et al., 2015).

In the 1960s, it was discovered that the rate of metamorphosis slows as temperatures decrease below 25 °C in *R. catesbeiana* tadpoles (Frieden et al., 1965). Metamorphosis halts entirely at 4-5 °C, even when tadpoles are injected with exogenous THs that would otherwise prompt metamorphosis at warmer temperatures (Ashley et al., 1968; Frieden et al., 1965). Additional research has established that circulating TH can still be taken up by transthyretin and transported to peripheral tissues at 4-5 °C. TH is still transported into cells and accumulates within the nucleus of nucleated red blood cells of *R. catesbeiana*, albeit at a slower rate (Murata and Yamauchi, 2005). Lastly, TH is still able to bind to TRs and initiate the expression of transcripts associated with cold temperature stress and lipid production at 4-5 °C (Hammond et al., 2016; Hammond et al., 2015; Suzuki et al., 2016).

The transcriptional machinery within the nucleus maintains its activity even at cold temperatures that do not permit metamorphosis (Yoshizato et al., 1975). However, TH-responsive transcripts such as *thrb* and *dio3* are not induced at 4-5 °C, even in the presence of TH (Hammond et al., 2015). The induction of TH signalling, and therefore the execution of the metamorphic program, is specifically halted by cold temperatures. Recent research has found that a small subset of induction phase transcripts is still induced by TH within the first 48 h of exposure at 4-5 °C (Hammond et al., 2016). These transcripts include *thibz* in multiple tissues, as well as CCAAT/enhancer binding protein 1 (*cebp1*) in the back skin. The cold temperature TH response is reproducible in whole tadpole exposure as well as in cultured organs (Hammond et al., 2016; Hammond et al., 2015). Interestingly, the expression of *thibz* is organ autonomous only in the tailfin, suggesting that other modulatory factors may be present *in vivo* or that there are tissue specific differences in the transcriptomic response at cold temperatures (Hammond et al., 2016). The expression of some, but not all, direct response transcripts under cold temperatures, implies further stratification during the induction phase (Figure 6). A subset of genes including *thibz* are responsive to TH early on even when the other components of the metamorphic program are not.

Epigenetic control may play a role in regulating the response to TH at different temperatures. TH exposure increases association of acetylated H3K9 with the promoter region of *thrb*, solely at warm temperatures (Mochizuki et al., 2012). Similarly, winter-acclimated bullfrog tadpoles had lower levels of the activation mark H3K9 in their livers compared to their summer-acclimated counterparts (Ishihara et al., 2019). It is still unknown if epigenetic modifications could play a role in the expression of TH-responsive transcripts at cold temperatures that do not permit metamorphosis.

1.8 Establishment of a Molecular Memory and the Accelerated Metamorphic Response

The TH signal is not lost at cold temperatures. A subset of induction phase transcripts is still TH-responsive at 4-5 °C, which indicates that cold temperatures stratify the initiation of the TH signaling from the execution of the metamorphic program. Moreover, cold temperatures do not abolish a later response to TH, merely pausing the downstream response. When tadpoles exposed to TH at cold temperatures are returned to warmer "permissive" temperatures of 24-25 °C, they undergo metamorphosis at an accelerated rate (Frieden et al., 1965). Tadpoles can restart metamorphosis even 40 days after their initial exposure to TH once returned to permissive temperatures (Ashley et al., 1968; Frieden et al., 1965). By this time, THs have since been excreted from the body and are no longer present. Thus, tadpoles retain a "molecular memory" of their prior exposure to TH molecules and can use it to later execute metamorphosis once temperatures rise.

Molecular memory allows the TH signal to be retained under nonpermissive temperatures and primes tadpoles to later undergo accelerated metamorphosis at permissive ones. Tadpoles undergo both phenotypic and transcriptomic changes associated with the metamorphic program after a shift from cold to warm temperatures. The tail regresses at 24-25 °C, though TH was only administered at 4-5 °C (Ashley et al., 1968; Frieden et al., 1965). Reddening of the hindlimbs due to vascularisation is visible 24 h after TH injection in tadpoles subjected to a temperature shift, compared to 48 h in permissive temperatures (Hammond et al., 2015). In addition, *thrb* undergoes similar or greater changes in abundance within 48 h of the temperature shift. The induction of direct response transcripts such as *thrb* occurs more quickly in tadpoles subjected to a temperature shift compared to those exposed to TH at only permissive temperatures (Hammond et al., 2016; Hammond et al., 2015). This in turn may contribute to the accelerated execution of TH-dependent gene cascades and precocious metamorphosis (Hammond et al., 2016). Molecular memory and the accelerated metamorphic response are organ autonomous and occur in both whole animal exposures and organ culture (Hammond et al., 2016; Koide et al., 2022).

Much remains unknown about the mechanisms of molecular memory that establish and maintain the TH signal at cold temperatures, and later prompts accelerated metamorphosis. Temperature-specific transcriptomic changes have been suggested as a potential component of molecular memory. *Thibz* is the sole transcript so far found to be TH-responsive at cold temperatures in multiple tissues including the tailfin and back skin of whole tadpoles (Hammond et al., 2016; Hammond et al., 2015). In addition, *thibz* undergoes changes in abundance in response to TH ahead of known induction phase transcripts such as *thrb* (Koide et al., 2022). This further suggests that *thibz* may play an important role in establishing the TH signal at nonpermissive temperatures and in the early initiation of the accelerated response. Over 400 genes were identified as TH-responsive at permissive temperatures; many of these direct-response genes associated with transcriptional regulation (Das et al., 2009). Other, unknown transcripts may potentially be responsive in cold temperatures where molecular memory is established, besides *thibz*.

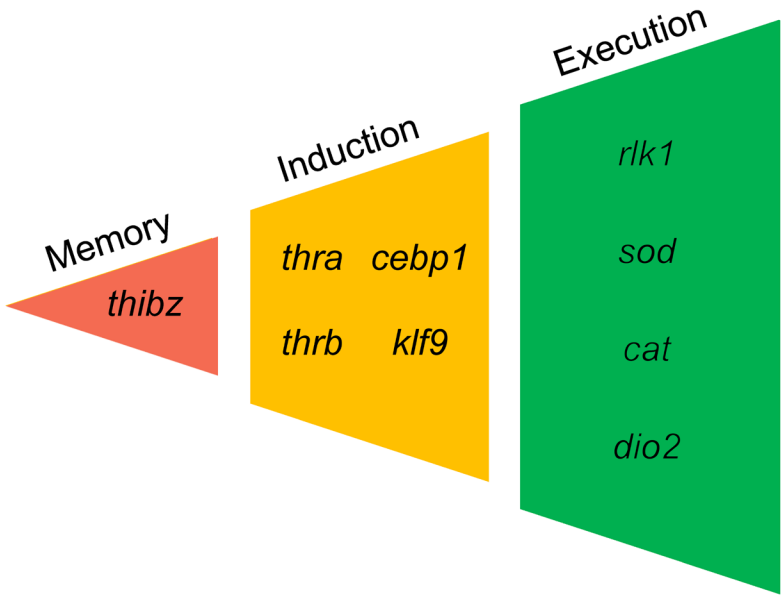

Figure 6. Stratification of the early thyroid hormone response in *R. catesbeiana* tailfin
Exposure to TH produces a transcriptomic response in *R. catesbeiana* tadpoles that can be stratified by temperature. In cold temperatures, only a certain subset of transcripts (including *thibz*) is TH-responsive in the tailfin. Exposure to TH at cold temperatures is later sufficient to prompt the metamorphic response program in full. The metamorphic response program is biphasic, consisting of an induction and execution phase. The induction phase includes the expression of direct response genes that do not require *de novo* protein synthesis. The execution phase involves the downstream expression of genes that do require *de novo* protein synthesis and can be prevented by inhibitors of translation. Adapted from (Hammond et al., 2016).

Epigenetic modifications may also contribute to molecular memory and the accelerated response. A shift from cold to warm temperatures increased the acetylation of H3K9 in tadpole liver (Ishihara et al., 2019). Global increases in transcriptionally active marks could subsequently make the transcription of *thrb* and other direct TH-response transcripts more accessible. In turn, this could potentially accelerate the execution of gene signalling cascades associated with the metamorphic program. As stated, it is uncertain how epigenetic modifications could influence the transcription of genes like *thibz* in cold temperatures as well as how they could contribute to the retention of the TH signal over time.

Putative components of the molecular memory in the tailfin were identified by transcriptomic analysis of cultured tailfin (C-Fin) exposed to TH at 4 °C for 48 h (Koide et al., 2022). Eighty-one transcripts, including 14 transcripts encoding transcription factors, were TH-responsive under conditions where molecular memory was established. Transcripts encoding *thibz* and krueppel-Like Factor X *(klfX)*, a novel member of the krueppel-like factor (*klf)* family underwent significant changes in abundance at cold temperatures. Krueppel-like factors are a family of zinc-finger domain transcription factors known to regulate cell proliferation, differentiation, and apoptosis (Pearson et al., 2008). *Klf9* was previously found to be TH-responsive under permissive temperatures in multiple *R. catesbeiana* tissues (Maher et al.,

2016; Veldhoen et al., 2015). In addition, *klf9* transcript abundance increases in the tailfin one week after TH exposure at cold temperatures (Hammond et al., 2016; Hammond et al., 2015). Among the transcripts encoding transcription factors identified in this study, the magnitude and timing of transcript abundance changes differed between transcripts and in 4 °C and 4-24 °C temperature shift conditions. This suggests that several transcripts encoding transcription factors are responsive under cold conditions where the molecular memory is established, and under conditions which prompt accelerated metamorphosis. The molecular memory of the tailfin also looks to be complex, with multiple components responding uniquely to the TH signal early after exposure.

Transcriptomic analysis has established that transcription factors are likely important components of the molecular memory in the tailfin. Previous research on the tadpole back skin shows that this tissue produces a transcriptomic response to TH at temperatures that do not permit metamorphosis (Hammond et al., 2015). However, *thibz* was only expressed in back skin *in vivo*, which suggests that other modulatory factors may be required to induce the expression of this transcript in this tissue (Hammond et al., 2016). The back skin's molecular memory and accelerated metamorphic response is not well-characterized. It is unknown if the molecular memory of the back skin includes transcripts encoding transcription factors, and if these transcripts are shared with the tailfin. The tailfin and back skin undergo different developmental programs in response to the same TH signal. Molecular memory is a useful tool for investigating the early initiation of TH signalling.

1.9 Hypothesis and Objectives

1.9.1 Hypothesis

My hypothesis is that transcripts encoding transcription factors expressed in cold temperatures are a component of the molecular memory of the back skin of *R. catesbeiana* tadpoles. These transcription factors may initiate the TH signal as well as priming for an accelerated metamorphic program after the temperature shift in the back skin, a tissue that undergoes extensive remodelling during metamorphosis.

1.9.2 Objectives

My objectives are to identify the transcriptomic response to thyroid hormones in the back skin under different temperatures.

1) Examine the expression dynamics of known TH-responsive transcripts under cold conditions in which molecular memory is established.

2) Examine the expression dynamics of known TH-responsive transcripts after a temperature shift which induces an accelerated metamorphic program.

3) Identify putative components of the molecular memory – novel TH-sensitive transcripts expressed at cold temperatures – in the back skin, using RNA-Sequencing.

2 Materials and Methods

2.1 Animal Husbandry

Premetamorphic *Rana catesbeiana* tadpoles (Taylor and Kollros (TK) stage VI-VIII) (Taylor and Kollros, 1946) were collected by WestWind SeaLab Supplies (Victoria, British Columbia, Canada) from freshwater lakes surrounding Victoria, BC. Tadpoles were housed in the University of Victoria's Outdoor Aquatics Unit in covered 100-gallon fiberglass tanks and experienced a natural photoperiod. Tanks contained recirculated, dechlorinated municipal water at a temperature of 15 ± 1 °C with a pH of 6.8 and 96-98% dissolved oxygen. Tadpoles were fed twice daily with Spirulina flakes (Nutrafin Max, Rolf C. Hagen, Montreal, PQ, Canada) once in the morning and afternoon. The care and treatment of animals was in accordance with guidelines established by the Canadian Council on Animal Care and approved by the University of Victoria Animal Care Committee (Protocol No. 2019-025).

2.2 Quantification of Treatments by Mass Spectrometry

Final concentrations of 400 nM NaOH and 10 nM T_3 were selected as control and TH treatment, respectively, to reflect biologically relevant concentrations of THs at metamorphic climax (Veldhoen et al., 2014b; White and Nicoll, 1981). A 10^{-3} M solution of T_3 was made from 3,3',5-Triiodo-L-thyronine sodium salt (Sigma Aldrich, CAT No. T-2752 55-06-01) in 40 mM NaOH (Sigma Aldrich, CAT No. 1310-73-2). The 10^{-3} M T_3 and 40 mM NaOH solutions were then filter sterilized with 0.22-micron nylon filters. All subsequent steps were performed in a laminar flow hood to maintain sterility. Serial dilution was used to produce a 10^{-5} M (10 µM T_3) in 400 µM NaOH stock solution, as well as a 400 µM NaOH in ddH_2O stock solution. These stock solutions were added to 70% Leibovitz L-15 with GlutaMAX media (Thermo Fisher, CAT No. 31415-029) to produce final concentrations of 400 nM NaOH and 10 nM T_3 for the C-Skin assays.

Aliquots of 1/100 dilutions of the 10 µM T_3 and 400 µM NaOH stock solutions in ddH_2O were shipped on ice to the University of Victoria's Proteomics Centre, BC, for quantification by Liquid Chromatography-Multiple-reaction monitoring/Mass Spectrometry (LC-MRM/MS). An Agilent 1290 UHPLC system coupled to an Agilent 6495B QQQ instrument (Agilent Technologies Canada Inc., Mississauga, ON, Canada) was operated in the positive-ion multiple-reaction monitoring (MRM) detection mode. An internal standard solution containing 13C6-T_3 and 13C6-T_4 was prepared in 50% aqueous methanol containing 0.05 M of ammonium hydroxide. A standard solution of a mixed stock solution containing T_3 and T_4 standard substances was prepared at 10 nmol/mL in internal standard solution, then serially diluted 1 to 4 (v/v) with internal standard solution.

Four hundred µL of each sample was aliquoted into a 1.5-mL Eppendorf tube alongside 50 µl of internal standard solution. The combined solutions were frozen at -80 °C for two hours and then lyophilized to dryness. The residues were then reconstituted in 100 µL of 50% methanol/0.05 M ammonium hydroxide. Ten µL aliquots of the sample and the standard solutions were injected to run UPLCMRM/MS using a C18 column (2.1 x 150 mm, 1.7 µm) for LC

separation and with the use of 0.1% formic acid/water (A) and 0.1% formic acid/acetonitrile (B) as the mobile phase for gradient elution (25% to 60% B in 10 min), at 0.4 mL/min and 50 °C. Concentrations of the detected analytes were calculated with internal standard calibration by interpolating the linear-regression curves of individual compounds constructed from the data acquired from injections of standard solutions, with the analyte-to-internal standard peak ratios measured from sample solutions.

2.3 C-Skin Assay

All experiments were performed with cultured back skin (C-Skin) biopsies from premetamorphic TK stage VI-VIII *R. catesbeiana* tadpoles. Tadpoles were euthanized by immersion in a solution of 1 g/L tricaine methanesulfonate (Syndel Laboratories, Nanaimo, Canada) in dechlorinated municipal water from the Outdoor Aquatics Unit, buffered with 1 g/L $NaHCO_3$. All chemicals were sourced from Fisher Chemical unless otherwise stated. All subsequent experimentation was performed aseptically within a laminar flow hood.

Euthanized tadpoles were rinsed with sterile 150 mL Magnesium-Free Media (MFM: 88 mM NaCl, 1 mM KCl, 2.4 mM $NaHCO_3$, 7.5 mM Tris-HCl and 0.88 mM $CaCl_2$, pH 7.6) four times in succession. Tadpoles were placed into a 150 x 20 mm sterile cell culture dish (Sarstedt, CAT No. 83-1803). Sterile dissection scissors and forceps were used to dissect away the back skin in one piece (beginning posterior to the head and terminating before the tail) and placed on sterile surgical gauze soaked in MFM. Six biopsies were taken from the back skin of an individual tadpole with a six mm biopsy punch (Integra Miltex, CAT No. 33-36). As multiple biopsies can be taken from a single animal and cultured under different treatment conditions, C-Skin assays help decrease intra-subject variation and can be used for repeated measures statistics. The similarity of biopsies taken from different locations within the same tissue was previously demonstrated (Hinther et al., 2010; Koide et al., 2022).

In each assay, the six mm C-Skin biopsies were transferred into the individual wells of sterile, polystyrene 24-well tissue culture plates (Falcon, CAT No. 353047). Tissue culture plates contained 500 µL of 70% Leibovitz L-15 with GlutaMAX media (Thermo Fisher, CAT No. 31415-029) modified with 10 mM sterile HEPES (pH 7.6) and 50 µg/mL penicillin, 50 µg/mL streptomycin, 100 µg/mL neomycin (Thermo Fisher, CAT No. 15640-055). Biopsies were acclimated overnight for 24 h before treatment and were incubated at either 4 °C or 24 °C depending on the experiment. Following acclimation, another 500 µL of 70% Leibovitz L-15 media was added containing a 2X concentration solution of 800 nM NaOH (control) or 20 nM T_3 in 800 nM NaOH (treatment). Therefore, biopsies were treated with either a final concentration of 400 nM NaOH control or a 10 nM T_3 in 400 nM NaOH (T_3 treatment) in 70% L-15 media.

For assays using permissive temperatures (24 °C), L-15 media was warmed to room temperature and exposures took place at 24 °C. For assays using nonpermissive temperatures (4 °C), L-15 media and tissue culture plates were kept on cold blocks to avoid exposure to warmer temperatures. Biopsies were either incubated at 4 °C or 24 °C for the duration of the experiment. Tissue culture plates were inspected for fungal and bacterial growth daily, but no contamination was detected during any experiments. After an exposure was finished, biopsies

were individually transferred into 8-well PCR tube strips containing 125 µL RNALater (Ambion, CAT No. AM7021) and held at 4 °C for 48 hours. Samples in RNALater were then transferred to -20 °C for long term storage.

2.4 Exposure Design

2.4.1 Transcriptomic Response to T_3 in C-Skin within 12 h at permissive temperatures with or without 48 h of cold temperatures

Six C-Skin biopsies from six premetamorphic *R. catesbeiana* tadpoles were acclimated overnight for 24 h in 24 °C or 4 °C incubators. For each individual animal, one biopsy was treated with a 400 nM NaOH control or a 10 nM T_3 treatment for each of the three temperature regimes. Biopsies were held at permissive temperatures of 24 °C for 12 h, nonpermissive temperatures of 4 °C for 48 h, or subjected to a temperature shift after 48 h from 4 °C to 24 °C for an additional 12 h (Figure 7).

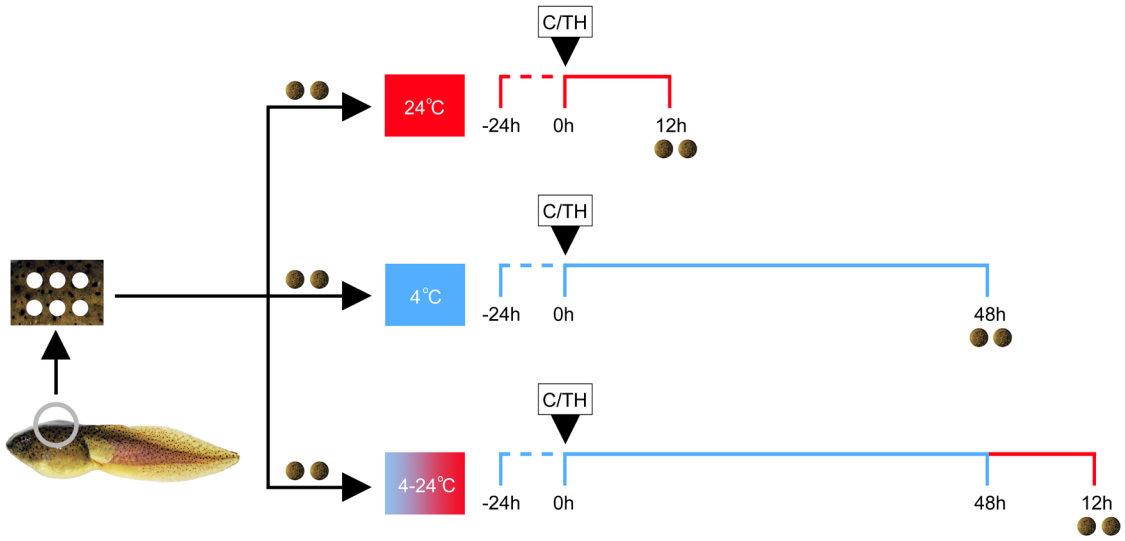

Figure 7. 12 h C-Skin exposure
Six back skin (C-Skin) biopsies per *R. catesbeiana* tadpole (n=6 tadpoles) were cultured separately in the wells of tissue culture plates. Colour indicates temperature, with red representing warm temperatures of 24 °C and blue representing cold temperatures of 4 °C. The dashed line indicates the acclimation period before treatment, and the solid line represents the time after exposure. Biopsies were treated with 400 nM NaOH control or 10 nM T_3 treatment, and then incubated in one of three temperature regimes. For the temperature shift, tissue culture plates were incubated at 4 °C for 48 h, then transferred to 24 °C for an additional 12 h.

2.4.2 Transcriptomic Response to T_3 in C-Skin within 24 h at permissive temperatures with or without 48 h of cold temperatures

Another independent C-Skin assay was performed with ten premetamorphic *R. catesbeiana* tadpoles to assess the TH-dependent transcriptomic changes that occurred within a longer 24 h period. Six biopsies per animal were acclimated overnight for 24 h in 24 °C or 4 °C incubators. For each individual animal, one biopsy was treated with a 400 nM NaOH control or 10 nM T_3 treatment for each of the three temperature regimes. Biopsies were held at permissive temperatures of 24 °C for 24 h, nonpermissive temperatures of 4 °C for 48 h, or subjected to a temperature shift after 48 h from 4 °C to 24 °C for an additional 24 h (Figure 8).

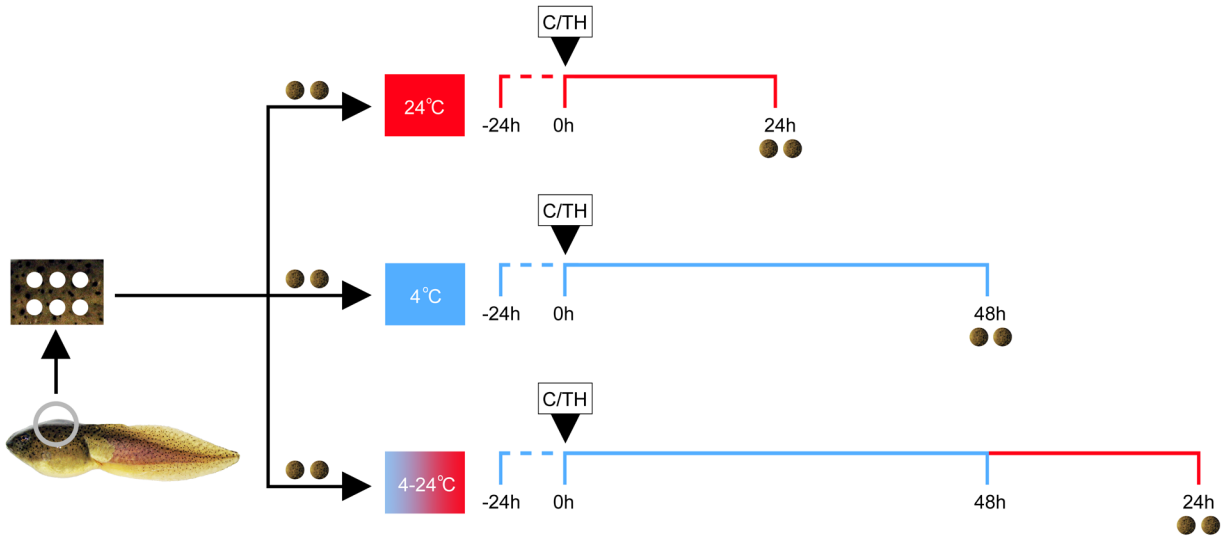

Figure 8. 24 h C-Skin exposure
Six back skin (C-Skin) biopsies per *R. catesbeiana* tadpole (n=10 tadpoles) were cultured separately in the wells of tissue culture plates. For the temperature shift, tissue culture plates were incubated at 4 °C for 48 h, then transferred to 24 °C for an additional 24 h. All other conditions were the same as in Figure 7.

2.4.3 Early Transcriptomic Response to T_3 During Three Time Course Experiments at Warm, Cold and Temperature Shift Conditions

To measure the changes in TH-responsive transcript abundance over time, six C-Skin biopsies from twelve tadpoles were treated with 10 nM T_3 and incubated for multiple timepoints. Three independent experiments were performed, with one exposure taking place at 24 °C, another at 4 °C, and one incorporating a temperature shift from 4 to 24 °C (Figure 9). During the 24 °C and 4 °C experiments, one biopsy per tadpole was immediately removed after treatment at the 0 h timepoint. The other biopsies were incubated at their respective temperatures and then removed at the 1,2,4,8 and 24 h marks.

In the temperature shift experiment, six biopsies from twelve tadpoles were treated with 10 nM T_3 and were incubated at 4 °C (Figure 9). One biopsy per animal was immediately removed after T_3 treatment at 4 °C at the 0 h mark. A second biopsy was removed after 48 h of incubation at 4 °C. The remaining biopsies were subsequently transferred to a new set of well plates with 1 mL of clean L-15 media containing no T_3 treatment to wash them at room temperature. Biopsies were then transferred to a new set of well plates containing 1 mL clean 70% Leibovitz L-15 media and incubated at 24 °C for 1,2,4, and 8 h time periods.

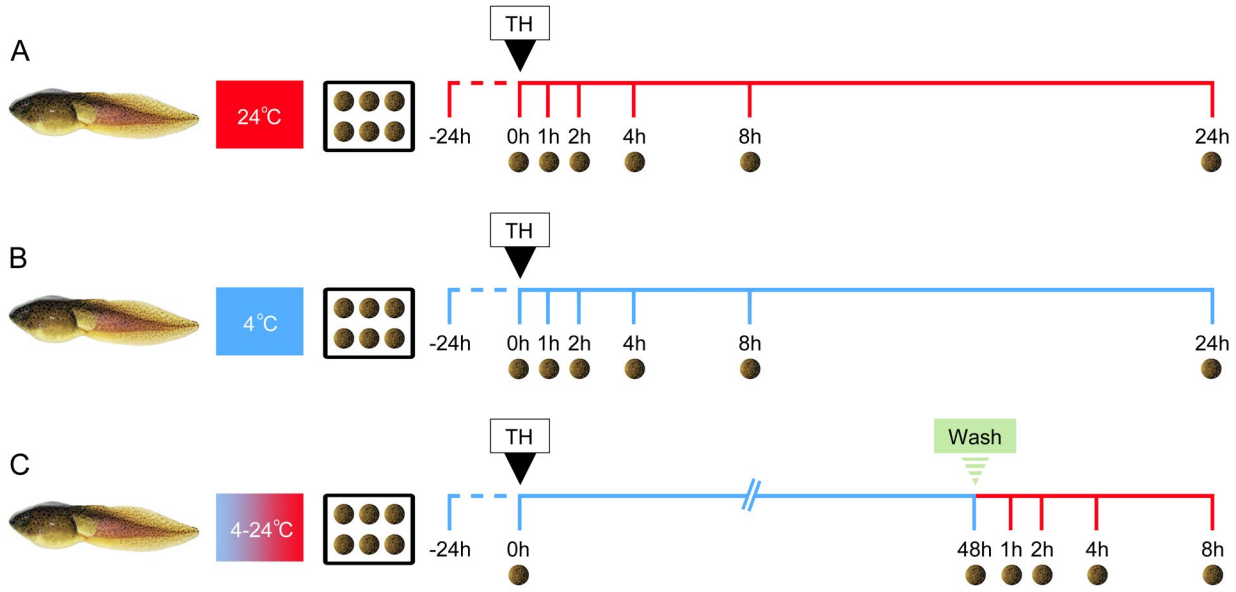

Figure 9. Warm (24 °C), cold (4 °C), and temperature shift (4-24 °C) time course experiments
Six back skin (C-Skin) biopsies of *R. catesbeiana* tadpoles were cultured separately in the wells of tissue culture plates. Three experiments were performed independently with 12 individual tadpoles each (A, B, C). The dashed line indicates the acclimation period before treatment, and the solid line represents the time after exposure. Biopsies were treated with 10 nM T_3 at the 0 h mark. At the end of each time point, one biopsy is removed from culture and preserved in RNALater. A) 24 h exposure at warm temperatures of 24 °C, in red. B) 24 h exposure at cold temperatures of 4 °C, in blue. C) Temperature shift exposure where initial TH exposure took place at 4 °C. C-Skin was held at 4 °C for 48 h. Brackets indicate the timeline is not to scale with the other two exposures. Biopsies then were washed with clean L-15 media and placed into new tissue culture plates for an 8 h time course at 24 °C.

2.5 Isolation of Total RNA

Samples were randomized prior to processing and RNA extraction, to minimize experimenter bias and batch effects. All isolations were performed on ice, with sterile, DNase-, RNase- free plasticware. Total RNA (1.3 µL) was later run on a NanoDrop 1000 Spectrophotometer (Thermo Fisher Scientific, Ottawa, Canada) to estimate RNA concentration and obtain a 260/280 and 260/230 ratio for each sample.

2.5.1 Extraction of RNA using TRIzol

RNA from the 12 h temperature shift assay (Figure 7) was extracted with TRIzol, followed by chloroform, isopropanol, and ethanol treatments as described in (Hammond et al., 2016) with the following modifications. Biopsies were placed in individual 1.5 mL Eppendorf Safe-Lock microfuges tubes (Eppendorf, CAT No. 022363611) containing 300 µL TRIzol (Invitrogen, CAT No. 15596-018). Biopsies were homogenized with a 3 mm tungsten carbide bead and a Retsch MM301 Mixer Mill (Thermo Fisher Scientific, Ottawa, Canada). Mechanical homogenization took place at 24 Hz, for two three-minute intervals with a 180° rotation between intervals. The homogenate was combined with 60 µL chloroform (Sigma Aldrich, CAT No. 437581) and centrifuged at 12,000 xg for 15 min at 4 °C for phase separation. The aqueous phase was transferred to a new microfuge tube and 20 µg glycogen (Roche Applied Sciences, CAT No. 10901393001) was added to maximize RNA yield. One hundred and fifty µL molecular-grade isopropanol (Fisher Scientific, CAT No. BP1150500) was used to precipitate the RNA. Isolated total RNA was resuspended in 40 µL UltraPure RNAse Free water (Invitrogen, CAT No. 10977023) and stored at -80 °C.

2.5.2 Extraction of RNA using Qiagen miRNeasy Tissue/Cells Advanced Mini Kit

RNA from all other exposures (Figure 8, Figure 9) was extracted with the use of Qiagen miRNeasy Tissue/Cells Advanced Mini Kits (Qiagen, CAT No. 217604). Extraction was performed according to the manufacturer's handbook (Qiagen HB-2672-003) with the following modifications. Biopsies were homogenized with a 3 mm stainless steel bead and a Retsch MM301 Mixer Mill (Thermo Fisher Scientific, Ottawa, Canada). Mechanical homogenization took place at 24 Hz, for two three-minute intervals with a 180° rotation between intervals. Two washes with 500 µL 80% RNase-free ethanol were performed in the RNA washing stage. Isolated total RNA was resuspended in 50 µL UltraPure RNAse Free water (Invitrogen, CAT No. 10977023) and stored at -80 °C.

2.6 cDNA synthesis

RNA was reverse transcribed to cDNA using an applied high-capacity cDNA reverse transcription kit with RNase inhibitor (Applied Biosystems Inc., CAT No. 4374967) following the manufacturer's protocol. RNA was diluted to approximately 1 µg of RNA per reaction prior to cDNA synthesis. Reverse transcription was carried out on a MyCycler™ Thermal Cycler (Bio-Rad Laboratories Inc., Hercules, CA). The reverse transcription reaction consisted of a 10 min primer

ligation at 24 °C, followed by a 2 h DNA polymerization at 37 °C and 5 min enzyme deactivation at 85 °C. Synthesized cDNA was stored at -20 °C. A 1/20 dilution was done to generate working stocks of cDNA for qPCR. Dilute cDNA was also stored at -20 °C.

2.7 qPCR analysis

TH-responsive transcripts were measured with targeted quantitative polymerase chain reaction (qPCR). Primer and probe sequences, as well as annealing temperatures are listed in Table 1. All reactions had been previously validated and described by (Veldhoen et al., 2014a), apart from *klfX* (Koide et al., 2022). Taqman based multiplex reactions were used to detect the TR transcripts *thra* and *thrb*, as well as the normalizer transcripts ribosomal protein L8 (*rpl8*), eukaryotic elongation factor 1A (*eef1a*) and ribosomal protein S10 (*rps10*) using a MX3005P qPCR system (Agilent Technologies Canada Inc., Mississauga, ON, Canada) as described in (Hammond et al., 2013; Wojnarowicz et al., 2013). A Taqman based simplex reaction was used to detect the *klfX* transcript on the MX3005P qPCR system (Agilent Technologies Canada Inc., Mississauga, ON, Canada), as described in (Koide et al., 2022). A SYBR based reaction was used to detect *thibz* on a CFX Connect real-time PCR detection system (Bio-Rad Laboratories Inc., Hercules, CA, USA), as described in (Veldhoen et al., 2014a).

All samples were run in quadruplicate. The mean of the cycle threshold (Ct value) was used for subsequent analysis. Quadruplicates with a standard deviation > 0.5 were removed as were outliers with abnormal melt curves. To account for input variation, the target TH-responsive transcripts were normalized to the geomean of the normalizer transcripts *rpl8*, *eef1a*, and *rps10*. Relative fold change to control samples was calculated with the $2^{\Delta\Delta\text{-Ct}}$ method as described in (Schmittgen and Livak, 2008).

Table 1. Primer and probe information

Primer and probe sequences (5'→ 3'), as well as annealing temperatures used for the normalizer and TH-responsive transcripts detected through qPCR in the present study. All probes used FAM fluorophores quenched with ZEN/Iowa Black™ FQ (ZEN/IB).

Transcript name	Up Primer Sequence	Down Primer Sequence	Probe Sequence	Annealing Temperature (°C)	Source
Ribosomal protein L8 *(rpl8)*	AGGCAGGTCGTGCN TACCA	GGGATGTTCTACAG GATTCATAGC	FAM-AAACTGCTGGCCACGTGTCC GT-ZEN/IB	64	Hammond et al., 2013; Wojnarowicz et al., 2013
Ribosomal Protein S10 *(rps10)*	GCTGCTGGTGTTGG TGART	AGCATGTTGTCACC RTTCC	FAM-TACATCAAGAAGATTGGTTA CAACCC-ZEN/IB	60	Hammond et al., 2013; Wojnarowicz et al., 2013
Eukaryotic translation elongation factor 1A *(eef1a)*	GCYTGGCGTCACTTT TACTG	CACGTCCAAAYCCTC CTCTAA	FAM-AAGGCTGAGGCTGGWGCT GGAG-ZEN/IB	60	Hammond et al., 2013; Wojnarowicz et al., 2013
Thyroid hormone receptor α *(thra)*	TGATAAGGCCACAG GRTACCACTA	CGGGTGATCTTGTC GATRA	FAM-ACTATCCAGAAGAACCTGCA CCCCTC-ZEN/IB	64	Hammond et al., 2013; Wojnarowicz et al., 2013
Thyroid hormone receptor β *(thrb)*	CTCATAGAAGAAAA CAGAGAAAARAGA	GAAGGCTTCTAAGT CCACTTTTCC	FAM-CATGTGGCCACCAATGCACA GG-ZEN/IB	64	Hammond et al., 2013; Wojnarowicz et al., 2013
Thyroid hormone induced bZip *(thibz)*	ASCTCCRCAGAAYCA GCA	TCACGTACCAGGCC AAAA	N/A	62	Veldhoen et al., 2014a
Krueppel-like factor X *(klfX)*	ACATCGGTAGCAGC GTTAT	TGAACTGAGATACA TGGAAGGT	FAM-CCTGCCACGGAAGAGACTA CACTGC-ZEN/IB	60	Koide et al., 2022

2.8 Statistical Analysis

Normality and homogeneity of variance of fold change data were tested using a Shapiro-Wilk and Levene's test. The data did not pass assumptions of normality and homogeneity of variance required for parametric testing. Repeated measures statistics were performed, as multiple biopsies from the same individual were subjected to all control and treatment conditions. Therefore, a non-parametric, repeated-measures Friedman test was used to assess significance among conditions alongside a post hoc Wilcoxon signed-rank test (p-value ≤ 0.05).

2.9 RNA-Sequencing (RNA-Seq) of C-Skin Samples from the 24 h C-Skin Assay

Samples from the 24 C-Skin assay (Figure 8) were assessed for their suitability for RNA-Seq. The 24 h C-Skin assay was performed with 10 premetamorphic *R. catesbeiana* tadpoles. For each individual animal, one biopsy was treated with a 400 nM NaOH control or a 10 nM T_3 treatment under one of three temperature regimes. Biopsies were held at permissive temperatures of 24 °C for 24 h, nonpermissive temperatures of 4 °C for 48 h or subjected to a temperature shift after 48 h from 4 °C to 24 °C for an additional 24 h (Figure 8). RNA was extracted using a QIAgen miRNeasy Tissue/Cells Advanced Mini Kit. qPCR was used to assess responsiveness to T_3 in these tissue samples with primers targeting *thra* and *thrb* at 24 °C, and *thibz* at 4 °C. *Thibz* responded to T_3 treatment as anticipated (Figure 10B). RNA concentration and quality were assessed using a Bioanalyzer 2100 (Agilent, Mississauga, Ontario, Canada) and RNA 6000 Nano Kit (Agilent, CAT No. 5067-1511). Samples were considered of sufficient quality for sequencing if they had an RNA Integrity Number (RIN) greater than seven. RNA from five individual tadpoles, with a paired 400 nM NaOH and 10 nM T_3 sample for each of the three temperature conditions (4 °C, 24 °C, 4-24 °C) were subjected to RNA sequencing (RNA-Seq). Thirty samples in total were shipped at -20 °C to the Michael Smith Genome Sciences Centre in Vancouver, BC. The Illumina HiSeq 2500 (Illumina, San Diego, California, USA) platform was used to generate strand-specific polyA+ mRNA libraries with 75 bp paired-end sequencing.

2.10 Bioinformatics

2.10.1 Alignment and DESeq2 Analysis

Raw RNA-seq reads were mapped to the *R. catesbeiana* genome version (https://www.bcgsc.ca/downloads/supplementary/bullfrog/) (Hammond et al., 2017) using the STAR two-pass alignment (version 2.6.1) (Dobin et al., 2013). StringTie (version 1.3.4) was used to assemble mapped reads with a minimum read coverage of 1 for multiple-exon transcripts, and 4.75 for single-exon transcripts (Pertea et al., 2015; Razmara et al., 2021). Coverage describes the average number of reads that align or "cover" known base pairs in the reference genome. Multiple-exon transcripts required full coverage for each isoform. A fully covered transcript has all internal exons fully covered by reads in the input alignment, and each intron has at least one spliced read aligned across it. Single exon transcripts required each base pair to be covered 4.75 bp on average across the gene (Pertea et al., 2015).

Aligned and assembled reads were then used to generate counts for individual transcripts, as well as generating gene counts by grouping transcript isoforms together. Both transcript and gene counts were calculated for biological replicates, to compare treatments to controls for each of the three temperature regimes. Transcript counts were used for DESeq2 analysis, whereas gene counts were used for Gene Annotation (GO) enrichment analysis.

Differential expression of T_3-treated versus control samples was calculated with DESeq2 (Love et al., 2014). The Wald test statistic was used to control for repeated measures through the addition of animal to the generalized linear model design (Koide et al., 2022). A cut off rate for transcripts with normalized counts that fell below 0.1 counts per million in five or more samples was used to minimize low count false positives. Differences in transcript abundance between the controls and treatment were considered statistically significant when the Benjamini-Hochberg multiple testing adjusted p-value ($p\text{-}_{adj}$) was ≤ 0.05. A false discovery rate (FDR) of 0.05 was applied (Love et al., 2014).

2.10.2 Transcript Annotation and Gene Ontology Analysis

BLASTn (version 2.6.0) and BLASTx were used to annotate transcripts using the National Center for Biotechnology Information (NCBI) nucleotide (nt) and non-redundant (nr) protein databases. The highest percent e-value sequence alignment was selected for each transcript. Trinotate (version 3.2.0) was used to assign gene ontology (GO) terms to genes marked as differentially expressed (DE) by DESeq2 (Bryant et al., 2017). GOseq was used to compare GO terms assigned to DE genes against GO terms assigned to all genes identified in the C-Skin samples (counts per million < 0.1). GOseq (version 1.42.0) was then used to identify GO term enrichment ($p_{adj} \leq 0.05$, FDR ≤ 0.05) (Young et al., 2010). GO term enrichment identified putative functions of enriched molecular pathways associated with the DE genes in each temperature condition. Cytoscape was used to generate and visualize connections between enriched GO terms (version 3.8.2) (Young et al., 2010).

3 Results and Discussion

3.1 The TH-dependent Transcriptomic Response of C-Skin is Temperature Sensitive

In order to examine the transcriptomic changes that occur in the back skin early after TH exposure, C-Skin biopsies were exposed to T_3 in the 12 h C-Skin experiment (Figure 7). C-Skin biopsies were treated with either a 400 nM NaOH control or a 10 nM T_3 treatment under one of three temperature regimes. Biopsies were held at permissive temperatures of 24 °C for 12 h, nonpermissive temperatures of 4 °C for 48 h, or subjected to a temperature shift after 48 from 4 °C to 24 °C for an additional 12 h (See Figure 7 for details).

The 12 h exposure period for 24 °C was chosen as tail regression can be blocked by both transcriptional and translational inhibitors within the first 24 h of TH exposure (Ji et al., 2007). After 48 h, the induction of the TH-dependent metamorphic program passes the commitment point and further development can no longer be prevented by inhibitors (Gilbert et al., 1996; Wang and Brown, 1993). Therefore, a 12 h time point should allow for the investigation of early transcriptomic changes that are essential for establishing the TH signal prior to the commitment point. The 48 h exposure period for 4 °C was chosen as previous studies have shown that a response to TH can be seen within this time period at nonpermissive temperatures (Hammond et al., 2016). An accelerated metamorphic response in permissive temperature after initial TH exposure at 4 °C has also been noted over similar time periods (Hammond et al., 2016; Hammond et al., 2015).

3.1.1 *Thrb* is Expressed in the C-Skin Solely in Permissive Temperatures Contrasting the Expression of *thibz* in Cold, Molecular Memory Conditions

There were no significant changes in abundance for the *thra* transcript in response to T_3 in any of the three temperature conditions (Figure 10A). The *thrb* transcript was responsive to T_3 only in temperatures that permit metamorphosis. *Thrb* underwent a significant 2.3-fold increase in abundance at 24 °C, 12 h after T_3 exposure. *Thibz* also underwent a 4.7-fold increase 12 h after T_3 exposure at 24 °C. This indicates that C-Skin retains the ability to respond to TH in culture and that two known TH-response transcripts increase in abundance under warm temperatures that permit metamorphosis.

Thrb did not change significantly in abundance in response to TH at 4 °C, conditions under which the molecular memory is established (Figure 10A). This result is consistent with prior research suggesting that *thrb* is not part of the transcriptomic response to TH at nonpermissive temperatures (Hammond et al., 2016). Unlike *thrb*, *thibz* underwent a 6.9-fold increase in response to T_3 at 4 °C after 48 h (Figure 10A). *Thibz* is responsive to TH in C-Skin at cold temperatures which permit the initiation of a TH signal, but not the metamorphic program. *Thibz* is similarly responsive under molecular memory conditions in the lung, liver, brain, tailfin, and back skin tissue of whole animals, as well as in C-Fin (Hammond et al., 2016; Hammond et al., 2015). In C-Fin, *thibz* increased 5-fold after 24 h of exposure to 10 nM T_3, which is a change in transcript abundance of a similar magnitude to C-Skin in our study (Hammond et al., 2016). However, in the Hammond et al. 2016 study, *thibz* was not TH-responsive in C-Skin. This study

used four mm biopsy punches of C-Skin, but otherwise used comparable methods for RNA extraction, qPCR, and statistical analysis to our study (Hammond et al., 2016). It was thought that the expression of thibz was not organ autonomous in this tissue and would require additional modulatory factors present in the whole animal to be expressed in this tissue (Hammond et al., 2016). Our current research shows the induction of *thibz* by TH in multiple C-Skin assays (Figure 10, Figure 11). *Thibz* may be an organ autonomous component of the molecular memory in the back skin, unlike what was previously thought.

Furthermore, exposure to TH at cold temperatures can prime biopsies to later undergo changes in transcript abundance after a temperature shift as part of accelerated metamorphosis. *Thrb* increased 6.7-fold in abundance after the 12 h shift to 24 °C, following exposure to T_3 at 4 °C (Figure 10A). *Thibz* also increased 30-fold after the temperature shift. The greater abundance increases in this group in comparison to the solely 24 °C group is indicative of an accelerated metamorphic program, where the expression of TH-responsive transcripts is compressed within the same time frame.

The novel krueppel-like factor *klfX* did not undergo significant changes in abundance in response to TH for all three temperature regimes in C-Skin (Figure 10A). These results contrast previous observations in C-Fin where *klfX* increased 5-fold in abundance in response to T_3 at 4 °C after 48 h (Koide et al., 2022). Expression of TH-responsive transcripts such as *Rana* larval keratin 1 (*rlk1*) has previously been noted as restricted to certain tissues (Hammond et al., 2015). *KlfX* may similarly be restricted to the tailfin.

3.2 *Thrb* and *thibz* Undergo Greater Changes in Transcript Abundance in Response to TH After a 24 h Temperature Shift

An independent assay with a 24 h TH exposure in permissive temperatures was performed. C-Skin biopsies were treated with either a 400 nM NaOH control or a 10 nM T_3 treatment under one of three temperature regimes. Biopsies were held at permissive temperatures of 24 °C for 24 h, nonpermissive temperatures of 4 °C for 48 h, or subjected to a temperature shift after 48 h from 4 °C to 24 °C for an additional 24 h (See Figure 8 for details). The 24 h exposure period for 24 °C was chosen to investigate changes occurring after the first 12 h following induction with TH. Tail regression can be blocked by both transcriptional and translational inhibitors within the first 24 h of TH exposure; a 24 h exposure period will capture transcriptomic changes that occur during the establishment of the metamorphic program at warm temperatures (Ji et al., 2007). In addition, vascularisation of the hindlimbs is visible 24 h after TH injection in tadpoles subjected to a temperature shift, compared to 48 h in permissive temperatures (Hammond et al., 2015). A tadpole exposed to TH and then subjected to a 24 h temperature shift is comparable to a tadpole at the 48 h timepoint at warm temperatures, where commitment to the metamorphic program occurs (Skirrow et al., 2008; Wang and Brown, 1993).

Similarly, there were no significant changes in abundance for *thra* in response to T_3, in any of the three temperature regimes (Figure 10B). *Thrb* increased 3-fold and *thibz* increased 89-fold at 24 °C after 24 h (Figure 10B). These results indicate that C-Skin continues to respond

to TH over the longer time period at permissive temperatures. *Thrb* did not respond to T_3 at 4 °C, which is consistent with results from the 12 h assay using the same conditions (Figure 10B). At 4 °C, *thibz* underwent a 6.5-fold increase in abundance after 48 hours (Figure 10B). This result is comparable to the previous assay using the same cold temperature condition, which further verifies that *thibz* is TH-responsive under molecular memory conditions in the back skin.

After the 24 h temperature shift, *thrb* increased 8.4-fold and *thibz* increased 120-fold (Figure 10B). The greater increases in *thrb* and *thibz* after the temperature shift are suggestive of the accelerated metamorphic response that occurs after initial TH exposure at 4 °C. The increases in transcript abundance in the 24 h assay's warm and temperature shift groups were greater than those of their 12 h counterparts (Figure 10). This may suggest that abundance of the two transcripts continues to increase from the 12 to 24 h mark. However, these assays were completed with separate animal subjects and cannot be directly compared. Lastly, *klfX* did not undergo significant changes in abundance in response to TH in the 24 h C-Skin assay (Figure 10B). *KlfX* was not TH-responsive at 24 °C or 4 °C in either assay.

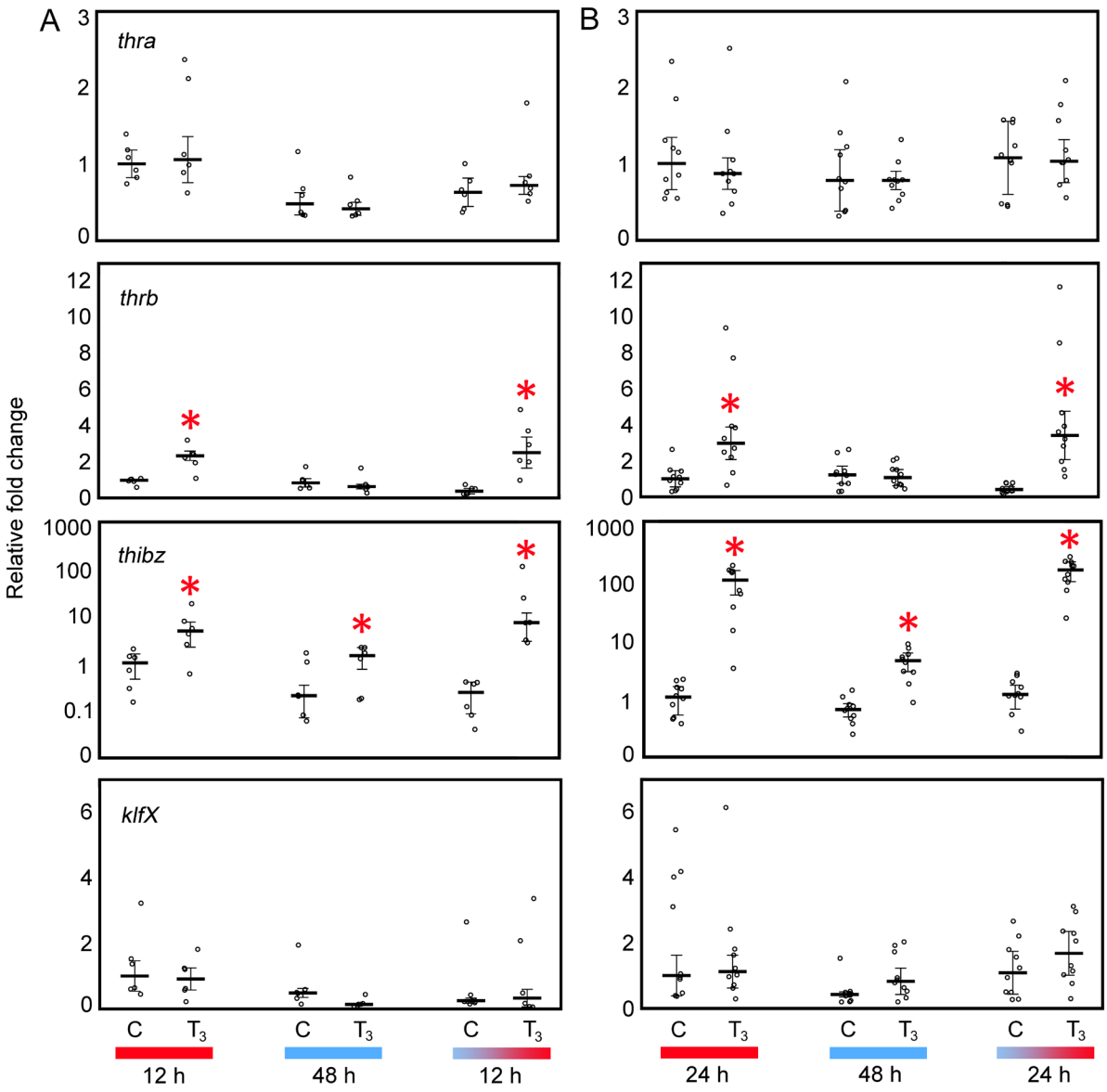

Figure 10. Exposure to 10 nM T_3 prompts changes in relative transcript abundance in *thrb* at warm temperatures and *thibz* at cold temperatures in 12 and 24 h C-Skin assays.
Use of cultured back skin (C-Skin) for repeated measures evaluation of TH effects on transcript abundance. Six C-Skin biopsies from premetamorphic *R. catesbeiana* tadpoles were exposed to a 400 nM NaOH control (C) or 10 nM T_3 (T_3) treatment at one of three temperature regimes. qPCR was used to measure abundance of the TH-responsive transcripts *thra*, *thrb*, *thibz* and *klfX* in the C-Skin biopsies. The left column (A) shows results from the 12 h C-Skin assay (see Figure 7 for details) and the right column (B) shows results from a separate 24 h C-Skin assays (see Figure 8 for details). The Y-axis indicates relative fold change in transcript abundance in comparison to the corresponding control. The X-axis indicates 400 nM NaOH "C" and 10 nM T_3 treatment "T_3", as well in the time in hours after which a biopsy was taken for RNA extraction. Red indicates warm temperatures (24 °C), blue represents cold temperatures (4 °C), and the gradient represents a temperature shift (4 to 24 °C). The open circles represent the relative fold change of individual data points with the median designated by the bar and median absolute deviation (MAD) designated by the whiskers. An asterisk indicates significance in the median relative fold change from the control ($p \leq 0.05$).

3.3 *Thibz* is an Early Responder to TH At Cold Temperatures, and is Induced Prior to *thrb* at Warm Temperatures in Time Course Experiments

To measure the abundance of TH-responsive transcripts over time, C-Skin biopsies were treated with 10 nM T_3 and incubated for a 0 to 24 h time course. Three independent experiments were performed with cold, warm and temperature shift conditions, each with repeated measures (See Figure 9 for details).

Thra was not temperature- or TH-responsive in all three time course experiments (Figure 11). In the 24 °C assay, *thrb* increased 5.8-fold in response to T_3 at the 24 h mark. *Thibz* had increased 4.5-fold by 4 h and continued to increase to 133-fold by 24 h. Notably, this increase in *thibz* abundance occurs before increases in *thrb* in this experiment. *Thrb* was not responsive to T_3 at 4 °C within the first 8 h of exposure, which was expected at temperatures that do not permit metamorphosis. In the 4 °C assay, *thibz* increased 2.3-fold by the 24 h mark. Under nonpermissive temperatures where the molecular memory is induced, *thibz* undergoes changes in abundance within the first 24 hours of initial TH exposure. *Thibz*, unlike *thrb*, is responsive in cold temperatures when molecular memory first initiates a TH signal (Figure 10, Figure 11). In addition, *thibz* is responsive ahead of other direct TH-response transcripts such as *thrb* at permissive temperatures (Figure 11). Together, these results are suggestive of the further stratification of the induction phase of TH response.

There were no significant changes in *thrb* abundance in the temperature shift assay, where biopsies were held at 24 °C for 8 h after initial TH exposure at 4 °C (Figure 11). It is possible that changes in *thrb* abundance in the back skin take place after 8 h, as *thrb* increases were seen in the other 12 h and 24 h experiments (Figure 10). These experiments were performed with different subjects, however, and cannot be directly compared. In the temperature shift experiment, *thibz* increased 2.8-fold 48 h after treatment with T_3 at 4 °C (Figure 11). *Thibz* continued to increase in abundance at 24 °C, even after being placed into clean media where T_3 was no longer present (Figure 11). *Thibz* increased 30-fold by 1 h and continued to increase to 498-fold by the 8 h mark. Additionally, increases in *thibz* in the temperatures shift experiment occurred 3 hours earlier and were of a greater magnitude than those in the warm experiment (Figure 11). These two experiments cannot be directly compared due to their use of different subject animals. Nevertheless, the two results suggest that *thibz* is an early responder in the initiation of TH signalling in the back skin.

3.3.1 The Novel Krueppel-Like Factor *klfX* is not Temperature- or TH-Responsive in C-Skin

Lastly, *klfX* was not TH-responsive in the C-Skin assays for any of the three time course experiments, across all temperatures and timepoints (Figure 11). This is in contrast to previous C-Fin results where *klfX* increased 2-fold 12 h after exposure to T_3 at 4 °C and increased 6.6-fold after 72 h (Koide et al., 2022). *KlfX* in C-Fin assays increased 4.4-fold 48 h after TH exposure at 4 °C but did not undergo any further changes in abundance after a temperature shift. At permissive temperatures, *klfX* was TH responsive after 1 h at 24 °C and was significantly increased throughout a 16 h time course (Koide et al., 2022). Comparison of *klfX* levels between C-Fin and C-Skin controls revealed that they were similar suggesting that *klfX* gene expression is

induced by TH in the C-Fin. *KlfX* did not display the same TH-responsiveness in the two tissues, despite comparable treatments and similar experimental designs. Potentially, other transcriptomic changes or modulatory processes may be present in the back skin's early response to TH signal. There is an indication that the molecular memory of the tailfin and back skin differ, as *klfX* was previously shown to be responsive in nonpermissive temperature in cultured tailfin (Koide et al., 2022).

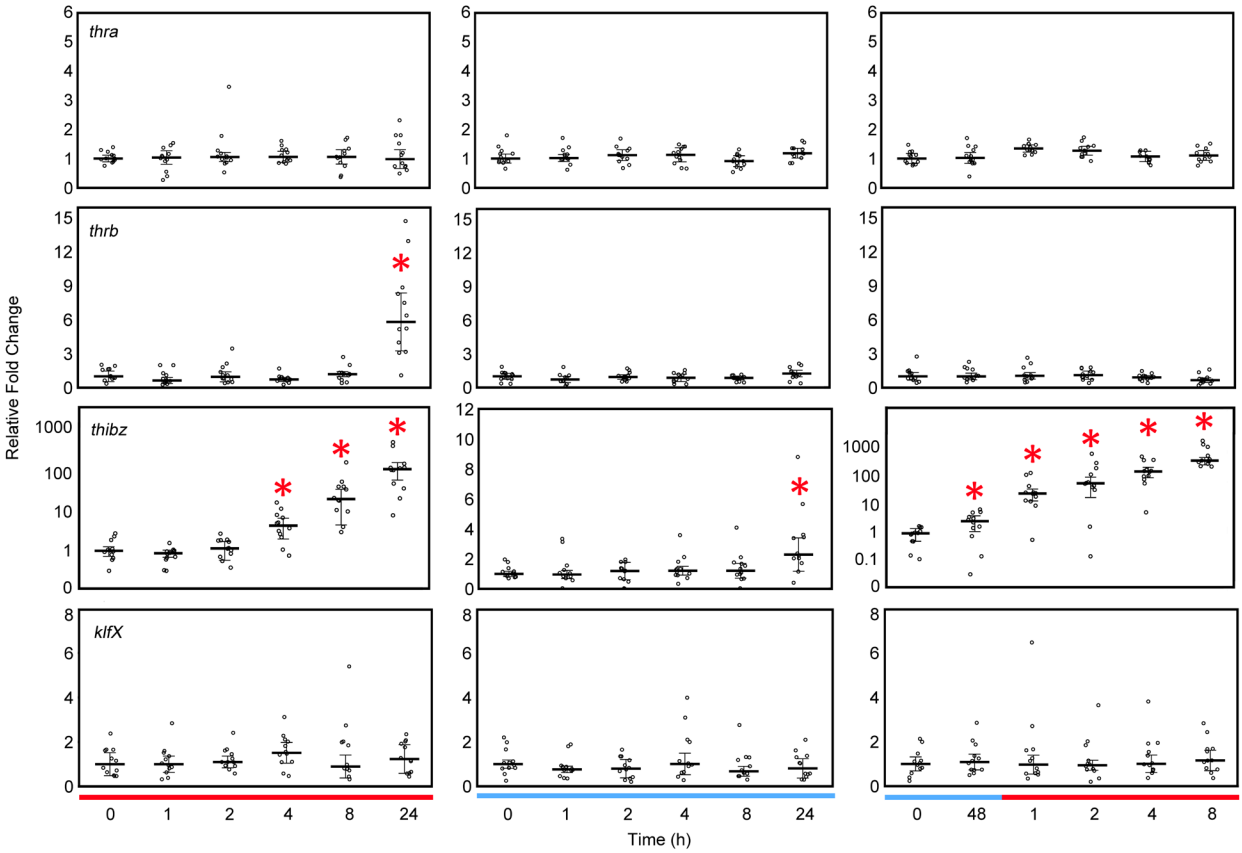

Figure 11. Exposure to 10 nM T_3 prompts increases in thibz transcript abundance in cold temperatures, as well as increases in *thibz* abundance in warm or temperature shift conditions prior to increases in *thrb*

Use of premetamorphic *R. catesbeiana* C-Skin (n = 12 per assay) for repeated measures evaluation of TH effects on transcript abundance changes. See Figure 9 for assay details. qPCR was used to measure the TH-responsive transcripts *thra*, *thrb*, *thibz* and *klfX*. The Y-axis indicates relative fold change in transcript abundance in comparison to the 0 h control. An asterisk indicates significance in the median relative fold change of a group of samples in comparison to the corresponding 0 h control ($p \leq 0.05$). See Figure 10 for additional plot details.

3.4 Investigation of the C-Skin Transcriptome by RNA-Sequencing

To investigate the broader transcriptomic response of the back skin at different temperatures, RNA from the C-Skin of five premetamorphic *R. catesbeiana* tadpoles was sent for RNA-Sequencing. Six biopsies from the same individual were exposed to either a 400 nM NaOH control or a 10 nM T_3 treatment for 24 h at 24 °C, 48 h at 4 °C, or a shift after 48 h at 4 °C to 24 °C for an additional 24 h were used (See Figure 8 for details).

The average number of raw RNA reads per library was 33.8 million for the cold (4 °C) condition, 36.5 million for the warm (24 °C) condition, and 32.1 million for the temperature shift (4-24 °C) condition (Supplementary Table 1). RNA-Seq reads were mapped to the annotated *R. catesbeiana* genome version 3 (Hammond et al., 2017) with similar levels of success across control and treatment groups, as well as across temperature conditions. Within the cold condition, 78.6 ± 0.2% paired end reads were mapped, 78.5 ± 0.2 % reads were mapped for the warm condition, and 78.5 ± 0.2% of reads were mapped for the temperature shift condition. After removing transcripts with a counts per million (cpm) of < 0.1 as false positives, there were 15,146 total transcripts identified in the cold condition, 15,359 transcripts in the warm condition and 15,178 transcripts in the temperature shift condition (Table 2). Approximately 88% of total transcripts were annotated using BLASTx and BLASTn against the NCBI non-redundant database for all three temperature conditions (Table 2). DESeq2 identified transcripts that were differentially expressed (DE) in response to T_3 treatment in the three temperature conditions. Of the DE transcripts, 95% in the cold condition, 89% in the warm condition, and 89% in the temperature shift condition were successfully annotated (Table 2).

Table 2. Transcript count and annotations
Total number of transcripts from C-Skin RNA libraries sequenced from *R. catesbeiana* tadpoles kept in one of three temperature conditions – cold, warm, and temperature shift. Total transcripts include those detected in any of the control or T_3 treatment animals for each respective temperature group. Transcripts were annotated using BLASTx and BLASTn (version 2.6.0, National Centre for Biotechnology Information). A transcript was considered differentially expressed (DE) if there was a statistically significant ($p_{adj} \leq 0.05$) difference in transcript abundance between the paired control and treatment samples in the repeated measures design with a false discovery rate (FDR) of 0.05.

Condition	Total Transcripts	% Transcripts Annotated	DE Transcripts	% DE Transcripts Annotated
Warm	15,359	88.45	570	89.47
Cold	15,146	88.70	44	95.45
Temperature Shift	15,178	88.66	890	88.99

Principal component analysis (PCA) of the DE transcripts shows strong separation between the control and treatment samples with the first component accounting for 75-86% of variation in all three temperature conditions (Figure 12). This highlights the robust transcriptomic response tadpoles exhibit upon exposure to TH at different temperatures.

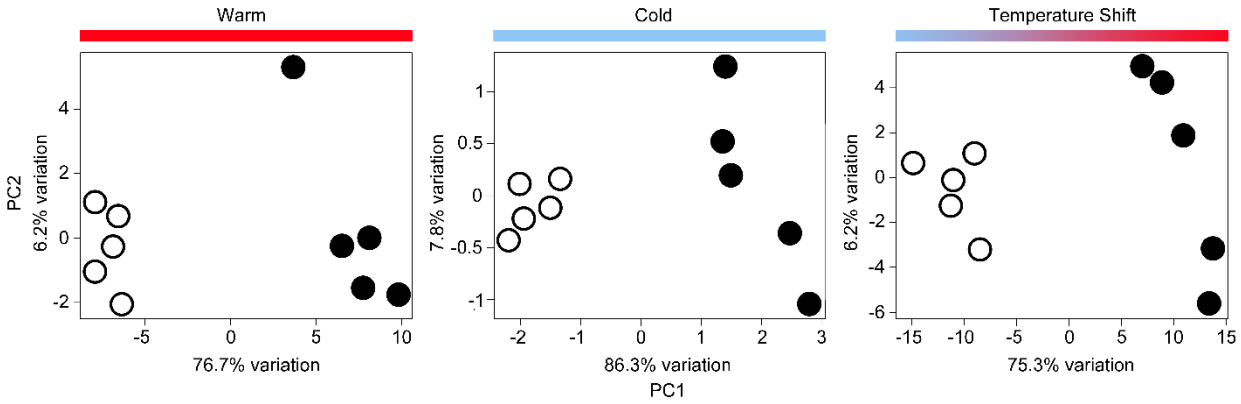

Figure 12. Principal component analysis (PCA) shows clear differentiation between the transcripts differentially expressed in *R. catesbeiana* tadpole C-Skin exposed to either control or TH treatment

Principal component analysis (PCA) of differentially expressed transcripts ($p_{adj} \leq 0.05$) identified in *R. catesbeiana* tadpole C-Skin (n = 5 tadpoles per temperature condition) exposed to either a 400 nM NaOH control (represented by open circles) or 10 nM T_3 treatment (represented by closed circles) in each of the three temperature conditions. Red represents the warm condition, where samples were held for 24 h at 24 °C, blue represents the cold temperature condition, where samples were held for 48 h at 4 °C and the gradient represents the temperature shift condition, where samples were held for 48 h at 4 °C, then held for an additional 24 h at 24 °C

Volcano plots highlight the differences in magnitude of the transcriptomic response to T_3 among the three temperature conditions (Figure 13). The warm condition has 345 unique DE transcripts, with another 220 shared between the warm and temperature shift conditions (Figure 13). The cold temperature condition has the fewest number of DE transcripts, with 37 unique transcripts (Figure 14). Only five DE transcripts are shared between the cold and warm conditions, with another 2 transcripts shared amongst the cold and temperature shift conditions (Table 5). The temperature shift condition has the largest number of DE transcripts, with 668 unique transcripts in this group (Figure 14). There were no transcripts marked as DE in all three conditions. Of the differentially expressed transcripts, 95 % in the cold condition were annotated, 89.7 % were annotated in the warm condition, and 88.9 % were annotated in the temperature shift condition (Table 2).

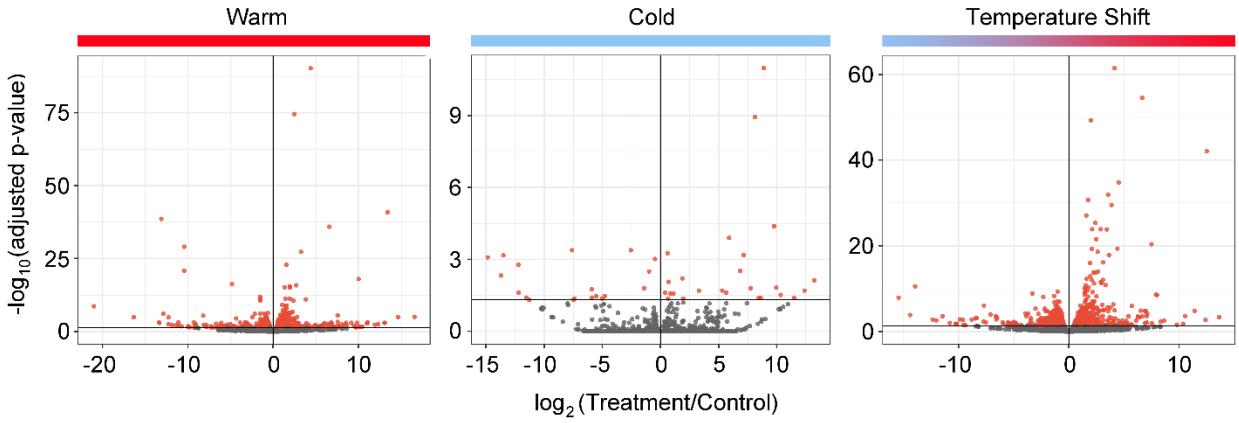

Figure 13. Volcano plots indicate differences in the magnitude of the transcriptomic response of *R. catesbeiana* tadpole C-Skin under different temperature conditions
Volcano plot of differentially expressed transcripts in *R. catesbeiana* tadpole C-Skin in cold, warm, and temperature shift conditions (n = 5 tadpoles per temperature condition). DESeq2 analysis was used to identify statistically significant changes in transcript abundance upon exposure to 10 nM T_3 treatment in comparison to 400 nM NaOH control. Red dots indicate differentially expressed transcripts ($p_{adj} \leq 0.05$), whereas grey dots indicate non-differentially expressed transcripts.

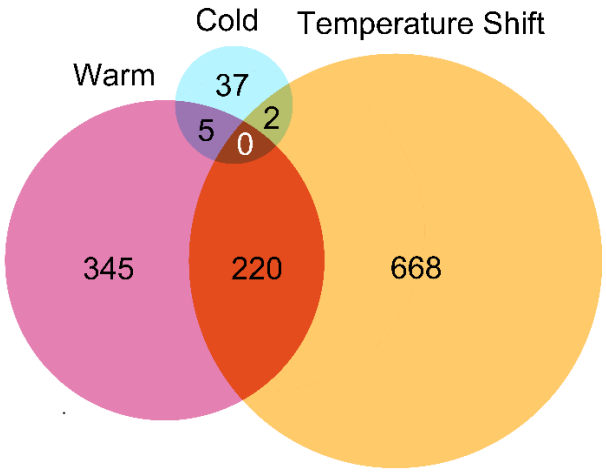

Figure 14. Venn diagram of differentially expressed transcripts in *R. catesbeiana* tadpole C-Skin indicates both shared and unique transcriptomic responses in the three temperature conditions
Comparison of differentially expressed transcripts in *R. catesbeiana* tadpole C-Skin treated with 10 nM T_3 in one of three temperature conditions. Pink represents the warm temperature condition, where samples were held for 24 h at 24 °C, blue represents the cold temperature condition, where samples were held for 48 h at 4 °C, and orange represents the temperature shift condition, where samples were held for 48 h at 4 °C, then held an additional 24 h at 24 °C. Differentially expressed transcripts ($p_{adj} \leq 0.05$) were identified with DESeq2 (Love et al., 2014). Circles were approximately scaled to represent the difference in total transcripts expressed in response to T_3 in the different temperature conditions.

3.5 RNA-Seq Assessment of Known TH-Responsive Transcripts

We first queried RNA-Seq data for known TH-responsive transcripts to further verify our qPCR results. We assessed the transcript abundance of *thra*, *thrb*, and *thibz*, the deiodinases *dio2* and *dio3,* and *heket*, a noncoding RNA previously found to be TH-responsive in the olfactory epithelium (Jackman et al., 2018).

Thra was detected in the cold, warm, and temperature shift conditions (Table 3). As in the qPCR analysis, there were no significant changes in *thra* abundance in response to TH. *Thrb* was also detected in all three temperature conditions. Transcript abundance increased 3.5-fold in the warm condition. *Thrb* was not significantly changed in the cold temperature condition, as expected. *Thrb* increased 7.9-fold in the temperature shift condition. The greater increase in *thrb* in the temperature shift condition is consistent with the augmented transcriptomic response seen in accelerated metamorphosis.

Thibz underwent a 111-fold increase in the warm temperature condition and a 160-fold increase in the temperature shift condition (Table 3). These results were consistent with prior qPCR data (Figure 4). *Thibz* was detected in the cold temperature condition with RNA-Seq (Table 3) but did not display significant changes in transcript abundance in response to T_3 when assessed with DESeq2 analysis (Supplementary Table 2). This contrasts the qPCR results for the

same samples chosen for RNA-Seq, as *thibz* significantly increased between 2- to 7-fold in response to T_3 at cold temperatures in these samples in comparison to their matched biopsy controls (Figure 10B). We do not know why there is this discrepancy between the qPCR and RNA-Seq data at cold temperatures. Perhaps one difference may stem from the differences in sample preparation. Generation of the RNA-Seq libraries is strand-specific whereas qPCR allows for amplification of either strand. In addition, *thibz* is TH-responsive *in vivo* in the back skin, but there are differing results regarding its expression in C-Skin. Our research has shown *thibz* to be TH-responsive in multiple C-Skin assays (Figure 10, Figure 11), but previous research did not find *thibz* expression in C-Skin under cold temperatures (Hammond et al., 2016). Regardless, the continued prominence of *thibz* as an early response transcript is notable and efforts to discover the role of this putative transcription factor in TH signaling in amphibians is underway.

The deiodinases mediate conversion between different forms of thyroid hormones. Localized deiodinase expression aids in the timing of metamorphosis by regulating the concentration of bioactive thyroid hormones in peripheral tissues (Brown, 2005). Dio2 converts T_4 to T_3 and is highly expressed in tissues such as the intestine during metamorphic climax (Bianco et al., 2002). Dio3 converts T_3 to T_2 and T_4 to reverse triiodothyronine (rT_3), which do not bind to TRs (Bianco and Kim, 2006). *Dio2* was detected in all three temperature conditions but was not differentially expressed in response to T_3. *Dio3* was detected in the warm and temperature shift conditions and was not differentially expressed in either condition (Table 3). These results suggest that T_3 exposure does not prompt deiodinase-mediated conversion as part of the TH response in C-Skin.

Heket, a previously identified long noncoding RNA in *R. catesbeiana*, increased 17-fold in the warm temperature condition and 25-fold in the temperature shift condition in response to T_3 (Table 3). Long non-coding RNAs (lncRNAs) are known to regulate processes such as chromatin remodelling, transcriptional activation, and mRNA translation (Statello et al., 2021). TH causes changes in expression among 1,000 putative lncRNA genes identified in the *R. catesbeiana* transcriptome (Hammond et al., 2017). *Heket* may play a role in modulating the TH response in the back skin, by influencing transcriptional pathways or chromatin remodelling as a lncRNA (Gao et al., 2020; Zhang et al., 2019). Many lncRNAs are expressed in a tissue-specific manner, however, it is unknown what role *heket* could play in the development of the back skin (Cabili et al., 2011).

Table 3. Transcript abundance changes of known TH-responsive transcripts are temperature-dependent in *R. catesbeiana tadpole* C-Skin
Median fold change in thyroid hormone responsive transcripts across temperature conditions of C-Skin exposed to 10 nM T_3 ($p \leq 0.05$). Significantly changed transcripts are marked with an asterisk. These transcripts are TH receptor α (*thra*), TH receptor β (*thrb*), TH-induced basic region leucine zipper-containing transcription factor (*thibz*), the long noncoding RNA heket (*heket),* and the deiodinases Dio2 (*dio2)* and Dio3 (*dio3).*

	Warm		Cold		Temperature Shift	
Transcript	FC	p-adj	FC	p-adj	FC	p-adj
Thyroid hormone receptor α *(thra)*	0.83	0.97	0.90	0.99	1.15	0.83
Thyroid hormone receptor β *(thrb)*	3.55*	2.75E-05	1.17	0.99	7.86*	1.32E-24
Thyroid hormone induced bZip *(thibz)*	111.32*	1.08E-36	1.53	0.99	159.87*	2.89E-55
Heket (*heket)*	16.76*	9.25E-12	0.95	0.99	24.68*	1.66E-35
Deiodinase 2 *(dio2)*	0.53	0.60	0.67	0.99	2.11	0.59
Deiodinase 3 *(dio3)*	3.33	0.56	NA	NA	1.38	0.91

3.6 Expression of Krueppel-Like Factor Transcripts in Warm and Temperature Shift Conditions

Krueppel-like factors are a family of zinc-finger domain transcription factors known to regulate cell proliferation, differentiation, and apoptosis (Pearson et al., 2008). *Klf9* specifically is strongly induced by T_3 in *X. laevis*, and associates with the *thrb* promoter region in tailfin and brain (Denver and Williamson, 2009). It is essential for proper postembryonic brain development in rats and *X. laevis* (Denver and Williamson, 2009; Hoopfer et al., 2002). Studies of *klf9* expression kinetics suggest that its thyroid hormone responsive elements allow direct activation by liganded TH receptors (Bagamasbad et al., 2008; Furlow and Kanamori, 2002). *Klf9* is TH-responsive under permissive temperatures in *R. catesbeiana* intestine, lung, and tailfin (Maher et al., 2016; Veldhoen et al., 2015). In addition, *klf9* transcript abundance increases in brain, back skin, and tailfin tissue one week after T_3 exposure at cold temperatures (Hammond et al., 2016; Hammond et al., 2015). *Klf9* was not TH-responsive over shorter time periods at in cold temperatures. The novel krueppel-like factor, *klfX* was upregulated at 5 °C within the first 96 h of TH exposure in C-Fin (Koide et al., 2022). Phylogenetically, *klfX* was most closely related to *klf5*. *Klf5* has not been previously implicated in TH signalling; however, it is associated with the regulation of the estrogen and retinoic acid nuclear receptors in mammalian models and cell lines (Guo et al., 2010; Kada et al., 2008).

Consistent with the qPCR results above, the *klfX* transcript was detected in the RNA-Seq data (Table 4) but did not undergo significant changes in abundance at any of the temperatures or time points examined (Figure 10, Figure 11). The DESeq2 pipeline also putatively annotated several other transcripts as krueppel-like factors. None of the transcripts identified as krueppel-like factors were differentially expressed in response to T_3 in the cold temperature condition. In both the warm and temperature shift conditions, *klf3, klf5* and *klf9* were significantly increased

in response to T_3 (Table 4). BLASTn alignment was used to confirm that the transcript annotated as *klf5* in our study was not the same sequence as *klfX*. In the warm temperature condition, *klf8* and *klf15* were also differentially expressed. *Klf7* was solely expressed in the temperature shift condition (Table 4).

The current results do not support a role for *klfX* in the back skin's early TH response including in cold temperatures wherein the molecular memory is established. Unlike in the C-Fin, *klfX* transcript abundance did not change significantly in C-Skin across multiple temperature conditions and timepoints studied (Koide et al., 2022). *KlfX* may be a tissue-specific regulatory factor that initiates TH-driven gene expression programs specifically associated with the development of the tailfin. Alternatively, additional modulatory elements that are not present in C-Skin might be required to prompt *klfX* expression in this tissue. The molecular memory is organ-autonomous and can be recapitulated in cultured tissue; however, previous research has shown differences in TH-responsive gene expression during *in vivo* versus *in vitro* studies of *R. catesbeiana* (Hammond et al., 2016; Veldhoen et al., 2015).

The current results also indicate that other members of the krueppel-like factor family are upregulated in response to T_3 at warm temperatures, or after a temperature shift. This suggests that these regulatory factors may play a role in the induction of TH response at temperatures that permit metamorphosis. In the back skin, the initiation of the TH signal at nonpermissive temperatures occurs prior to changes in abundance in krueppel-like factors. Some krueppel-like factors, excluding *klfX*, may play a role in development of the back skin downstream of the initial TH signal. In the tailfin, *klfX* undergoes changes in abundance at cold temperatures in a similar timeframe to *thibz* (Koide et al., 2022). Both are part of the early transcriptomic response when the TH signal is first established under molecular memory conditions. The components of molecular memory may be tissue-specific, and shared transcripts may be stratified differently in the TH response of different tissues. Alternatively, *klf9* in C-Skin was previously only increased significantly one week after exposure to T_3 at cold temperatures. It was suggested that *klf9* may play a role in maintaining the TH signal in overwintering tadpoles over time (Hammond et al., 2015). It is currently unknown if *klfX* could be similarly expressed in the C-Skin at a later timepoint after TH exposure at 4 °C , as opposed to early in the response when the molecular memory is first established.

Table 4. A subset of krueppel-like factor-encoding transcripts are TH-responsive in *R. catesbeiana* C-Skin in warm and temperature shift conditions
Median fold change in krueppel-like factor transcripts across temperature groups of C-Skin exposed to 10 nM T_3 ($p \leq 0.05$). Significantly changed transcripts are denoted by an asterisk.

	Warm		Cold		Temperature Shift	
Transcript Annotation	FC	p-adj	FC	p-adj	FC	p-adj
Krueppel-like factor 2 *(klf2)*	0.91	0.98	0.84	0.99	1.24	0.34
Krueppel-like factor 3 *(klf3)*	2.13*	0.01	0.88	0.99	2.40*	0.01
Krueppel-like factor 5 *(klf5)*	1.28	0.81	0.89	0.99	1.64	0.22
Krueppel-like factor 6 *(klf6)*	0.81	0.93	0.95	0.99	0.74	0.75
Krueppel-like factor 7 *(klf7)*	1.77	0.11	0.68	0.99	2.07*	0.01
Krueppel-like factor 8 *(klf8)*	0.46*	2.59E-03	0.87	0.99	0.24	0.81
Krueppel-like factor 9 *(klf9)*	12.32*	4.69E-28	0.83	0.99	10.77*	7.38E-17
Krueppel-like factor 10 *(klf10)*	1.10	0.86	1.08	0.99	0.70	0.64
Krueppel-like factor 11 *(klf11)*	1.28	0.21	1.06	0.99	1.18	0.98
Krueppel-like factor 13 *(klf13)*	1.42	0.87	1.31	0.99	0.89	0.83
Krueppel-like factor 15 *(klf15)*	0.92*	4.52E-03	0.76	0.99	0.73	0.53
Krueppel-like factor X *(klfX)*	0.52	0.89	3.17	0.99	1.44	0.78

3.7 Gene Ontology Analysis Indicates Changes in Transcription Factor Activity and Tissue Remodelling in the Warm and Temperature Shift Conditions

RNA-Seq reads were used to generate gene counts by grouping transcript isoforms together. Gene counts were tabulated to compare treatment and controls across the three temperature conditions and annotated for use in Gene Ontology enrichment analysis (Supplementary Table 3). Gene Ontology analysis was used to determine enriched functional groups associated with the DE genes in each temperature condition. Cytoscape was then used to visualize connections among the biological pathways that were affected by TH exposure. There were too few DE genes for network analysis of GO terms in the cold temperature condition (Supplementary Figure 3). However, there were enough DE genes in the warm and temperature shift conditions to visualize broad clusters of GO term categories.

In the warm temperature condition, there was a large group of genes associated with transcription factor and DNA binding activity (Figure 15). Terms corresponding to thyroid hormone metabolism, ammonia metabolism, transmembrane transport of amino acids, and aldolase activity were also enriched in this condition. GO term enrichment was also suggestive of changes in cell adhesion and development initiated by TH signalling in this tissue.

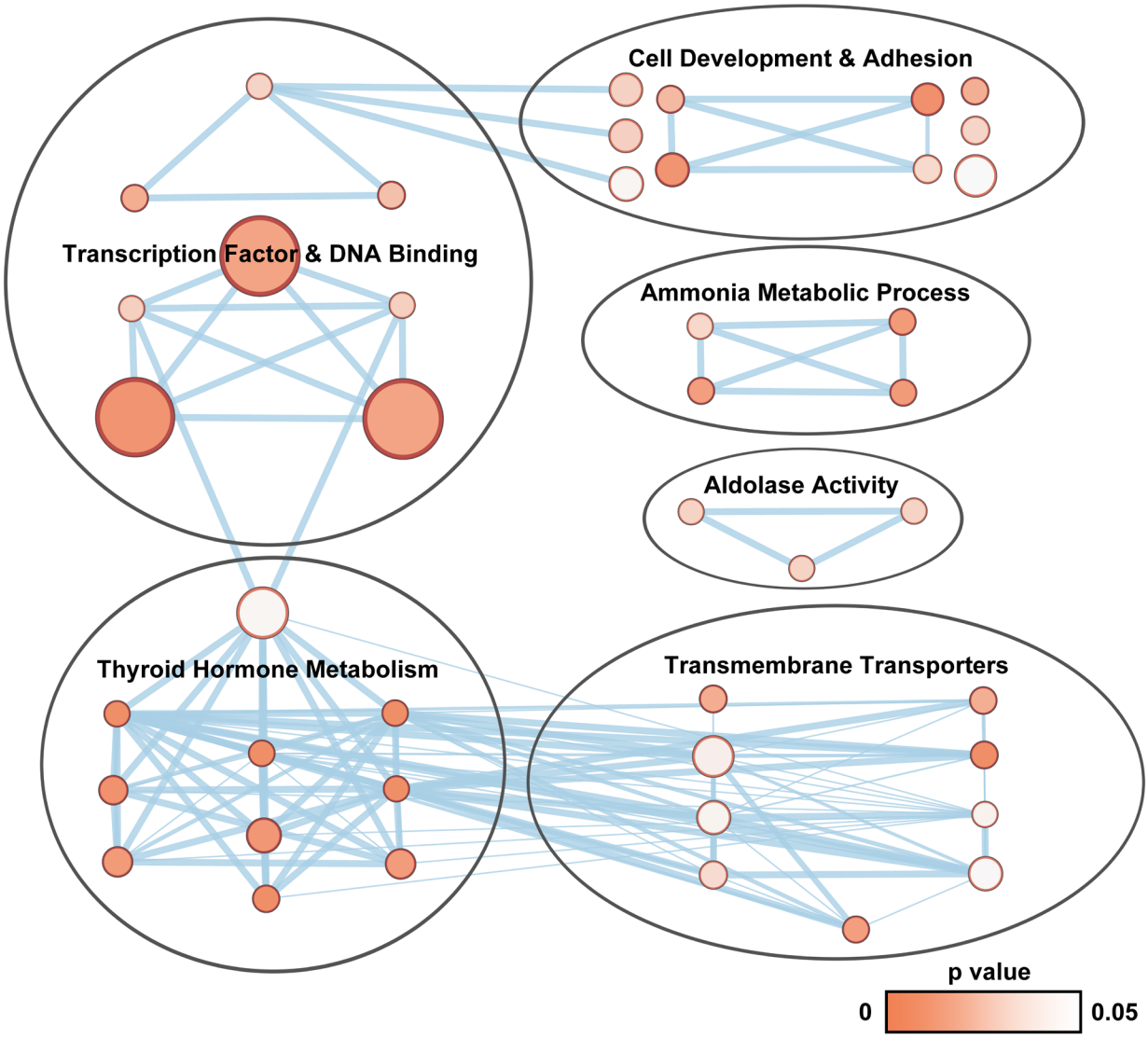

Figure 15. Gene ontology enrichment network for the warm temperature condition indicates changes in transcription factor activity, cell development and metabolism in response to TH
Significantly enriched gene ontology categories of differentially expressed genes in *Rana catesbeiana* C-Skin exposed to 10 nM T_3 for 24 h at 24 °C ($p \leq 0.05$). Each node represents a GO term, with node size corresponding to the number of genes associated with the GO term. Lines represent overlap between genes within related ontology categories, with line thickness indicating the number of overlapping genes. Darker node color represents a lower p-value.

The temperature shift condition had both unique GO term groups and ones similar to the warm condition. Terms relating to transcription factor and DNA binding activity, thyroid hormone metabolism, and transmembrane transport were enriched in both the warm and temperature shift conditions (Figure 15, Figure 16). Nodes corresponding to chromatin, RNA metabolic processes, retinoid binding and the response to abiotic stimulus, were enriched solely in the temperature shift condition (Figure 16).

GO analysis broadly suggests that transcription factor and DNA binding activity play a role in the TH response at warm temperatures or after a temperature shift. Enriched terms relating to tissue remodelling were also present in both temperature regimes (Figure 15, Figure 16). A larger group of terms corresponding to cellular adhesion and development, such as pigment granule organization and collagen binding, were enriched in the temperature shift condition (Figure 16). This result may be suggestive of accelerated metamorphosis, where TH prompts developmental changes associated with metamorphosis on a condensed time scale after exposure at 4 °C.

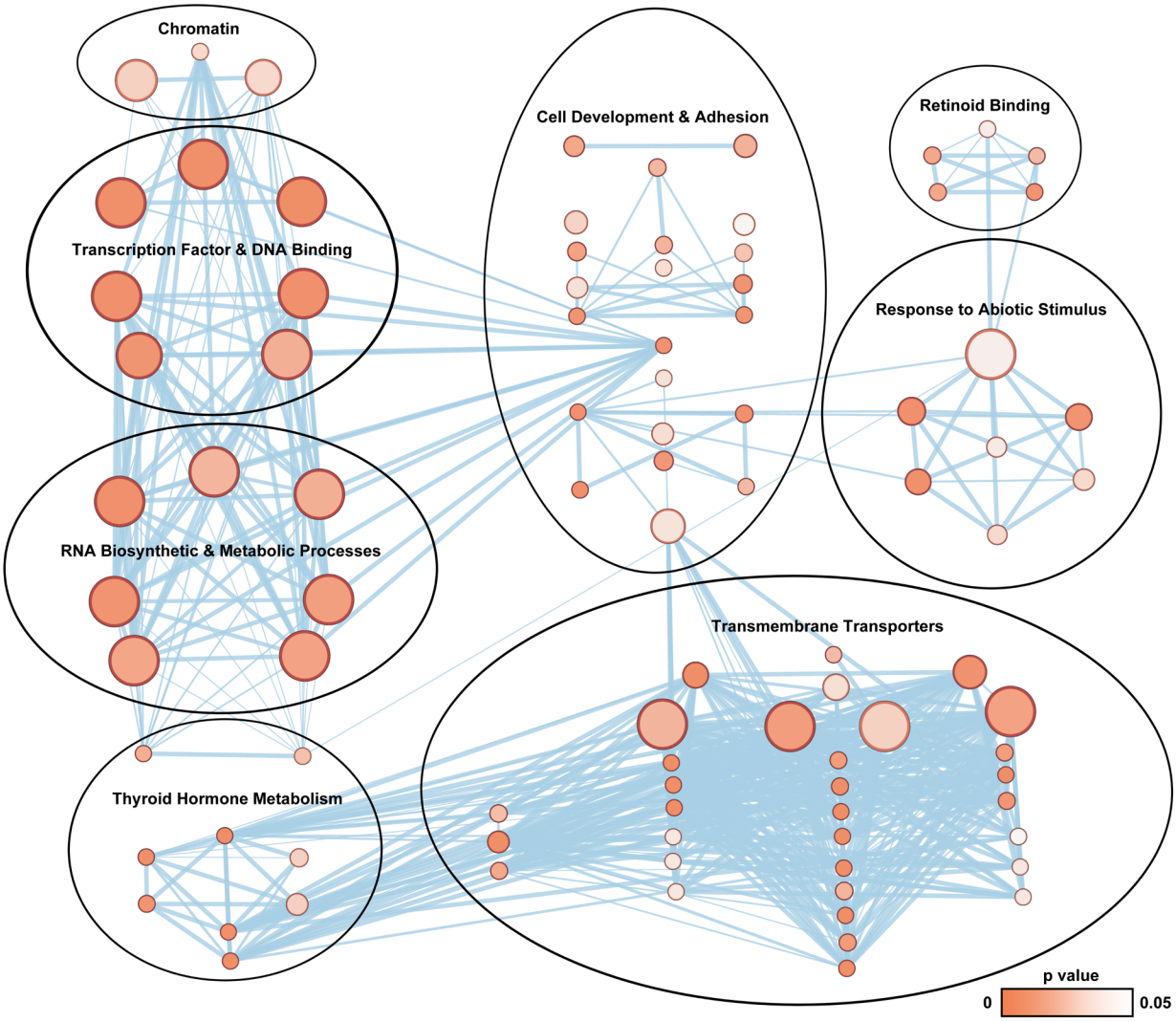

Figure 16. Gene ontology enrichment network for the temperature shift condition indicates changes in transcription factor activity, chromatin, and cell development in response to TH
Significantly enriched gene ontology categories of differentially expressed genes in *Rana catesbeiana* C-Skin exposed to 10 nM T_3 for 48 h at 4 °C, followed by a shift to 24 °C for an additional 24 h ($p \leq 0.05$). Refer to Figure 15 for further details.

3.8 Transcripts Shared Between the Cold, Warm, and Temperature Shift Conditions

There were 44 transcripts that were significantly affected by TH in the cold temperature condition. Twenty-five transcripts increased and 19 transcripts decreased in response to TH. No differentially expressed transcripts common to all three temperature conditions were detected (Figure 14). Only two transcripts were shared between the cold and temperature shift condition, and five transcripts were shared between the cold and warm condition (Table 5).

Table 5. Differentially expressed transcripts shared between the cold temperature condition and the warm and temperature shift conditions
Transcripts marked as differentially expressed by DESeq2 in more than one temperature condition. FC denotes a median fold change in transcript abundance in 10 nM T_3 treated samples in comparison to the corresponding 400 nM NaOH control. A significant change in transcript abundance is denoted by an asterisk ($p \leq 0.05$). Inf –infinity, denominator was 0.

	Warm			Cold			Temperature Shift		
Transcript Annotation	FC	Log_2 FC	p-adj	FC	Log_2 FC	p-adj	FC	Log_2 FC	p-adj
No Annotation (Contig ID: AB205_00398331-RC)	1.97	1.1	0.178	5.84*	1.89*	0.01	5.33*	3.61*	4.11E-03
ATP Binding Cassette Subfamily A Member 2 (ABCA2)	0.97	0.06	0.985	Inf*	5.31*	0.02	0.42*	-1.31*	0.02
Fc Receptor-Like Protein 6	0*	-6.60*	0.028	0*	-7.63*	4.16E-04	3.87	2.03	0.31
Nucleolar RNA Helicase 2-A-Like (Contig ID: AB205_00398508-RA)	0.00012*	-12.27*	1.33E-05	5.07E-05*	-13.53*	6.72E-04	0.96	0.04	0.97
Nucleolar RNA Helicase 2-A-Like (Contig ID: AB205_00398508-RB)	1415*	8.5*	0.001	895.86*	9.75*	4.14E-05	1.06	-0.84	0.83
Apoferritin Pseudogene	0*	-12.27*	0.003	0*	-12.19*	0.02	1.22	-0.24	0.98
Signal Induced Proliferation Associated 1 Like 2 (SIPA1L2)	0*	-8.2*	3.55E-06	Inf*	6.84*	3.06E-03	1.33	1.04	0.9

A transcript encoding ATP binding cassette subfamily A member 2 (ABCA2) was shared between the cold and temperature shift conditions (Table 5). Members of the ATP-binding cassette transporter superfamily are associated with the transport of molecules across intra- and extracellular membranes. Research suggests ABCA2 plays a role in cholesterol homeostasis and sphingolipid metabolism (Davis, 2011). It is unclear, what, if any role ABCA2 plays in the TH response of amphibians. There was also an unannotated transcript that was increased 5.8-fold in the cold temperature condition and 5.3-fold in the temperature shift condition (Table 5). A BLASTn search found that the only annotation found for this 3,909 bp transcript was an uncharacterized *Rana temporaria* locus (Accession Number: XM_040335092.1) with a 92.7% match in identity (Supplementary Figure 4A). When translated into a protein in reading frame 1 this transcript produced a putative 1,302 amino acid protein (Supplementary Figure 4B). A BLASTx search found that the closest matches were hypothetical proteins from *R. catesbeiana* and *R. temporaria.* High similarity to other to nucleotide and protein sequences from *Ranid* species indicates that this transcript is not an assembly artifact and may be a novel, unidentified transcript responsive to TH in the back skin of *R. catesbeiana*.

The transcripts shared between the cold and temperature conditions had a variety of annotations. One differentially expressed transcript was Fc receptor-like (FCRL) 6. FC receptor-like proteins are preferentially expressed by mammalian B-cells and have a variety of extracellular immunoglobin-like domains (Davis, 2007). FCRL6 is a transmembrane glycoprotein

with multiple immunoreceptor tyrosine activating and inhibiting motifs (Rostamzadeh et al., 2018). Notably, another member of this family, FCRL4 expresses a cytoplasmic tyrosine-based motif that binds the p85 regulatory subunit of phosphatidylinositol-3 kinase (PI3K), a pathway also non-genomically induced by T_4 (Rostamzadeh et al., 2018; Sidorenko and Clark, 2003). The cold and warm temperature conditions also share differential expression of signal induced proliferation associated 1 like 2 (SIPA1L2). SIPA1L2 contains a GTPase activating domain and a C-terminal coiled-coil domain with a leucine zipper. In rats, SIPA1L2 has been found to act as an activating protein for a GTPase associated with neuron development (Spilker et al., 2008). A transcript encoding an apoferritin gene was also differentially expressed in both conditions. Differential expression of apoferritin had been previously noted in the liver of winter-acclimated *R. catesbeiana* bullfrogs (Wu et al., 2002). However, no prior research suggests a strong mechanistic role in initiating TH signalling for these three transcripts.

3.9 Transcripts Associated with Changes in mRNA Structure and Stability Expressed in the Cold Temperature Condition

There were also striking increases in two transcripts annotated as nucleolar RNA helicase 2A, also known as DEAD-box helicase 21 (DDX21) in both the cold and warm temperature conditions. DDX21 plays multifaceted roles during ribosomal biogenesis and mRNA processing, which makes this an intriguing prospect in the control of the TH-response. Two DDX21 transcripts were expressed in the cold and warm conditions (Table 5), referred to by their contig IDs in the *R. catesbeiana* genome, AB205_00398508-RA and AB205_00398508-RB. AB205_00398508-RA was 1,112 bp long, and AB205_00398508-RB was 2,040 bp long, with the first 1,112 bp being shared sequence (Supplementary Figure 5A). AB205_00398508-RA decreased significantly in the cold and warm temperature conditions and AB205_00398508-RB increased in both the cold and warm conditions over 800-fold (Table 5). These transcripts may produce different proteins with different functionalities if translated, as DDX21 is a multifunctional enzyme with an N-terminal domain, middle D1 and D2 domains, and C-terminal domain (Chen et al., 2020). When translated into a protein in reading frame 1, AB205_00398508-RA produced a sequence of 373 amino acids and AB205_00398508-RB produced a sequence of 679 amino acids (Supplementary Figure 5B).

DEAD-box helicases are a family of RNA helicases characterised by a conserved Asp-Glu-Ala-Asp (DEAD) motif. They play a broad variety of roles in ribosomal biogenesis, transcriptional regulation, and mRNA editing, storage, and decay (Linder and Jankowsky, 2011). DDX21's role in ribosomal biogenesis is its most well-understood. In the nucleolus, DDX21 binds ribosomal RNAs (rRNAs) and small nucleolar RNAs (snoRNAs) to promote ribosomal biogenesis (Calo et al., 2015). In the nucleoplasm, DDX21 has also been shown to associate with small nuclear ribonucleoprotein (snRNP) complexes to bind the promoters of RNA polymerase II transcribed genes. DDX21 then facilitates the transcription of select mRNAs (Calo et al., 2015).

Furthermore, DDX21 is an important regulator of cellular proliferation and differentiation in oncogenesis, outside of its function in rRNA regulation. DDX21 promotes the transcription of the proto-oncogenes c-Myc, cyclin D1, and c-Jun (Cao et al., 2018). DDX21 was specifically found to be an interaction partner of c-Jun that promotes activation of its' target

genes. c-Jun is a transcription factor responsive to extracellular stimuli including apoptotic and stress signals (Zhang et al., 2014). It stimulates mRNA synthesis through enhancing activation at promoter regions, in combination with specific co-factors such as DDX21 (Westermarck et al., 2002).

DDX21 also aids in resolving estrogen-induced R loops on estrogen-responsive genes in breast cancer cells (Song et al., 2017). R loops are three-stranded structures that harbour an RNA–DNA hybrid and have been implicated in genome instability in cancerous cells. However, the programmed formation of R loops is also used to regulate chromatin formation, gene expression and transcriptional termination (Niehrs and Luke, 2020). DDX21 was found to prevent the blocking of transcriptional elongation of estrogen-responsive genes and may additionally play a role in genome integrity (Song et al., 2017).

Lastly, DDX21 may be able to alter the secondary structure of mRNA to alter transcription and translation. DDX21 has ATP-dependent helicase action that unwinds double stranded RNA during the host's innate immune response to viral infection (Chen et al., 2020). It also has ATP-independent foldase activity that adds secondary structure to single-stranded RNA (Valdez et al., 1997). Emerging research also suggests that DDX21 may be able to bind and unwind RNA guanine quadruplexes (McRae et al., 2018). Four-stranded guanine quadruplexes form from guanine-rich nucleic acid sequences and current research supports that RNA G-quadruplexes are regulatory elements. G-quadruplexes in the 5'-UTRs of mRNAs are shown to modulate translation initiation and efficiency (Bugaut and Balasubramanian, 2012). 3'-UTR G-quadruplexes are found to impact alternative polyadenylation and produce shortened mRNAs with variable stability and translation efficiency (Beaudoin and Perreault, 2013). G-quadruplexes have also been shown to be highly stable structures that require specialized helicases for a change in conformation (McRae et al., 2017). The DDX21 helicase was found to bind and unwind G-quadruplexes through interaction with a motif on its' C-terminus. DDX21 resolves G-quadruplex structures by direct binding in both an ATP-dependent and -independent manner. Furthermore, DDX21 was able to supress the expression of a β-galactosidase gene with a G-quadruplex in the 3'-UTR region, which suggests that DDX21 recruitment may be able to modulate transcription by altering G-quadruplex structure (McRae et al., 2017).

Thus, taken together, DDX21 isoforms may act as transcription factors to promote gene expression at warm temperatures or may post-transcriptionally modify mRNA in temperatures that do not permit the metamorphic program to occur.

3.10 Expression of Transcripts Encoding Transcription Factors in the Cold Temperature Group

Seven transcripts encoding transcription factors were differentially expressed in the cold temperature condition (Table 6). There was no overlap with the transcripts encoding transcription factors differentially expressed in the C-Skin, and those previously identified as differentially expressed in response to TH in the C-Fin (Koide et al., 2022). Of those putative transcription factors identified in the C-Fin, transcripts encoding SIX homeobox 1, cyclin L2, cysteine and serine rich nuclear protein 1, Cbl proto-oncogene C, SRY-box 21, forkhead box Q1,

and high mobility group protein B2 were detected but not significantly TH-responsive in the C-Fin (data not shown).

The transcripts encoding transcription factors in the C-Skin include mediator complex subunit 1 (MED1) and mothers against decapentaplegic 4-like (SMAD4) (Table 6). MED1 protein is a component of multisubunit complexes which interact with TRs to initiate transcription (Femia et al., 2020; Park et al., 2005). SMAD4 is part of the SMAD family of transcription factors which mediate TGF-B signal transcription factors (Hill, 2016). Strikingly, zinc finger ZZ-type and EF-hand domain containing 1 (ZZEF1) transcript increased 366-fold in response to TH (Table 6). ZZEF1 was found to interact with the histone H3 tail to modulate the expression of *klf6* and *klf9* in 2021, however its biological role remains unknown (Yu et al., 2021). The role of these transcripts encoding transcription factors hasn't yet been determined. However, given their responsiveness at cold temperatures, they may be a component of the molecular memory in the C-Skin. These results suggest transcription factors may play a role in the early initiation of TH signaling under cold conditions. The transcripts encoding transcription factors also differ from those found in the tailfin, which may suggest that the early response to TH has tissue-specificity. Additional modulatory factors apart from transcripts encoding transcription factors may also be present in the back skin as other transcripts were differentially expressed in response to TH at cold temperatures (Table 7).

Table 6. Tissue-specific, differentially expressed transcripts encoding transcription factors in the cold temperature condition
Transcripts encoding transcription factors marked as differentially expressed by DESeq2 in the cold temperature condition. FC denotes a median fold change in transcript abundance in 10 nM T_3 treated samples in comparison to the corresponding 400 nM NaOH control. Inf –infinity, denominator was 0.

Transcript Annotation	FC	Log_2 FC	p-adj
Mothers Against Decapentaplegic Homolog 4-Like	Inf	9.96	1.5E-02
ABL Proto-Oncogene 1, Non-Receptor Tyrosine Kinase (ABL1)	Inf	11.48	4.1E-02
Zinc Finger ZZ-Type and EF-Hand Domain Containing 1 (ZZEF1)	366.50	7.77	1.6E-02
Mediator Complex Subunit 1 (MED1)	12.06	3.31	2.0E-02
Up-Regulator of Cell Proliferation-Like	1.94	0.85	2.6E-02
Matrix Metallopeptidase 9 (MMP9)	1.57	0.60	5.6E-04
Activating Transcription Factor 7-Interacting Protein 1-Like	1.36	0.41	2.4E-02

Epigenetic control may play a role in the response of the back skin to TH at cold temperatures. (Table 7). E1A binding protein p400 (EP400) increased 1.6-fold in response to TH in C-Skin. EP400 aids in the acetylation of histone H2A and H3.3 to positively regulate transcription (Pradhan et al., 2016). As part of the NuA4 histone acetyltransferase complex, EP400 activates the transcription of select genes by both altering nucleosome-DNA interactions and promoting histone-protein interactions (Mattera et al., 2010; Zhao et al., 2017). As part of the SWR1-like complex, it can replace H2A with H2A.Z to regulate gene expression in plants in a temperature-dependent manner (Aslam et al., 2019). Chromatin modifications could promote

the expression of certain early TH-responsive transcripts at cold temperatures whilst preventing the induction of the metamorphic program.

Non-genomic signalling may also play a part in the initiation of the TH signal in the back skin. There was also a 7-fold increase in a Von Willebrand Domain-containing Protein 8 (VWA8) transcript in the cold temperature condition (Table 7). Conserved eukaryote Von Willebrand Domain-containing proteins are intracellular and play a role in cell adhesion, as well as in transcription and DNA repair as part of multiprotein complexes (Whittaker and Hynes, 2002). VWA8 is a relatively novel protein with undetermined activity and function (Luo et al., 2017). It has been demonstrated to localize to the matrix of the inner mitochondrial membrane in mice (Luo et al., 2020). It has a long and short isoform produced by alternative splicing. (Luo et al., 2020; Luo et al., 2017). VWA8 has potential TR co-regulator TH activity and has been found in mammalian cell culture to selectively interact with the TRβ2 isoform in mammalian cell culture and could bind TRβ1 through the shared E/F domain (Hahm and Privalsky, 2013). The function of VWA8 is not well understood in vertebrates, though research suggests it may have nucleotide-binding or ATPase activity (Hahm and Privalsky, 2013; Umair et al., 2021). If VWA8 binds TRs in amphibians in response to TH as coregulator, it may be able to regulate the expression of certain transcripts at cold temperatures.

Table 7. All differentially expressed transcripts in the cold temperature condition
Transcripts marked as differentially expressed by DESeq2 in the cold temperature condition. FC denotes a median fold change in transcript abundance in 10 nM T_3 treated samples in comparison to the corresponding 400 nM NaOH control. Inf –infinity, denominator was 0.

Transcript Annotation	FC	Log_2 FC	p-adj
Aminoadipate-Semialdehyde Synthase (AASS)	Inf	8.62	4.1E-02
Signal Induced Proliferation Associated 1 Like 2 (SIPA1L2)	Inf	6.84	3.1E-03
ATP Binding Cassette Subfamily A Member 2 (ABCA2)	Inf	5.31	2.0E-02
Clustered Mitochondria Protein Homolog	Inf	10.34	3.1E-02
Tenascin C (TNC)	Inf	8.46	4.1E-02
Mothers Against Decapentaplegic Homolog 4-Like	Inf	9.96	1.5E-02
Microtubule-Associated Protein 4-Like	Inf	8.12	1.2E-09
ABL Proto-Oncogene 1, Non-Receptor Tyrosine Kinase (ABL1)	Inf	11.48	4.1E-02
Tyrosine Kinase Non-Receptor 2 (TNK2)	Inf	12.38	2.0E-02
Cytoplasmic Actin Type 5	Inf	13.23	7.3E-03
RERG Like (RERGL)	Inf	5.66	2.4E-02
Von Willebrand Factor A Domain Containing 8 (VWA8)	Inf	7.15	6.7E-04
Biliverdin Reductase B (BLVRB)	Inf	8.88	1.1E-11
Nucleolar RNA Helicase 2-A-Like (Contig ID: AB205_00398508-RB)	895.86	9.75	4.1E-05
Zinc Finger ZZ-Type And EF-Hand Domain Containing 1 (ZZEF1)	366.50	7.77	1.6E-02
Glutamine Synthetase-Like	116.60	5.90	1.3E-04
Mediator Complex Subunit 1 (MED1)	12.06	3.31	2.0E-02
No Annotation (Contig ID: AB205_00398331-RC)	5.84	1.89	6.2E-03
Phosphatidylserine Decarboxylase Proenzyme, Mitochondrial-Like	4.37	1.93	4.3E-02
WAP Four-Disulfide Core Domain Protein 3-Like	2.03	0.65	4.3E-02
Up-Regulator Of Cell Proliferation-Like	1.94	0.85	2.6E-02
E1A-Binding Protein P400-Like	1.63	0.70	8.5E-03
Matrix Metallopeptidase 9 (MMP9)	1.57	0.60	5.6E-04
VHA-A mRNA For Vacuolar Proton-ATPase A-Subunit	1.56	1.11	2.7E-02
Activating Transcription Factor 7-Interacting Protein 1-Like	1.36	0.41	2.4E-02
Caspase Recruitment Domain Family Member 9	0.70	-0.47	9.7E-04
Family With Sequence Similarity 53 Member A (FAM53A)	0.43	-0.99	3.2E-03
mRNA For Annexin A1 (ANX1)	0.35	-1.41	1.6E-02
No Annotation (Contig ID: AB205_00393477-RB)	0.13	-2.55	4.2E-04
SID1 Transmembrane Family Member 2 (SIDT2)	0.05	-4.82	3.4E-02
FUS RNA Binding Protein (FUS)	0.00	-7.48	4.8E-02
Senataxin (SETX)	0.00	-7.40	4.3E-02
Nucleolar RNA Helicase 2-A-Like (Contig ID: AB205_00398508-RA)	0.00	-13.53	6.7E-04
Trafficking Kinesin Protein 1 (TRAK1)	0.00	-11.53	4.1E-02
Ribonuclease T2 (RNASET2)	0.00	-12.23	1.7E-03
Circularly Permutated Ras Protein 1-Like	0.00	-5.92	1.8E-02
Coronin 2B (CORO2B)	0.00	-5.52	3.5E-02
Fc Receptor-Like Protein 6	0.00	-7.63	4.2E-04
Trafficking Protein Particle Complex 4 (TRAPPC4)	0.00	-11.28	5.0E-02
Apoferritin Pseudogene	0.00	-12.19	2.4E-02
Cytoplasmic Actin Type 5 mRNA	0.00	-14.86	8.3E-04
RERG Like (RERGL)	0.00	-5.90	4.1E-02
Exportin 1 (XPO1)	0.00	-13.71	4.8E-03
Cytochrome P450 2U1	0.00	-5.04	4.3E-02

3.11 Transcripts Encoding Transcription Factors Expressed After a Temperature Shift that Prompts Accelerated Metamorphosis

Exposure to TH at cold temperatures primes tadpoles to later undergo metamorphosis after a temperature shift. Induction of the molecular memory is sufficient to prompt an accelerated metamorphic program. Twenty-seven transcripts encoding transcription factors were identified as TH-responsive in the temperature shift condition (Table 8). These transcripts included cAMP responsive element binding protein 3 like 4 (CREB3L4) which increased 25-fold. CREB3L4 is a membrane-bound bZIP domain-containing transcription factor induced by androgens in murine models (Aicha et al., 2007; Asada et al., 2011) . CREB3L4 was found to regulate the expression of a diverse group of transcripts associated with transcriptional regulation, small molecule transport and signal transduction in the prostate (Aicha et al., 2007). Transcription factors such as CREB3L4 may contribute to the accelerated metamorphic response after a temperature shift by enhancing the transcription of other TH-responsive genes.

Table 8. Differentially expressed transcripts encoding transcription factors in the temperature shift condition excluding *TH-induced basic region leucine zipper-containing transcription factor (thibz)*

Transcripts encoding transcription factors marked as differentially expressed by DESeq2 in the temperature shift condition. FC denotes a median fold change in transcript abundance in 10 nM T_3 treated samples in comparison to the corresponding 400 nM NaOH control. Inf –infinity, denominator was 0.

Transcript Annotation	Fc	Log_2 Fc	p-adj
Forkhead Box Protein O6-Like	Inf	7.04	2.3E-04
Forkhead Box Protein O6-Like	Inf	8.00	2.9E-09
Camp Responsive Element Binding Protein 3 Like 4 (CREB3L4)	25.00	4.14	1.2E-05
POU Class 3 Homeobox 1 (POU3F1)	11.84	3.32	1.4E-11
BARX Homeobox 2 (BARX2)	6.05	2.39	2.1E-14
SRY-Box 4 (SOX4)	5.81	2.89	2.6E-12
CCAAT/enhancer-binding protein (C/EBP-1)	4.26	2.22	1.5E-14
E74 Like ETS Transcription Factor 3 (ELF3)	4.12	2.18	3.1E-05
Transcription Factor 7 Like 2 (TCF7L2)	2.62	1.55	1.1E-10
Iroquois Homeobox 5 (IRX5)	2.36	1.06	1.7E-04
Iroquois Homeobox 1 (IRX1)	1.97	1.23	4.1E-02
Signal Transducer and Activator of Transcription 5B	1.76	0.78	2.3E-03
Signal Transducer and Activator of Transcription 5B	1.76	0.78	2.3E-03
Homeobox Protein MSX-2-Like	1.60	1.40	2.7E-03
Homeobox B3 (HOXB3)	1.57	0.88	3.5E-02
Zinc Finger E-Box Binding Homeobox 2 (ZEB2)	1.40	0.66	3.4E-02
Transcriptional Regulating Factor 1 (TRERF1)	0.71	-0.58	2.8E-02
RB Transcriptional Corepressor Like 2 (RBL2)	0.70	-0.50	3.6E-02
Sp2 Transcription Factor (SP2)	0.69	-0.69	3.8E-02
TRAF Interacting Protein With Forkhead Associated Domain (TIFA)	0.61	-0.70	4.8E-02
Zinc Finger Homeobox 3 (ZFHX3)	0.57	-1.07	2.0E-04
Forkhead Box Q1 (FOXQ1)	0.42	-1.30	1.5E-07
Camp Responsive Element Binding Protein 3 Like 4 (CREB3L4)	0.38	-1.77	1.9E-03
Sp1 Transcription Factor (SP1)	0.15	-1.84	2.0E-03
Up-Regulator of Cell Proliferation-Like	0.14	-3.45	8.3E-04
Sterol Regulatory Element Binding Transcription Factor 2 (SREBF2)	0.00	-7.55	7.1E-03
Sp9 Transcription Factor (SP9)	0.00	-5.51	3.1E-02

3.12 Transcripts Associated with Changes in mRNA Structure and Stability Expressed in the Temperature Shift Condition

There were also several transcripts upregulated in the temperature shift condition that suggest potential mechanisms of action for producing an accelerated response after initial exposure to TH at cold temperatures (Table 9). Heterogenous nuclear ribonucleoprotein (hnRNP) complexes are RNA and protein complexes that play a role in pre-mRNA processing, transport, and stability (Chaudhury et al., 2010). A heterogenous nuclear riboprotein L transcript increased 3,470-fold solely in the temperature shift condition (Table 9). Heterogenous nuclear riboprotein L (HNRNPL) is a component of hnRNP complexes with a binding preference for CA-rich elements. It is a splicing factor that can activate and repress exon inclusion through intron retention, inclusion / exclusion of cassette-type exons, and poly(A) site selection (Hung et al., 2008; Rossbach et al., 2014). Splicing targets are diverse and HNRNPL plays a role in T-cell activation in mammals, tumorigenesis, and apoptosis (Loh et al., 2015; Seo et al., 2017; Shankarling et al., 2014).

In addition, HNRNPL has also been implicated in post-transcriptional regulation by miRNA silencing activity in tumor cells. Hypoxia causes the translocation of HNRNPL to the cytoplasm, where it competes with miRNAs to bind to CA-rich elements on mRNA (Jafarifar et al., 2011). MicroRNAs silence gene expression by mRNA degradation and inhibiting translation. (Roush and Slack, 2006). Increases in HNRNPL transcript abundance may prevent the mRNA degradation and gene silencing, leading to the induction of the TH response after a temperature shift.

CCHC-type zinc finger nucleic acid binding protein (CNBP) also increased 100-fold solely in the temperature shift condition. CNBP is highly conserved amongst vertebrates and was first described as a DNA-binding protein and putative regulator of the sterol regulatory element (Armas et al., 2021; Rajavashisth et al., 1989). It has been implicated in the positive and negative transcriptional regulation of a diverse set of genes related to craniofacial development, the murine innate immune system, and oncogenesis (Armas et al., 2021; David et al., 2019; Lee et al., 2017). In *X. laevis* CNBP may modulate transcription by binding to a conserved region on the 5’ UTR of ribosomal protein mRNAs (Pellizzoni et al., 1997). CNBP has additionally been shown to act as a modulator of translation as well as transcription. CNBP acts as a nucleic acid chaperone to produce stable structures that repress translation and is a component of stress granules, a ribonucleoprotein structure that aids in the storage of mRNA and protein homeostasis (Armas et al., 2008; Rojas et al., 2012). Alternatively, CNBP can prevent G-quadruplex formation on mRNA to increase efficacy of translation without a change in mRNA abundance (Benhalevy et al., 2017). CNBP protein can be post-translationally modified and has distinct patterns of localization in both the nucleus and cytoplasm of *Bufo arenarum* oocytes as development progresses (Armas et al., 2001; Armas et al., 2021). CNBP may regulate numerous cellular signalling pathways in a variety of ways; it is still unclear what biochemical properties facilitate its’ multiple functions. CNBP could perhaps play a role in accelerated metamorphosis after a temperature shift by modulating transcription associated with the

induction of metamorphosis. CNBP may post-transcriptionally modify mRNA structure and stability or efficiency of translation.

Table 9. Putative accelerated response transcripts in the temperature shift condition
Transcripts of interest marked as differentially expressed by DESeq2 in the temperature shift condition. FC denotes a median fold change in transcript abundance in 10 nM T_3 treated samples in comparison to the corresponding 400 nM NaOH control

Transcript Annotation	FC	Log_2 FC	p-adj
Heterogeneous Nuclear Ribonucleoprotein L (HNRNPL)	3470	12.50	8.00E-43
CCHC-Type Zinc Finger Nucleic Acid Binding Protein (CNBP)	100	5.18	0.00289

4 Conclusions and Future Directions

Thyroid hormones (THs) are essential for the postembryonic development of all vertebrates. THs are signalling molecules which initiate complex cascades of gene expression responsible for a diverse set of developmental outcomes. The molecular mechanisms underlying TH signalling are conserved amongst mammals and amphibians. They possess similar nuclear hormone receptors, corepressors, coactivators, and TH-responsive elements on TH-responsive genes (Sachs and Buchholz, 2017). In both groups, the synthesis, transport and metabolism of TH molecules is carefully coordinated to ensure a successful transition between an aquatic and semiterrestrial environment. Perinatal mammals and amphibians undergo comparable developmental events in response to TH, including lung maturation, intestinal remodelling, and a switch from embryonic to adult keratins (Buchholz, 2015; Sachs and Buchholz, 2017). TH is the only signal required to prompt the metamorphosis from tadpole to froglet in amphibians. As amphibians undergo drastic developmental changes in virtually every tissue in response to exogenous TH, metamorphosis has been used to model TH signalling. Considerable attention has been paid to the initiation of TH signalling, to better understand how TH alone can induce a diverse set of response programs which must be carefully coordinated for healthy postembryonic development.

The metamorphosis of the American bullfrog, *Rana catesbeiana*, is influenced by temperature as well as TH. As temperatures decrease, the rate of metamorphosis also decreases. At cold temperatures of 4-5 °C, metamorphosis halts and does not occur even in the presence of exogenous THs that should otherwise prompt it (Ashley et al., 1968; Frieden et al., 1965). However, the TH signal is not lost. Once tadpoles are returned to warmer temperatures, they undergo metamorphosis at an accelerated rate. Tadpoles undergo metamorphosis 40 days after their initial TH exposure, long after the hormones have been excreted (Frieden et al., 1965). Therefore, tadpoles retain a “molecular memory” of their exposure to TH molecules. The molecular memory is capable of establishing and retaining a TH signal without inducing metamorphosis and is sufficient to prompt tadpoles to undergo an augmented TH response at a later point in time. Temperature inherently stratifies the initiation of TH signalling from the execution of the metamorphic program in *R. catesbeiana*. The molecular memory thus provides a unique opportunity to study the early events of TH signalling.

Herein, we investigated the molecular memory of cultured tadpole back skin (C-Skin), a tissue that undergoes extensive remodelling in response to TH. During metamorphosis, tadpole skin is transformed from a three-layer epidermis analogous to the mammalian periderm, to a froglet epidermis and dermis analogous to that of other terrestrial vertebrates (Brown and Cai, 2007). THs continue to be essential to skin homeostasis in adult humans. Thyroid disorders such as Graves’ disease and thyroiditis are associated with skin conditions such as alopecia, dermatitis, and eczema (Mancino et al., 2021). We hypothesized that transcripts encoding transcription factors expressed at cold temperatures were a component of the molecular memory in the back skin.

Thibz, an early response transcript, was found to be TH-responsive in C-Skin at cold temperatures, which diverges with previous research suggesting the expression of this transcript is not organ autonomous in C-Skin (Hammond et al., 2016). To date, *thibz* is the sole transcript found to be consistently TH-responsive in multiple tadpole tissues, including liver, lung, back skin, tailfin, and C-Fin (Hammond et al., 2016; Hammond et al., 2015). *Thibz* is notable as it is highly TH-responsive in both *R. catesbeiana* and *X. laevis* (Hammond et al., 2015). Transgenic *X. laevis* bearing a fluorescent TH/bZIP-GFP construct have used to identify disruptions in TH signalling by measuring GFP fluorescence (Fini et al., 2007; Li et al., 2022). Changes in *thibz* expression were detectable in response to 1 nM T_3 within the first 24 hours of exposure in premetamorphic *X. laevis* tadpoles (Li et al., 2022). *Thibz* has been used as an endpoint to identify the TH disrupting effects of bisphenol A, as well as 15 common chemicals found in human amniotic fluid (Fini et al., 2007; Fini et al., 2017). A short-term, 72 h exposure to these endocrine disrupting chemicals was found to measurably alter *thibz* expression, as well as TH-dependent transcription, gene expression, and brain development in *X. laevis* (Fini et al., 2017). As TH signalling is conserved amongst vertebrates, exposure to excess exogenous TH or TH disrupting chemicals could have adverse effects on both amphibian and mammalian postembryonic development (Abdelouahab et al., 2013; Fini et al., 2017). *Thibz* is TH-responsive, and its' expression has been used to identify disruptions of TH signalling in *X. laevis* (Li et al., 2022). *Thibz* may play a role in initiating TH signalling when molecular memory is established. (Hammond et al., 2016). Further research is warranted to discover the role of this putative transcription factor in TH signalling in amphibians.

RNA interference (RNAi) is a technique for gene silencing by targeting select mRNAs for degradation. RNAi has been used to knock down the expression of individual genes in cell culture (Han, 2018). RNAi by short interfering RNA (siRNAs) can knock down mRNA abundance by degrading mRNA in a sequence-specific manner dependent on complementary binding of the target mRNA (Wittrup and Lieberman, 2015). siRNA-mediated mRNA knockdown has recently been established in precision-cut mouse lung tissue slices cultured in media for 96 h (Ruigrok et al., 2018). Similar to organ culture biopsies, lung tissue explants are cultured *ex vivo* and maintain their cell heterogeneity and some of their higher-level structure (de Graaf et al., 2010). An exploration of siRNA mediated knockdown of *thibz* could aid in elucidating if *thibz* and other transcripts encoding transcription factors are components of molecular memory essential for establishing TH signalling. Specifically targeting *thibz* mRNA for degradation would also prevent future expression or accumulation of the thibz protein, which is useful in investigating its functionality as a transcription factor in molecular memory (Ruigrok et al., 2018). Targeted chromatin immunoprecipitation followed by massive parallel sequencing analysis (ChIP-Seq) could also shed light on the action of the TH/bZIP protein (Barski and Zhao, 2009; Nakato and Shirahige, 2016) . ChIP-Seq could identify interactions between specific DNA and the putative transcription factor encoded by *thibz* at temperatures that do not permit metamorphosis (Barski and Zhao, 2009).

Gene Ontology analysis provided a broad overview of the TH-response in the temperature shift condition, which was substantially enriched for terms relating to transcription factors and DNA binding. Our research suggests that transcription factors play an

important role in the accelerated response of the back skin. On the other hand, we found that transcripts encoding transcription factors were not the only significantly changed transcripts in the back skin under cold conditions. The transcripts encoding transcription factors in C-Skin (other than *thibz*) had no overlap with those previously identified in the C-Fin (Koide et al., 2022). This may suggest that the early initiation of TH signalling has tissue-specificity. There were also substantial increases in abundance for several transcripts associated with chromatin remodelling, the formation of heterogenous ribonucleoprotein complexes, and other post-transcriptional modifications that alter mRNA stability. These transcripts may shed light on possible alternate mechanisms of establishing a TH signal under cold temperature conditions which do not permit metamorphosis.

Previous research by Koide et al., 2022 noted that active transcription and translation was not required for the induction of all transcripts in the C-Fin. *Thibz* underwent significant abundance changes in TH at 4 °C which were not inhibited by inhibitors of transcription and translation. Transcript abundance is determined by the ratio of mRNA synthesis to decay. mRNA half-life can be impacted by the secondary and tertiary structure of its own nucleotide sequence, as well as elements such as the 5' cap and poly A tail (Boo and Kim, 2020; Jalkanen et al., 2014). In addition, mRNA can undergo a wide variety of post-transcriptional modifications that alter stability as well as storage into RNA granules (Peer et al., 2017; Tian et al., 2020). Current research suggests that alterations in mRNA stability may play an important role in tightly coordinating gene expression (Boo and Kim, 2020). Studies of estrogen, testosterone, and TH have demonstrated the ability of hormones to influence mRNA stability, and consequently transcript abundance (Park et al., 1996; Qian et al., 1993; Trojanowicz et al., 2011).

The HPT axis can repress gene expression associated with TH signalling. Current research suggests that the negative feedback loop that regulates TH production may also include post-transcriptional modifications to mRNA. TH destabilizes *thyroid stimulating hormone subunit beta (tshb)* mRNA; TH interacts non-genomically with the integrin αVβ3 membrane receptor to reduce length the poly (A) tail, thereby decreasing *tshb's* half-life (Bargi-Souza et al., 2018; Krane et al., 1991). In rats, TH increases the stability of uncoupling protein-1 and acetylcholinesterase mRNA, the latter possibly by phosphorylation (Guerra et al., 1996; Puymirat et al., 1995). In rat brain and neuronal cell culture, TH decreases the transcription rate of the mRNA stability regulator HuD. As HuD post-transcriptionally mediates the expression of many genes associated with neurodevelopment, TH may be able to regulate multiple processes by repressing genes associated with mRNA stability (Cuadrado et al., 2003).

The increases in *thibz* abundance without active transcription potentially suggests that TH influences mRNA stability at cold temperatures. It is currently unknown what post-transcriptional changes could impact the stability, and therefore the abundance, of TH-responsive transcripts under cold temperatures. Investigation into the half-life of *thibz* mRNA under different temperature conditions is warranted. Modifications to transcript stability may aid in retaining the TH signal. Several putative components of the molecular memory in C-Skin potentially possessed post-transcriptional modification activity, which provides another interesting avenue for investigation (Figure 17).

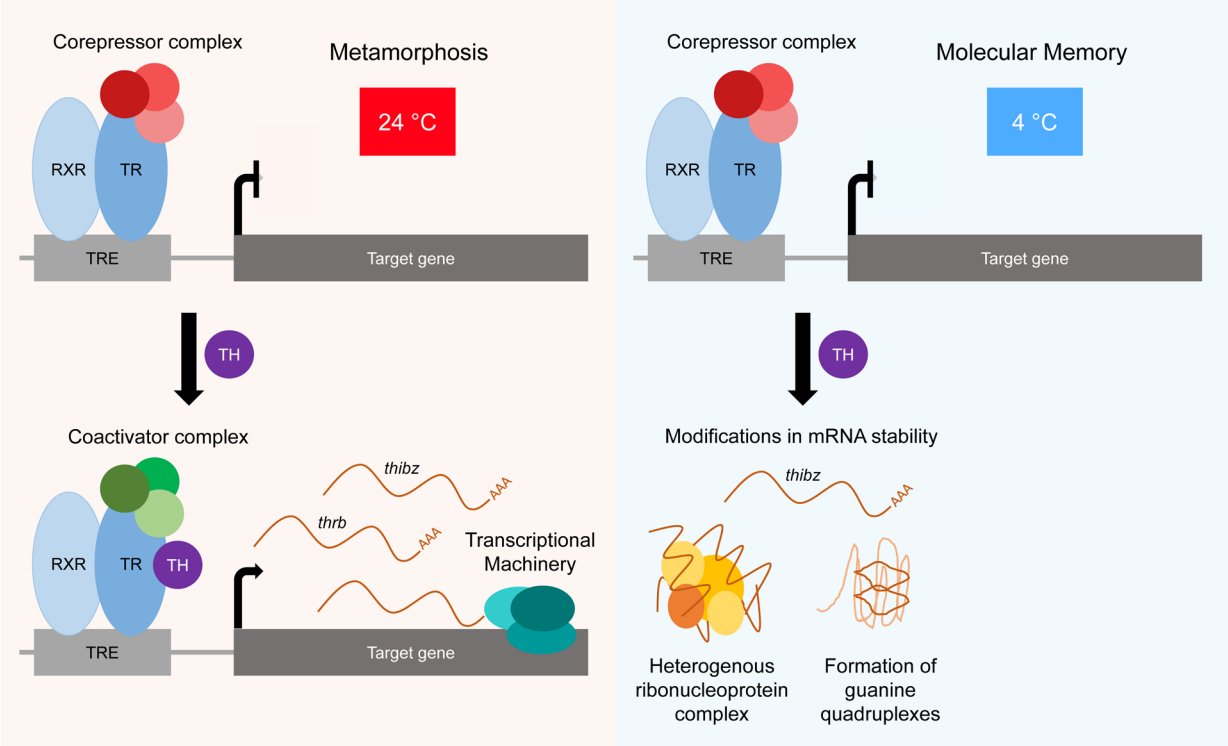

Figure 17. Alternative mechanisms of TH signaling at different temperatures. Multiple mechanisms may be at play in regulating transcript abundance in response to TH at different temperatures. At warm temperatures of 24 °C, TH induces primarily genome signalling that prompts the active transcription of transcripts such as thrb, and subsequent downstream response programs. At cold temperatures of 4 °C, changes in mRNA stability may possibility aid in retaining the TH signal and establishing the molecular memory. Adapted from Koide et al., 2022.

Exposure to TH at cold temperatures is sufficient to retain a TH signal and prompt an accelerated metamorphic program once temperatures rise. Multiple mechanisms may be at play in the response to TH at different temperatures (Koide et al., 2022). In cold temperatures, TH may modulate mRNA stability to influence the abundance of transcripts such as *thibz* to establish a TH signal without executing metamorphosis. At warm temperatures, TH induces genomic signalling that prompts the expression of transcripts such as *thrb*, and subsequent response programs. TH signalling is complex and involves an interplay of genomic and nongenomic signalling, epigenetic modifications and T_3- and T_4- specific coregulators. All these factors could facilitate the temperature-specific action of TH and contribute to the molecular memory and accelerated response. These mechanisms could also be tissue-specific, as this research shows differences in the transcriptomic responses of C-Skin and C-Fin even during the initiation of TH signalling at cold temperatures. Further research is needed to understand the mechanisms that contribute to molecular memory and the accelerated metamorphic response.

Amphibian metamorphosis has often been used as a model for how TH prompts complex developmental programs in many different tissues. Temperature can be used to stratify the initiation of a TH signal from the execution of metamorphosis in *R. catesbeiana*

tadpoles. The molecular memory provides a unique opportunity to study the initiation of TH signalling which is crucial in coordinating a diverse set of response programs. The TH response in *R. catesbeiana* likely requires multiple modes of gene regulation at different temperatures. Further research is needed to investigate the mechanisms of the molecular memory and the induction of TH signalling.

As TH is essential for postembryonic development in all vertebrates, understanding the early mechanisms of TH signalling is incredibly valuable. Disruptions in TH signalling during postembryonic development can be incredibly detrimental to neurological and physical health. For amphibians, metamorphosis may also be a period of development which is especially vulnerable to climate fluctuations (Narayan et al., 2019). Environmental cues such as temperature aid in regulating the initiation, timing, and duration of metamorphosis. Metamorphosis is energetically costly, and individuals in a transitional state are often ill-suited for both their larval and adult habitats (Lowe et al., 2021). For example, tadpoles of the tree frog *Hyla pseudopuma* are more susceptible to aquatic and terrestrial predators at their metamorphic climax (Crump, 1984). Changes in the timing and duration of metamorphosis could subsequently affect food availability, predation risk, and mortality (Lowe et al., 2021; Wilbur and Collins, 1973). Subsequently, climate variability may have disproportionately strong impacts on the overall survival and fitness of species which undergo metamorphosis (Lowe et al., 2021). The metamorphosis of *R. catesbeiana* is tightly regulated by both THs and temperature cues to ensure a successful, coordinated life-stage transition. A better understanding of temperature-dependent TH signalling in *R. catesbeiana* could provide valuable insight into the potential impacts of exogenous THs and temperate fluctuations in a time of increasing climate variability.

5 References

Abdelouahab, N., Langlois, M.-F., Lavoie, L., Corbin, F., Pasquier, J.-C., and Takser, L. (2013). Maternal and Cord-Blood Thyroid Hormone Levels and Exposure to Polybrominated Diphenyl Ethers and Polychlorinated Biphenyls During Early Pregnancy. American Journal of Epidemiology *178*, 701-713.

Aicha, S.B., Lessard, J., Pelletier, M., Fournier, A., Calvo, E., and Labrie, C. (2007). Transcriptional profiling of genes that are regulated by the endoplasmic reticulum-bound transcription factor AIbZIP/CREB3L4 in prostate cells. Physiological Genomics *31*, 295-305.

Allen, B.M. (1925). The effects of extirpation of the thyroid and pituitary glands upon the limb development of anurans. Journal of Experimental Zoology *42*, 13-30.

Armas, P., Cabada, M.O., and Calcaterra, N.B. (2001). Primary structure and developmental expression of *Bufo arenarum* cellular nucleic acid-binding protein: Changes in subcellular localization during early embryogenesis. Development, Growth & Differentiation *43*, 13-23.

Armas, P., Coux, G., Weiner, A.M.J., and Calcaterra, N.B. (2021). What's new about CNBP? Divergent functions and activities for a conserved nucleic acid binding protein. Biochimica et Biophysica Acta (BBA) - General Subjects *1865*, 129996.

Armas, P., Nasif, S., and Calcaterra, N.B. (2008). Cellular nucleic acid binding protein binds G-rich single-stranded nucleic acids and may function as a nucleic acid chaperone. Journal of Cellular Biochemistry *103*, 1013-1036.

Asada, R., Kanemoto, S., Kondo, S., Saito, A., and Imaizumi, K. (2011). The signalling from endoplasmic reticulum-resident bZIP transcription factors involved in diverse cellular physiology. The Journal of Biochemistry *149*, 507-518.

Ashley, H., Katti, P., and Frieden, E. (1968). Urea excretion in the bullfrog tadpole: effect of temperature, metamorphosis, and thyroid hormones. Developmental Biology *17*, 293-307.

Aslam, M., Fakher, B., Jakada, B.H., Cao, S., and Qin, Y. (2019). SWR1 Chromatin Remodeling Complex: A Key Transcriptional Regulator in Plants. Cells *8*, 1621.

Bagamasbad, P., Howdeshell, K.L., Sachs, L.M., Demeneix, B.A., and Denver, R.J. (2008). A role for basic transcription element-binding protein 1 (BTEB1) in the autoinduction of thyroid hormone receptor β. Journal of Biological Chemistry *283*, 2275-2285.

Bargi-Souza, P., Goulart-Silva, F., and Nunes, M.T. (2018). Posttranscriptional actions of triiodothyronine on Tshb expression in TαT1 cells: New insights into molecular mechanisms of negative feedback. Molecular and Cellular Endocrinology *478*, 45-52.

Barski, A., and Zhao, K. (2009). Genomic location analysis by ChIP-Seq. Journal of Cellular Biochemistry *107*, 11-18.

Beaudoin, J.-D., and Perreault, J.-P. (2013). Exploring mRNA 3'-UTR G-quadruplexes: evidence of roles in both alternative polyadenylation and mRNA shortening. Nucleic Acids Research *41*, 5898-5911.

Benhalevy, D., Gupta, S.K., Danan, C.H., Ghosal, S., Sun, H.-W., Kazemier, H.G., Paeschke, K., Hafner, M., and Juranek, S.A. (2017). The Human CCHC-type Zinc Finger Nucleic Acid-Binding Protein Binds G-Rich Elements in Target mRNA Coding Sequences and Promotes Translation. Cell Reports *18*, 2979-2990.

Berry, D.L., Rose, C.S., Remo, B.F., and Brown, D.D. (1998). The Expression Pattern of Thyroid Hormone Response Genes in Remodeling Tadpole Tissues Defines Distinct Growth and Resorption Gene Expression Programs. Developmental Biology *203*, 24-35.

Bianco, A.C., and Kim, B.W. (2006). Deiodinases: implications of the local control of thyroid hormone action. The Journal of Clinical Investigation *116*, 2571-2579.

Bianco, A.C., Salvatore, D., Gereben, B.z., Berry, M.J., and Larsen, P.R. (2002). Biochemistry, Cellular and Molecular Biology, and Physiological Roles of the Iodothyronine Selenodeiodinases. Endocrine Reviews *23*, 38-89.

Boo, S.H., and Kim, Y.K. (2020). The emerging role of RNA modifications in the regulation of mRNA stability. Experimental & Molecular Medicine *52*, 400-408.

Brown, D.D. (2005). The role of deiodinases in amphibian metamorphosis. Thyroid *15*, 815-821.

Brown, D.D., and Cai, L. (2007). Amphibian metamorphosis. Developmental Biology *306*, 20-33.

Bryant, D.M., Johnson, K., DiTommaso, T., Tickle, T., Couger, M.B., Payzin-Dogru, D., Lee, T.J., Leigh, N.D., Kuo, T.-H., and Davis, F.G. (2017). A tissue-mapped axolotl *de novo* transcriptome enables identification of limb regeneration factors. Cell reports *18*, 762-776.

Buchholz, D.R. (2015). More similar than you think: Frog metamorphosis as a model of human perinatal endocrinology. Developmental Biology *408*, 188-195.

Buchholz, D.R., Paul, B.D., Fu, L., and Shi, Y.-B. (2006). Molecular and developmental analyses of thyroid hormone receptor function in *Xenopus laevis*, the African clawed frog. General and Comparative Endocrinology *145*, 1-19.

Bugaut, A., and Balasubramanian, S. (2012). 5'-UTR RNA G-quadruplexes: translation regulation and targeting. Nucleic Acids Research *40*, 4727-4741.

Burrow, G.N., Fisher, D.A., and Larsen, P.R. (1994). Maternal and Fetal Thyroid Function. New England Journal of Medicine *331*, 1072-1078.

Cabili, M.N., Trapnell, C., Goff, L., Koziol, M., Tazon-Vega, B., Regev, A., and Rinn, J.L. (2011). Integrative annotation of human large intergenic noncoding RNAs reveals global properties and specific subclasses. Genes Dev *25*, 1915-1927.

Cai, L., and Brown, D.D. (2004). Expression of type II iodothyronine deiodinase marks the time that a tissue responds to thyroid hormone-induced metamorphosis in *Xenopus laevis*. Developmental Biology *266*, 87-95.

Calo, E., Flynn, R.A., Martin, L., Spitale, R.C., Chang, H.Y., and Wysocka, J. (2015). RNA helicase DDX21 coordinates transcription and ribosomal RNA processing. Nature *518*, 249-253.

Cao, J., Wu, N., Han, Y., Hou, Q., Zhao, Y., Pan, Y., Xie, X., and Chen, F. (2018). DDX21 promotes gastric cancer proliferation by regulating cell cycle. Biochemical and Biophysical Research Communications *505*, 1189-1194.

Cecil, S.G., and Just, J.J. (1979). Survival rate, population density and development of a naturally occurring anuran larvae (*Rana catesbeiana*). Copeia, 447-453.

Chaudhury, A., Chander, P., and Howe, P.H. (2010). Heterogeneous nuclear ribonucleoproteins (hnRNPs) in cellular processes: Focus on hnRNP E1's multifunctional regulatory roles. Rna *16*, 1449-1462.

Chen, Z., Li, Z., Hu, X., Xie, F., Kuang, S., Zhan, B., Gao, W., Chen, X., Gao, S., Li, Y.*, et al.* (2020). Structural Basis of Human Helicase DDX21 in RNA Binding, Unwinding, and Antiviral Signal Activation. Advanced Science *7*, 2000532.

Choi, J., Suzuki, K.-i.T., Sakuma, T., Shewade, L., Yamamoto, T., and Buchholz, D.R. (2015). Unliganded Thyroid Hormone Receptor α Regulates Developmental Timing via Gene Repression in *Xenopus tropicalis*. Endocrinology *156*, 735-744.

Corrie, L.M., Kempe, M.N., Blajkevitch, O., Shang, D., and Helbing, C.C. (2021). Dioctyl Sodium Sulfosuccinate as a Potential Endocrine Disruptor of Thyroid Hormone Activity in American bullfrog, *Rana (Lithobates) catesbeiana*, Tadpoles. Archives of Environmental Contamination and Toxicology *80*, 726-734.

Crump, M.L. (1984). Ontogenetic changes in vulnerability to predation in tadpoles of *Hyla pseudopuma*. Herpetologica, 265-271.

Cuadrado, A., Navarro-Yubero, C., Furneaux, H., and Muñoz, A. (2003). Neuronal HuD gene encoding a mRNA stability regulator is transcriptionally repressed by thyroid hormone. Journal of Neurochemistry *86*, 763-773.

Das, B., Heimeier, R.A., Buchholz, D.R., and Shi, Y.-B. (2009). Identification of direct thyroid hormone response genes reveals the earliest gene regulation programs during frog metamorphosis. Journal of Biological Chemistry *284*, 34167-34178.

David, A.P., Pipier, A., Pascutti, F., Binolfi, A., Weiner, A.M J., Challier, E., Heckel, S., Calsou, P., Gomez, D., Calcaterra, N.B.*, et al.* (2019). CNBP controls transcription by unfolding DNA G-quadruplex structures. Nucleic Acids Research *47*, 7901-7913.

Davis, P.J., Leonard, J.L., and Davis, F.B. (2008). Mechanisms of nongenomic actions of thyroid hormone. Frontiers in Neuroendocrinology *29*, 211-218.

Davis, P.J., Shih, A., Lin, H.-Y., Martino, L.J., and Davis, F.B. (2000). Thyroxine Promotes Association of Mitogen-activated Protein Kinase and Nuclear Thyroid Hormone Receptor (TR) and Causes Serine Phosphorylation of TR*. Journal of Biological Chemistry *275*, 38032-38039.

Davis, R.S. (2007). Fc receptor-like molecules. Annu Rev Immunol *25*, 525-560.

Davis, W. (2011). The ATP-binding cassette transporter-2 (ABCA2) regulates cholesterol homeostasis and low-density lipoprotein receptor metabolism in N2a neuroblastoma cells. Biochimica et Biophysica Acta (BBA) - Molecular and Cell Biology of Lipids *1811*, 1152-1164.

de Graaf, I.A.M., Olinga, P., de Jager, M.H., Merema, M.T., de Kanter, R., van de Kerkhof, E.G., and Groothuis, G.M.M. (2010). Preparation and incubation of precision-cut liver and intestinal slices for application in drug metabolism and toxicity studies. Nature Protocols *5*, 1540-1551.

Denver, R.J. (2013). Chapter Seven - Neuroendocrinology of Amphibian Metamorphosis. In Current Topics in Developmental Biology, Y.-B. Shi, ed. (Academic Press), pp. 195-227.

Denver, R.J., and Williamson, K.E. (2009). Identification of a Thyroid Hormone Response Element in the Mouse Krüppel-Like Factor 9 Gene to Explain Its Postnatal Expression in the Brain. Endocrinology *150*, 3935-3943.

Dobin, A., Davis, C.A., Schlesinger, F., Drenkow, J., Zaleski, C., Jha, S., Batut, P., Chaisson, M., and Gingeras, T.R. (2013). STAR: ultrafast universal RNA-seq aligner. Bioinformatics *29*, 15-21.

Femia, M.R., Evans, R.M., Zhang, J., Sun, X., Lebegue, C.J., Roggero, V.R., and Allison, L.A. (2020). Mediator subunit MED1 modulates intranuclear dynamics of the thyroid hormone receptor. J Cell Biochem *121*, 2909-2926.

Fini, J.-B., Le Mével, S., Turque, N., Palmier, K., Zalko, D., Cravedi, J.-P., and Demeneix, B.A. (2007). An *In Vivo* Multiwell-Based Fluorescent Screen for Monitoring Vertebrate Thyroid Hormone Disruption. Environmental Science & Technology *41*, 5908-5914.

Fini, J.-B., Mughal, B.B., Le Mével, S., Leemans, M., Lettmann, M., Spirhanzlova, P., Affaticati, P., Jenett, A., and Demeneix, B.A. (2017). Human amniotic fluid contaminants alter thyroid hormone signalling and early brain development in *Xenopus* embryos. Scientific Reports *7*, 43786.

Forhead, A.J., and Fowden, A.L. (2014). Thyroid hormones in fetal growth and prepartum maturation. Journal of Endocrinology *221*, R87-R103.

Frieden, E., Wahlborg, A., and Howard, E. (1965). Temperature control of the response of tadpoles to triiodothyronine. Nature *205*, 1173-1176.

Furlow, J.D., Berry, D.L., Wang, Z., and Brown, D.D. (1997). A set of novel tadpole specific genes expressed only in the epidermis are down-regulated by thyroid hormone during *Xenopus laevis* metamorphosis. Developmental Biology *182*, 284-298.

Furlow, J.D., and Kanamori, A. (2002). The transcription factor basic transcription element-binding protein 1 is a direct thyroid hormone response gene in the frog *Xenopus laevis.* Endocrinology *143*, 3295-3305.

Gao, N., Li, Y., Li, J., Gao, Z., Yang, Z., Li, Y., Liu, H., and Fan, T. (2020). Long Non-Coding RNAs: The Regulatory Mechanisms, Research Strategies, and Future Directions in Cancers. Frontiers in Oncology *10*.

Gilbert, L. (2013). Metamorphosis: a problem in developmental biology (Springer Science & Business Media).

Gilbert, L.I., Tata, J.R., and Atkinson, B.G. (1996). Metamorphosis: postembryonic reprogramming of gene expression in amphibian and insect cells (Academic Press).

Gilbert, M.E., Rovet, J., Chen, Z., and Koibuchi, N. (2012). Developmental thyroid hormone disruption: Prevalence, environmental contaminants and neurodevelopmental consequences. NeuroToxicology *33*, 842-852.

Grimaldi, A., Buisine, N., Miller, T., Shi, Y.-B., and Sachs, L.M. (2013). Mechanisms of thyroid hormone receptor action during development: lessons from amphibian studies. Biochimica et Biophysica Acta (BBA)-General Subjects *1830*, 3882-3892.

Gudernatsch, J.F. (1912). Feeding experiments on tadpoles. Archiv für Entwicklungsmechanik der Organismen *35*, 457-483.

Guerra, C., Roncero, C., Porras, A., Fernández, M., and Benito, M. (1996). Triiodothyronine Induces the Transcription of the Uncoupling Protein Gene and Stabilizes Its mRNA in Fetal Rat Brown Adipocyte Primary Cultures (∗). Journal of Biological Chemistry *271*, 2076-2081.

Guo, P., Dong, X.-Y., Zhao, K.-W., Sun, X., Li, Q., and Dong, J.-T. (2010). Estrogen-induced interaction between KLF5 and estrogen receptor (ER) suppresses the function of ER in ER-positive breast cancer cells. International Journal of Cancer *126*, 81-89.

Hahm, J.B., and Privalsky, M.L. (2013). Research Resource: Identification of Novel Coregulators Specific for Thyroid Hormone Receptor-β2. Molecular Endocrinology *27*, 840-859.

Hammond, S.A., Carew, A., and Helbing, C. (2013). Evaluation of the effects of titanium dioxide nanoparticles on cultured *Rana catesbeiana t*ailfin tissue. Frontiers in Genetics *4*, 251.

Hammond, S.A., Jackman, K.W., Partovi, S.H., Veldhoen, N., and Helbing, C.C. (2016). Identification of organ-autonomous constituents of the molecular memory conferred by thyroid hormone exposure in cold temperature-arrested metamorphosing *Rana (Lithobates) catesbeiana* tadpoles. Comparative Biochemistry and Physiology Part D: Genomics and Proteomics *17*, 58-65.

Hammond, S.A., Veldhoen, N., and Helbing, C.C. (2015). Influence of temperature on thyroid hormone signaling and endocrine disruptor action in *Rana (Lithobates) catesbeiana* tadpoles. General and Comparative Endocrinology *219*, 6-15.

Hammond, S.A., Warren, R.L., Vandervalk, B.P., Kucuk, E., Khan, H., Gibb, E.A., Pandoh, P., Kirk, H., Zhao, Y., and Jones, M. (2017). The North American bullfrog draft genome provides insight into hormonal regulation of long noncoding RNA. Nature Communications *8*, 1-8.

Han, H. (2018). RNA interference to knock down gene expression in disease gene identification: Methods and Protocols, J.K. DiStefano, ed. (New York, NY: Springer New York), pp. 293-302.

Hill, C.S. (2016). Transcriptional Control by the SMADs. Cold Spring Harb Perspect Biol *8*.

Hinther, A., Domanski, D., Vawda, S., and Helbing, C.C. (2010). C-fin: A cultured frog tadpole tail fin biopsy approach for detection of thyroid hormone-disrupting chemicals. Environmental Toxicology and Chemistry *29*, 380-388.

Hirahara, N., Nakamura, H.M., Sasaki, S., Matsushita, A., Ohba, K., Kuroda, G., Sakai, Y., Shinkai, S., Haeno, H., and Nishio, T. (2020). Liganded T3 receptor β2 inhibits the positive feedback autoregulation of the gene for GATA2, a transcription factor critical for thyrotropin production. PloS one *15*, e0227646.

Hoopfer, E.D., Huang, L., and Denver, R.J. (2002). Basic transcription element binding protein is a thyroid hormone-regulated transcription factor expressed during metamorphosis in *Xenopus laevis*. Development, growth & differentiation *44*, 365-381.

Hung, L.H., Heiner, M., Hui, J., Schreiner, S., Benes, V., and Bindereif, A. (2008). Diverse roles of hnRNP L in mammalian mRNA processing: a combined microarray and RNAi analysis. Rna *14*, 284-296.

Ishihara, A., Sapon, M.A., and Yamauchi, K. (2019). Seasonal acclimatization and thermal acclimation induce global histone epigenetic changes in liver of bullfrog *(Lithobates catesbeianus)* tadpole. Comparative Biochemistry and Physiology Part A: Molecular & Integrative Physiology *230*, 39-48.

Ishizuya-Oka, A. (2011). Amphibian organ remodeling during metamorphosis: Insight into thyroid hormone-induced apoptosis. Development, Growth & Differentiation *53*, 202-212.

Ishizuya-Oka, A., Hasebe, T., and Shi, Y.-B. (2010). Apoptosis in amphibian organs during metamorphosis. Apoptosis *15*, 350-364.

Jackman, K.W., Veldhoen, N., Miliano, R.C., Robert, B.J., Li, L., Khojasteh, A., Zheng, X., Zaborniak, T.S.M., van Aggelen, G., Lesperance, M.*, et al.* (2018). Transcriptomics investigation of thyroid hormone disruption in the olfactory system of the *Rana [Lithobates] catesbeiana* tadpole. Aquatic Toxicology *202*, 46-56.

Jafarifar, F., Yao, P., Eswarappa, S.M., and Fox, P.L. (2011). Repression of VEGFA by CA-rich element-binding microRNAs is modulated by hnRNP L. The EMBO Journal *30*, 1324-1334.

Jalkanen, A.L., Coleman, S.J., and Wilusz, J. (2014). Determinants and implications of mRNA poly(A) tail size – Does this protein make my tail look big? Seminars in Cell & Developmental Biology *34*, 24-32.

Ji, L., Domanski, D., Skirrow, R., and Helbing, C. (2007). Genistein prevents thyroid hormone-dependent tail regression of *Rana catesbeiana* tadpoles by targetting protein kinase C and thyroid hormone receptor α. Developmental Dynamics: An Official Publication of the American Association of Anatomists *236*, 777-790.

Kada, N., Suzuki, T., Aizawa, K., Munemasa, Y., Matsumura, T., Sawaki, D., and Nagai, R. (2008). Acyclic retinoid inhibits functional interaction of transcription factors Krüppel-like factor 5 and retinoic acid receptor-alpha. FEBS Letters *582*, 1755-1760.

Kim, H.-Y., and Mohan, S. (2013). Role and Mechanisms of Actions of Thyroid Hormone on the Skeletal Development. Bone Research *1*, 146-161.

Koide, E.M., Abbott, E.A., and Helbing, C.C. (2022). Uncovering early thyroid hormone signalling events through temperature-mediated activation of molecular memory in the cultured bullfrog tadpole tail fin. General and Comparative Endocrinology *323-324*, 114047.

Krane, I.M., Spindel, E.R., and Chin, W.W. (1991). Thyroid Hormone Decreases the Stability and the Poly(A) Tract Length of Rat Thyrotropin β-Subunit Messenger RNA. Molecular Endocrinology *5*, 469-475.

Lee, E., Lee, T.A., Kim, J.H., Park, A., Ra, E.A., Kang, S., Choi, H.j., Choi, J.L., Huh, H.D., Lee, J.E*., et al.* (2017). CNBP acts as a key transcriptional regulator of sustained expression of interleukin-6. Nucleic Acids Research *45*, 3280-3296.

Lee, S., and Privalsky, M.L. (2005). Heterodimers of Retinoic Acid Receptors and Thyroid Hormone Receptors Display Unique Combinatorial Regulatory Properties. Molecular Endocrinology *19*, 863-878.

Li, J., Li, Y., Zhu, M., Song, S., and Qin, Z. (2022). A Multiwell-Based Assay for Screening Thyroid Hormone Signaling Disruptors Using thibz Expression as a Sensitive Endpoint in *Xenopus laevis.* Molecules *27*.

Linder, P., and Jankowsky, E. (2011). From unwinding to clamping — the DEAD box RNA helicase family. Nature Reviews Molecular Cell Biology *12*, 505-516.

Loh, T.J., Cho, S., Moon, H., Jang, H.N., Williams, D.R., Jung, D.-W., Kim, I.-C., Ghigna, C., Biamonti, G., Zheng, X*., et al.* (2015). hnRNP L inhibits CD44 V10 exon splicing through interacting with its upstream intron. Biochimica et Biophysica Acta (BBA) - Gene Regulatory Mechanisms *1849*, 743-750.

Love, M.I., Huber, W., and Anders, S. (2014). Moderated estimation of fold change and dispersion for RNA-seq data with DESeq2. Genome biology *15*, 1-21.

Lowe, W.H., Martin, T.E., Skelly, D.K., and Woods, H.A. (2021). Metamorphosis in an Era of Increasing Climate Variability. Trends in Ecology & Evolution *36*, 360-375.

Luo, M., Ma, W., Sand, Z., Finlayson, J., Wang, T., Brinton, R.D., Willis, W.T., and Mandarino, L.J. (2020). Von Willebrand factor A domain-containing protein 8 (VWA8) localizes to the matrix side of the inner mitochondrial membrane. Biochemical and Biophysical Research Communications *521*, 158-163.

Luo, M., Mengos, A.E., Ma, W., Finlayson, J., Bustos, R.Z., Xiao Zhu, Y., Shi, C.-X., Stubblefield, T.M., Willis, W.T., and Mandarino, L.J. (2017). Characterization of the novel protein KIAA0564

(Von Willebrand Domain-containing Protein 8). Biochemical and Biophysical Research Communications *487*, 545-551.

Maher, S.K., Wojnarowicz, P., Ichu, T.-A., Veldhoen, N., Lu, L., Lesperance, M., Propper, C.R., and Helbing, C.C. (2016). Rethinking the biological relationships of the thyroid hormones, l-thyroxine and 3,5,3'-triiodothyronine. Comparative Biochemistry and Physiology Part D: Genomics and Proteomics *18*, 44-53.

Mancino, G., Miro, C., Di Cicco, E., and Dentice, M. (2021). Thyroid hormone action in epidermal development and homeostasis and its implications in the pathophysiology of the skin. Journal of Endocrinological Investigation *44*, 1571-1579.

Mangelsdorf, D.J., Thummel, C., Beato, M., Herrlich, P., Schütz, G., Umesono, K., Blumberg, B., Kastner, P., Mark, M., Chambon, P*., et al.* (1995). The nuclear receptor superfamily: The second decade. Cell *83*, 835-839.

Manzon, R.G., and Manzon, L.A. (2017). Lamprey metamorphosis: thyroid hormone signaling in a basal vertebrate. Molecular and Cellular Endocrinology *459*, 28-42.

Matsuda, H., Paul, B.D., Choi, C.Y., Hasebe, T., and Shi, Y.-B. (2009). Novel Functions of Protein Arginine Methyltransferase 1 in Thyroid Hormone Receptor-Mediated Transcription and in the Regulation of Metamorphic Rate in *Xenopus laevis*. Molecular and Cellular Biology *29*, 745-757.

Mattera, L., Courilleau, C., Legube, G., Ueda, T., Fukunaga, R., Chevillard-Briet, M., Canitrot, Y., Escaffit, F., and Trouche, D. (2010). The E1A-Associated p400 Protein Modulates Cell Fate Decisions by the Regulation of ROS Homeostasis. PLOS Genetics *6*, e1000983.

McRae, E.K.S., Booy, E.P., Moya-Torres, A., Ezzati, P., Stetefeld, J., and McKenna, S.A. (2017). Human DDX21 binds and unwinds RNA guanine quadruplexes. Nucleic Acids Research *45*, 6656-6668.

McRae, E.K.S., Davidson, D.E., Dupas, S.J., and McKenna, S.A. (2018). Insights into the RNA quadruplex binding specificity of DDX21. Biochimica et Biophysica Acta (BBA) - General Subjects *1862*, 1973-1979.

Mirth, C., Saunders, T., and Amourda, C. (2021). Growing Up in a Changing World: Environmental Regulation of Development in Insects. Annual Review of Entomology *66*.

Mochizuki, K., Goda, T., and Yamauchi, K. (2012). Gene expression profile in the liver of *Rana catesbeiana* tadpoles exposed to low temperature in the presence of thyroid hormone. Biochemical and Biophysical Research Communications *420*, 845-850.

Moeller, L.C., Cao, X., Dumitrescu, A.M., Seo, H., and Refetoff, S. (2006). Thyroid hormone mediated changes in gene expression can be initiated by cytosolic action of the thyroid hormone receptor β through the phosphatidylinositol 3-kinase pathway. Nuclear Receptor Signaling *4*, nrs.04020.

Moeller, L.C., Dumitrescu, A.M., and Refetoff, S. (2005). Cytosolic Action of Thyroid Hormone Leads to Induction of Hypoxia-Inducible Factor-1α and Glycolytic Genes. Molecular Endocrinology *19*, 2955-2963.

Mullur, R., Liu, Y.-Y., and Brent, G.A. (2014). Thyroid Hormone Regulation of Metabolism. Physiological Reviews *94*, 355-382.

Murata, T., and Yamauchi, K. (2005). Low-Temperature Arrest of the Triiodothyronine-Dependent Transcription in *Rana catesbeiana* Red Blood Cells. Endocrinology *146*, 256-264.

Nakato, R., and Shirahige, K. (2016). Recent advances in ChIP-seq analysis: from quality management to whole-genome annotation. Briefings in Bioinformatics *18*, 279-290.

Narayan, E.J., Forsburg, Z.R., Davis, D.R., and Gabor, C.R. (2019). Non-invasive Methods for Measuring and Monitoring Stress Physiology in Imperiled Amphibians. Frontiers in Ecology and Evolution *7*.

Niehrs, C., and Luke, B. (2020). Regulatory R-loops as facilitators of gene expression and genome stability. Nature Reviews Molecular Cell Biology *21*, 167-178.

Nishikawa, A., Kaiho, M., and Yoshizato, K. (1989). Cell death in the anuran tadpole tail: thyroid hormone induces keratinization and tail-specific growth inhibition of epidermal cells. Dev Biol *131*, 337-344.

Nishikawa, A., and Yoshizato, K. (1986). Hormonal regulation of growth and life span of bullfrog tadpole tail epidermal cells cultured in vitro. J Exp Zool *237*, 221-230.

Nussey, S.S., and Whitehead, S.A. (2001). Endocrinology: an integrated approach.

Okada, R., Miller, M.F., Yamamoto, K., Groef, B.D., Denver, R.J., and Kikuyama, S. (2007). Involvement of the corticotropin-releasing factor (CRF) type 2 receptor in CRF-induced thyrotropin release by the amphibian pituitary gland. General and Comparative Endocrinology *150*, 437-444.

Park, D., Cheon, M., Kim, C., Kim, K., and Ryu, K. (1996). Progesterone together with estradiol promotes luteinizing hormone beta-subunit mRNA stability in rat pituitary cells cultured in vitro. Eur J Endocrinol *134*, 236-242.

Park, S.W., Li, G., Lin, Y.-P., Barrero, M.J., Ge, K., Roeder, R.G., and Wei, L.-N. (2005). Thyroid Hormone-Induced Juxtaposition of Regulatory Elements/Factors and Chromatin Remodeling of Crabp1 Dependent on MED1/TRAP220. Molecular Cell *19*, 643-653.

Paul, B.D., Buchholz, D.R., Fu, L., and Shi, Y.-B. (2007). SRC-p300 Coactivator Complex Is Required for Thyroid Hormone-induced Amphibian Metamorphosis*. Journal of Biological Chemistry *282*, 7472-7481.

Pearson, R., Fleetwood, J., Eaton, S., Crossley, M., and Bao, S. (2008). Krüppel-like transcription factors: A functional family. The International Journal of Biochemistry & Cell Biology *40*, 1996-2001.

Peer, E., Rechavi, G., and Dominissini, D. (2017). Epitranscriptomics: regulation of mRNA metabolism through modifications. Current Opinion in Chemical Biology *41*, 93-98.

Pellizzoni, L., Lotti, F., Maras, B., and Pierandrei-Amaldi, P. (1997). Cellular nucleic acid binding protein binds a conserved region of the 5′ UTR of *Xenopus laevis* ribosomal protein mRNAs. Edited by M. Yaniv. Journal of Molecular Biology *267*, 264-275.

Pertea, M., Pertea, G.M., Antonescu, C.M., Chang, T.-C., Mendell, J.T., and Salzberg, S.L. (2015). StringTie enables improved reconstruction of a transcriptome from RNA-seq reads. Nature biotechnology *33*, 290-295.

Pradhan, S.K., Su, T., Yen, L., Jacquet, K., Huang, C., Côté, J., Kurdistani, S.K., and Carey, M.F. (2016). EP400 Deposits H3.3 into Promoters and Enhancers during Gene Activation. Molecular Cell *61*, 27-38.

Puymirat, J., Etongue-Mayer, P., and Dussault, J.H. (1995). Thyroid Hormones Stabilize Acetylcholinesterase mRNA in Neuro-2A Cells That Overexpress the β1 Thyroid Receptor (∗). Journal of Biological Chemistry *270*, 30651-30656.

Qian, K., Franklin, R.B., and Costello, L.C. (1993). Testosterone regulates mitochondrial aspartate aminotransferase gene expression and mRNA stability in prostate. The Journal of Steroid Biochemistry and Molecular Biology *44*, 13-19.

Rajavashisth, T.B., Taylor, A.K., Andalibi, A., Svenson, K.L., and Lusis, A.J. (1989). Identification of a Zinc Finger Protein That Binds to the Sterol Regulatory Element. Science *245*, 640-643.

Ramsey, M., and Crews, D. (2009). Steroid signaling and temperature-dependent sex determination—Reviewing the evidence for early action of estrogen during ovarian determination in turtles. Seminars in Cell & Developmental Biology *20*, 283-292.

Razmara, P., Imbery, J.J., Koide, E., Helbing, C.C., Wiseman, S.B., Gauthier, P.T., Bray, D.F., Needham, M., Haight, T., and Zovoilis, A. (2021). Mechanism of copper nanoparticle toxicity in rainbow trout olfactory mucosa. Environmental Pollution *284*, 117141.

Rice, E.S., Kohno, S., John, J.S., Pham, S., Howard, J., Lareau, L.F., O'Connell, B.L., Hickey, G., Armstrong, J., and Deran, A. (2017). Improved genome assembly of American alligator genome reveals conserved architecture of estrogen signaling. Genome research *27*, 686-696.

Robinson, D.H., and Heintzelman, M.B. (1987). Morphology of ventral epidermis of *Rana catesbeiana* during metamorphosis. The Anatomical Record *217*, 305-317.

Rojas, M., Farr, G.W., Fernandez, C.F., Lauden, L., McCormack, J.C., and Wolin, S.L. (2012). Yeast Gis2 and Its Human Ortholog CNBP Are Novel Components of Stress-Induced RNP Granules. PLOS ONE *7*, e52824.

Rossbach, O., Hung, L.-H., Khrameeva, E., Schreiner, S., König, J., Curk, T., Zupan, B., Ule, J., Gelfand, M.S., and Bindereif, A. (2014). Crosslinking-immunoprecipitation (iCLIP) analysis reveals global regulatory roles of hnRNP L. RNA biology *11*, 146-155.

Rostamzadeh, D., Kazemi, T., Amirghofran, Z., and Shabani, M. (2018). Update on Fc receptor-like (FCRL) family: new immunoregulatory players in health and diseases. Expert Opinion on Therapeutic Targets *22*, 487-502.

Roush, S.F., and Slack, F.J. (2006). Micromanagement: A Role for MicroRNAs in mRNA Stability. ACS Chemical Biology *1*, 132-134.

Rousset, B., Dupuy, C., Miot, F., and Dumont, J. (2000). Chapter 2 Thyroid Hormone Synthesis And Secretion. In Endotext, K.R. Feingold, B. Anawalt, A. Boyce, G. Chrousos, W.W. de Herder, K. Dhatariya, K. Dungan, J.M. Hershman, J. Hofland, S. Kalra*, et al.*, eds.

Ruigrok, M.J.R., Xian, J.-L., Frijlink, H.W., Melgert, B.N., Hinrichs, W.L.J., and Olinga, P. (2018). siRNA-mediated protein knockdown in precision-cut lung slices. European Journal of Pharmaceutics and Biopharmaceutics *133*, 339-348.

Sachs, L.M., and Buchholz, D.R. (2017). Frogs model man: *In vivo* thyroid hormone signaling during development. genesis *55*, e23000.

Santos, D.A., Shi, L., Tu, B.P., and Weissman, J.S. (2019). Cycloheximide can distort measurements of mRNA levels and translation efficiency. Nucleic Acids Research *47*, 4974-4985.

Sasaki, S., Matsushita, A., Kuroda, G., Nakamura, H.M., Oki, Y., and Suda, T. (2018). Chapter Five - The Mechanism of Negative Transcriptional Regulation by Thyroid Hormone: Lessons From the Thyrotropin β Subunit Gene. In Vitamins and Hormones, G. Litwack, ed. (Academic Press), pp. 97-127.

Schmittgen, T.D., and Livak, K.J. (2008). Analyzing real-time PCR data by the comparative CT method. Nature protocols *3*, 1101-1108.

Schreiber, A.M., and Brown, D.D. (2003). Tadpole skin dies autonomously in response to thyroid hormone at metamorphosis. Proceedings of the National Academy of Sciences *100*, 1769-1774.

Schreiber, A.M., and Specker, J.L. (1998). Metamorphosis in the summer flounder *(Paralichthys dentatus*): stage-specific developmental response to altered thyroid status. General and comparative endocrinology *111*, 156-166.

Schroeder, A., Jimenez, R., Young, B., and Privalsky, M.L. (2014). The Ability of Thyroid Hormone Receptors to Sense T4 as an Agonist Depends on Receptor Isoform and on Cellular Cofactors. Molecular Endocrinology *28*, 745-757.

Seo, J.-Y., Kim, D.-Y., Kim, S.-H., Kim, H.-J., Ryu, H.G., Lee, J., Lee, K.-H., and Kim, K.-T. (2017). Heterogeneous nuclear ribonucleoprotein (hnRNP) L promotes DNA damage-induced cell apoptosis by enhancing the translation of p53. Oncotarget *8*, 51108.

Shankarling, G., Cole, B.S., Mallory, M.J., and Lynch, K.W. (2014). Transcriptome-Wide RNA Interaction Profiling Reveals Physical and Functional Targets of hnRNP L in Human T Cells. Molecular and Cellular Biology *34*, 71-83.

Shi, Y.-B. (2000). Amphibian metamorphosis (Wiley-Liss).

Shi, Y.-B. (2009). Dual functions of thyroid hormone receptors in vertebrate development: the roles of histone-modifying cofactor complexes. Thyroid *19*, 987-999.

Shi, Y.-B. (2021). Life Without Thyroid Hormone Receptor. Endocrinology *162*.

Shi, Y.-B., Matsuura, K., Fujimoto, K., Wen, L., and Fu, L. (2012). Thyroid hormone receptor actions on transcription in Amphibia: The roles of histone modification and chromatin disruption. Cell & Bioscience *2*, 42.

Shi, Y., and Brown, D. (1993). The earliest changes in gene expression in tadpole intestine induced by thyroid hormone. Journal of Biological Chemistry *268*, 20312-20317.

Shibata, Y., Tanizaki, Y., and Shi, Y.-B. (2020). Thyroid hormone receptor beta is critical for intestinal remodeling during *Xenopus tropicalis* metamorphosis. Cell & Bioscience *10*, 46.

Sidorenko, S.P., and Clark, E.A. (2003). The dual-function CD150 receptor subfamily: the viral attraction. Nature Immunology *4*, 19-24.

Sirakov, M., and Plateroti, M. (2011). The thyroid hormones and their nuclear receptors in the gut: From developmental biology to cancer. Biochimica et Biophysica Acta (BBA) - Molecular Basis of Disease *1812*, 938-946.

Skirrow, R.C., Veldhoen, N., Domanski, D., and Helbing, C.C. (2008). Roscovitine inhibits thyroid hormone-induced tail regression of the frog tadpole and reveals a role for cyclin C/Cdk8 in the establishment of the metamorphic gene expression program. Developmental Dynamics *237*, 3787-3797.

Song, C., Hotz-Wagenblatt, A., Voit, R., and Grummt, I. (2017). SIRT7 and the DEAD-box helicase DDX21 cooperate to resolve genomic R loops and safeguard genome stability. Genes Dev *31*, 1370-1381.

Spilker, C., Acuña Sanhueza, G.A., Böckers, T.M., Kreutz, M.R., and Gundelfinger, E.D. (2008). SPAR2, a novel SPAR-related protein with GAP activity for Rap1 and Rap2. Journal of Neurochemistry *104*, 187-201.

Statello, L., Guo, C.-J., Chen, L.-L., and Huarte, M. (2021). Gene regulation by long non-coding RNAs and its biological functions. Nature Reviews Molecular Cell Biology *22*, 159-159.

Sun, G., Fu, L., and Shi, Y.-B. (2014). Epigenetic regulation of thyroid hormone-induced adult intestinal stem cell development during anuran metamorphosis. Cell & Bioscience *4*, 73.

Suzuki, K., Hayashita, H., Yoshizato, K., Bach Kristensen, D., Sato, K., and Katsu, K. (2001). Novel *Rana* keratin genes and their expression during larval to adult epidermal conversion in bullfrog tadpoles. Differentiation *68*, 44-54.

Suzuki, S., Awai, K., Ishihara, A., and Yamauchi, K. (2016). Cold temperature blocks thyroid hormone-induced changes in lipid and energy metabolism in the liver of *Lithobates catesbeianus* tadpoles. Cell & Bioscience *6*, 19.

Tagami, T., Madison, L.D., Nagaya, T., and Jameson, J.L. (1997). Nuclear receptor corepressors activate rather than suppress basal transcription of genes that are negatively regulated by thyroid hormone. Molecular and Cellular Biology *17*, 2642-2648.

Tagami, T., Park, Y., and Jameson, J.L. (1999). Mechanisms That Mediate Negative Regulation of the Thyroid-stimulating Hormone α Gene by the Thyroid Hormone Receptor*. Journal of Biological Chemistry *274*, 22345-22353.

Tata, J.R. (1993). Gene expression during metamorphosis: An ideal model for post-embryonic development. Bioessays *15*, 239-248.

Tata, J.R. (1999). Amphibian metamorphosis as a model for studying the developmental actions of thyroid hormone. Biochimie *81*, 359-366.

Taylor, A.C., and Kollros, J.J. (1946). Stages in the normal development of *Rana pipiens* larvae. The Anatomical Record *94*, 7-23.

Thambirajah, A.A., Koide, E.M., Imbery, J.J., and Helbing, C.C. (2019). Contaminant and Environmental Influences on Thyroid Hormone Action in Amphibian Metamorphosis. Front Endocrinol (Lausanne) *10*, 276.

Thanas, C., Ziros, P.G., Chartoumpekis, D.V., Renaud, C.O., and Sykiotis, G.P. (2020). The Keap1/Nrf2 Signaling Pathway in the Thyroid—2020 Update. Antioxidants *9*, 1082.

Tian, S., Curnutte, H.A., and Trcek, T. (2020). RNA Granules: A View from the RNA Perspective. Molecules *25*, 3130.

Tomita, A., Buchholz, D.R., and Shi, Y.-B. (2004). Recruitment of N-CoR/SMRT-TBLR1 corepressor complex by unliganded thyroid hormone receptor for gene repression during frog development. Molecular and Cellular Biology *24*, 3337-3346.

Trojanowicz, B., Dralle, H., and Hoang-Vu, C. (2011). AUF1 and HuR: possible implications of mRNA stability in thyroid function and disorders. Thyroid Research *4*, S5.

Umair, M., Farooq Khan, M., Aldrees, M., Nashabat, M., Alhamoudi, K.M., Bilal, M., Alyafee, Y., Al Tuwaijri, A., Aldarwish, M., Al-Rumayyan, A.*, et al.* (2021). Mutated VWA8 Is Associated With Developmental Delay, Microcephaly, and Scoliosis and Plays a Novel Role in Early Development and Skeletal Morphogenesis in Zebrafish. Frontiers in Cell and Developmental Biology *9*.

Valdez, B.C., Henning, D., Perumal, K., and Busch, H. (1997). RNA-unwinding and RNA-folding Activities of RNA Helicase II/Gu — Two Activities in Separate Domains of the Same Protein. European Journal of Biochemistry *250*, 800-807.

Veldhoen, N., Propper, C.R., and Helbing, C.C. (2014a). Enabling comparative gene expression studies of thyroid hormone action through the development of a flexible real-time quantitative PCR assay for use across multiple anuran indicator and sentinel species. Aquatic toxicology *148*, 162-173.

Veldhoen, N., Skirrow, R.C., Brown, L.L., van Aggelen, G., and Helbing, C.C. (2014b). Effects of acute exposure to the non-steroidal anti-inflammatory drug ibuprofen on the developing North

American bullfrog *(Rana catesbeiana)* tadpole. Environmental Science & Technology *48*, 10439-10447.

Veldhoen, N., Stevenson, M.R., and Helbing, C.C. (2015). Comparison of thyroid hormone-dependent gene responses in vivo and in organ culture of the American bullfrog *(Rana (Lithobates) catesbeiana)* lung. Comparative Biochemistry and Physiology Part D: Genomics and Proteomics *16*, 99-105.

Visser, W.E., Friesema, E.C.H., and Visser, T.J. (2011). Minireview: Thyroid Hormone Transporters: The Knowns and the Unknowns. Molecular Endocrinology *25*, 1-14.

Wang, Z., and Brown, D.D. (1993). Thyroid hormone-induced gene expression program for amphibian tail resorption. Journal of Biological Chemistry *268*, 16270-16278.

Watanabe, Y., Kobayashi, H., Suzuki, K.-i., Kotani, K., and Yoshizato, K. (2001). New epidermal keratin genes from *Xenopus laevis*: hormonal and regional regulation of their expression during anuran skin metamorphosis: GeneBank accession number of sequences: AB045599, AB045600, and AB045601.1. Biochimica et Biophysica Acta (BBA) - Gene Structure and Expression *1517*, 339-350.

Wen, L., and Shi, Y.-B. (2015). Unliganded thyroid hormone receptor α controls developmental timing in *Xenopus tropicalis*. Endocrinology *156*, 721-734.

Wen, L., and Shi, Y.-B. (2016). Regulation of growth rate and developmental timing by *Xenopus* thyroid hormone receptor α. Development, Growth & Differentiation *58*, 106-115.

Westermarck, J., Weiss, C., Saffrich, R., Kast, J., Musti, A.-M., Wessely, M., Ansorge, W., Séraphin, B., Wilm, M., Valdez, B.C.*, et al.* (2002). The DEXD/H-box RNA helicase RHII/Gu is a co-factor for c-Jun-activated transcription. The EMBO Journal *21*, 451-460.

White, B.A., and Nicoll, C.S. (1981). Hormonal Control of Amphibian Metamorphosis. In Metamorphosis: A Problem in Developmental Biology, L.I. Gilbert, and E. Frieden, eds. (Boston, MA: Springer US), pp. 363-396.

Whittaker, C.A., and Hynes, R.O. (2002). Distribution and Evolution of von Willebrand/Integrin A Domains: Widely Dispersed Domains with Roles in Cell Adhesion and Elsewhere. Molecular Biology of the Cell *13*, 3369-3387.

Wilbur, H.M., and Collins, J.P. (1973). Ecological Aspects of Amphibian Metamorphosis. Science *182*, 1305-1314.

Wittrup, A., and Lieberman, J. (2015). Knocking down disease: a progress report on siRNA therapeutics. Nature Reviews Genetics *16*, 543-552.

Wojnarowicz, P., Ogunlaja, O.O., Xia, C., Parker, W.J., and Helbing, C.C. (2013). Impact of wastewater treatment configuration and seasonal conditions on thyroid hormone disruption and stress effects in *Rana catesbeiana* tailfin. Environmental science & technology *47*, 13840-13847.

Wu, Q., Sugimoto, K., Moriyama, K., Adachi, Y., Nakayama, A., and J. Mori, K. (2002). Cloning of hibernation-related genes of bullfrog *(Rana catesbeiana)* by cDNA subtraction. Comparative Biochemistry and Physiology Part B: Biochemistry and Molecular Biology *133*, 85-94.

Wu, Y., and Koenig, R.J. (2000). Gene Regulation by Thyroid Hormone. Trends in Endocrinology & Metabolism *11*, 207-211.

Yaoita, Y., and Brown, D.D. (1990). A correlation of thyroid hormone receptor gene expression with amphibian metamorphosis. Genes Dev *4*, 1917-1924.

Yoshizato, K. (1992). Death and Transformation of Larval Cells during Metamorphosis of Anura. Development, Growth & Differentiation *34*, 607-612.

Yoshizato, K., Kistler, A., and Frieden, E. (1975). Binding of Thyroid Hormones by Nuclei of Cells from Bullfrog Tadpole Tail Fins. Endocrinology *97*, 1030-1035.

Young, M.D., Wakefield, M.J., Smyth, G.K., and Oshlack, A. (2010). Gene ontology analysis for RNA-seq: accounting for selection bias. Genome biology *11*, 1-12.

Yu, Y., Tencer, A., Xuan, H., Kutateladze, T.G., and Shi, X. (2021). ZZEF1 is a Histone Reader and Transcriptional Coregulator of Krüppel-Like Factors. Journal of Molecular Biology *433*, 166722.

Zhang, X., Wang, W., Zhu, W., Dong, J., Cheng, Y., Yin, Z., and Shen, F. (2019). Mechanisms and functions of long non-coding RNAs at multiple regulatory levels. International journal of molecular sciences *20*, 5573.

Zhang, Y., Baysac, K.C., Yee, L.-F., Saporita, A.J., and Weber, J.D. (2014). Elevated DDX21 regulates c-Jun activity and rRNA processing in human breast cancers. Breast Cancer Research *16*, 449.

Zhao, L.J., Loewenstein, P.M., and Green, M. (2017). Enhanced MYC association with the NuA4 histone acetyltransferase complex mediated by the adenovirus E1A N-terminal domain activates a subset of MYC target genes highly expressed in cancer cells. Genes Cancer *8*, 752-761.

Zoeller, R.T., Tan, S.W., and Tyl, R.W. (2007). General Background on the Hypothalamic-Pituitary-Thyroid (HPT) Axis. Critical Reviews in Toxicology *37*, 11-53.

6 Supplementary Figures

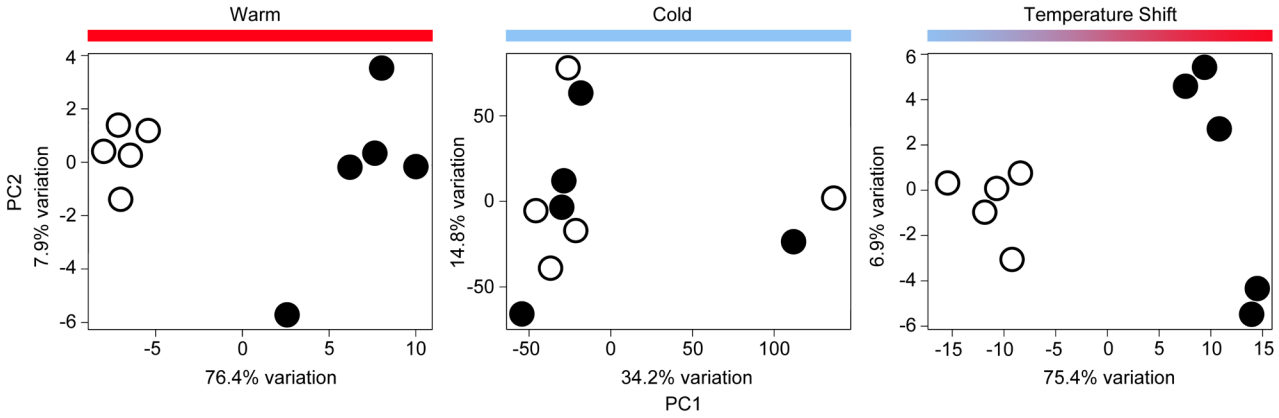

Supplementary Figure 1. Principal component analysis (PCA) of differentially expressed genes in *R. catesbeiana* tadpole C-Skin.
Principal component analysis (PCA) of differentially expressed genes (padj ≤ 0.05) identified in *R. catesbeiana* tadpole C-Skin (n = 5 tadpoles per temperature condition) exposed to either a 400 nM NaOH control (represented by open circles) or 10 nM T_3 treatment (represented by closed circles) in one of three temperature conditions. Red represents the warm condition, where samples were held for 24 h at 24 °C, blue represents the cold temperature condition, where samples were held for 48 h at 4 °C and the gradient represents the temperature shift condition, where samples were held for 48 h at 4 °C, then held for an additional 24 h at 24 °C.

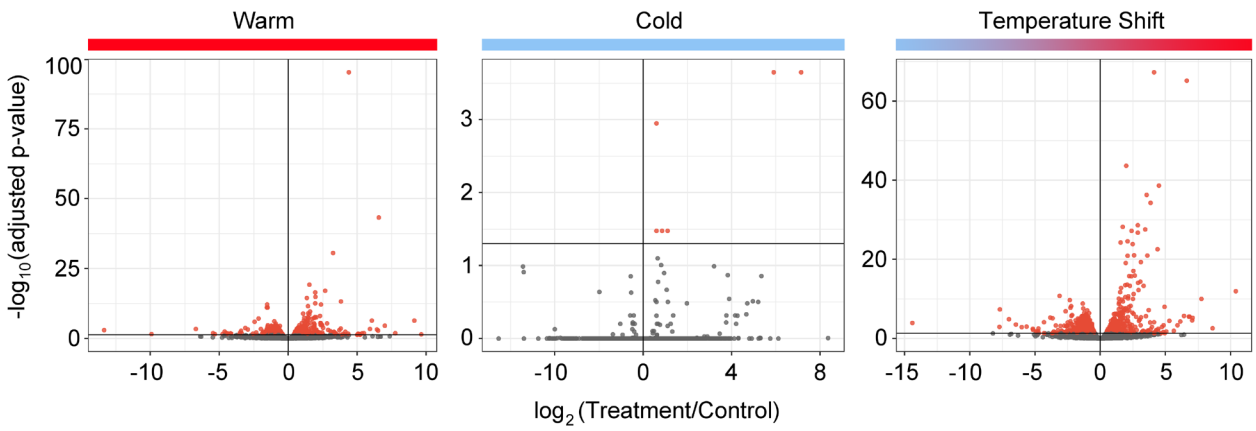

Supplementary Figure 2. Volcano plots of differentially expressed genes in *R. catesbeiana* tadpole C-Skin under different temperature conditions
Volcano plot of differentially expressed genes in *R. catesbeiana* tadpole C-Skin in cold, warm, and temperature shift conditions (n = 5 tadpoles per condition). DESeq2 analysis was used to identify statistically significant changes in gene abundance upon exposure to 10 nM T_3 treatment in comparison to 400 nM NaOH control. Red dots indicate differentially expressed genes ($p_{adj} \leq 0.05$), whereas grey dots indicate non-differentially expressed genes.

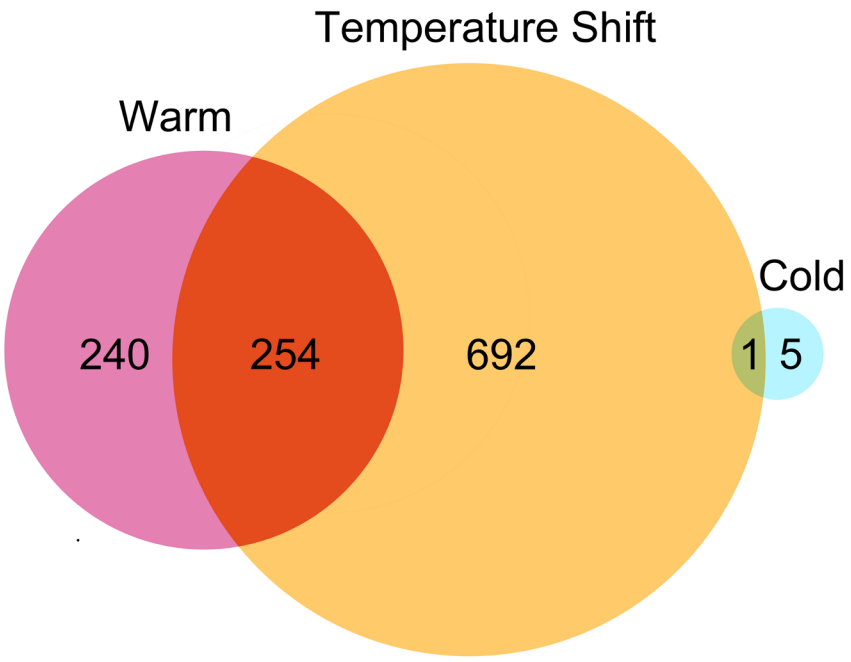

Supplementary Figure 3. Venn diagram of differentially expressed genes in *R. catesbeiana* C-Skin in three temperature conditions
Comparison of differentially expressed genes in *R. catesbeiana* tadpole C-Skin treated with 10 nM T_3 in one of three temperature conditions. Pink represents the warm temperature condition, where samples were held for 24 h at 24 °C, blue represents the cold temperature condition, where samples were held for 48 h at 4 °C, and orange represents the temperature shift condition, where samples were held for 48 h at 4 °C, then held an additional 24 h at 24 °C. Differentially expressed genes ($p_{adj} \leq 0.05$) were identified with DESeq2 (Love et al., 2014). Circles were approximately scaled to represent the difference in total genes expressed in response to T_3 in the different temperature conditions.

> Contig ID: AB205_00398331-RC

ATGGGTTGTGCCACTTGGGCTCTTCTCCTTGATATTGTGAATGACCCTCCTTCTGATGCACTGGAAGGCCAGCACCCAGACTATCAAGGCGCAGAAG
TCACTCGCAGCAATGAAATTAAGGTTATAGAGTCGACAGAATCGAAAAACATAGTGGTCATACCCCACAATGTCCAAAGCATTGTTAATCAGGAACA
GGTGAACCCTCCTGACCTGCTAGAGTTGAAAAAAAAAGTATTGATTGGTTGTGAAATTAAAGTTTCCCAGTATGAAGAAGAACTCACAAGTAGGGTT
GAAAATTTGGAAGACAATGAGCCTTCGGGGAACTCAGAGCATAAAGTCTATAAAGGTGGACAACATACTGGAGAACCATCTTCTGATGGTCAGTATG
AAGAAAGTCTCTTTCAGCCAATTACCTTACAAAGTCTTTCATTTGAAGATCAGAAACAGCTGGTGGGCACTACTGGACAAGAGGAGGAAGAAAAAAT
TAAAAGTCTTATCGAAATCACAACAGAAAAATGGGAATATAGCATAGCTACTGAACAAGAAGCACAGGTATTGGAGGAGTCTATAGATTCTACGGTC
ACATTGGAGTTTGATGTTGATACCATTTTAGATGTGATTGAAAACAACAAGAAACTGGTAACACCGGTGGATGAACCAGAAAGCTCTTCCAGCCAAG
GAGGAGATAGCAGGAAGACATTGGAAGACCTACTGGAGACAGCCAACCGCTTAGCAAAGCACTGTGATTTATTTCAAAAAGTTGAGGATCAAAAAGG
TTCTGATAACCTACGCGATCTTGATGAAACTTTAGGTTCAATGCCAGCGTCGATCTTATCCACAGACCTAGGGTACACAGAGGAGAATCTGACATCT
GTGGATGTGTCATTAACAAAAAGCAATTTTTTTTTAGAACAGAATGAAAATAAACAAACCAATTTGGAAGAAGAAACCATAAAAACACAATCTTTGG
TGTTTGGACAAAGCAATAGAAATTTTGAGGAAGAAGGGAAGGAAGTTTCAGCAAAGGACCTAAGCAAACCTACCAACAAGGAAGACGTACAGGGTAT
AGAAGGGCATCTGACAGAAAAACAGGAGGAAAAACATCAATTTAAGGAATCTGAGAGGCAGCCTAATATTTCCAAAAAACAAAAGATTAAGAGAAGG
GTTCACTTTTCTCCAAGTACAGAAGATTTATTCAAAAAATCTGAACGTGCATCGAGAAATACACTTCAGATGGTTTGTGATGAAATTCTTGAAGGGG
AATTGCAACCAGGAGAAGATCGTGAACAATTAGGAAGTTCATACATAATTAAAGACTTGGGTGAGTCTCCTAGCAAAGAAAGAGAAGGGAACTATCT
TGGAGGTACCACCTGCAGCTATGATAGTCATTATGATGGACAGTCAACCAGTGAGGAAGAAGAGACAAATGGATTAAACGAGGGTCAAACAGTGTGG
TATGATGAATACCCAGCTCAAGCAGAGCATGGTGAGAGATGTGATTCCTTGGGAGCCGTGACCGACCAAAATGTGCATGTGGATTTCAAAATGGAGG
AGTCATTTGCGACTGCAACAGATAGCAGATCAAAAGAAGAACATTTGGATCACATTCCTTCCAGTGAAGAAACACTTTCATTTGAAACGGAGTCTGC
TGGAAATCGAGATAAGTCCAATATTAACAATGTAAATCTTGAGCAAACACTCTTTACGGAAAATAAAAACGAGTCACATGCTTTGCGAGAAACAGTG
AACAAATCAGAAAAGGAATCTCTTGCTGCCTCAGATGGCACAGAAGAGACTGTAAGAAAAGAGGACTCTTTCTTAGAGGAAGAAAAGTACCAGGTAG
AATACCTATTAGAAGATAGGAAAGATCTTCTAGAATGTGACCCCACACATGTGAAAGAATCTATAGATGATATTAGACAATCAAGTGACACATTAGA
CACAAAGAATGTTGGTGTACCAAAAGATTTCACAGATGAGCAAAAGCAGACTGATATCCTGTTTCTGGAACAGGCAATCCTTGGTCAAGACTACCCA
ACTGAGGACACTGATAACAAACAGCTTCAAAACATAATTCATTATTCAGCCCATAGGGACATAACAGAGACTGCATCAGCTGAGAATGATCTTACCT
TAGTTCAATGTAGTATACTGAAAACTGATAAGATTATCAAAAGTGAACAGGATGGAAAAGAGGTTCAAGACGAAACCTTTTTATCAGACGCAAAAGA
TGTTCTGAAGTCTTTTGAAGAGCAAACGCGATCCGGCATTGTCCAGTTTGAAGAGGACACACTACTCAGACAACCAGTTTCCAGAAATGGTGATGAT
GGATACCCCGAAAATTTGCATGGAACACAGCTAAGCACGTCAGTGGATGAAATATGTATGTCATTGGTGGGAGATGTCGAATTAAGAGATGGTCCAC
CATCAGAAGAACACAAAGAGGTCTTCAGAGATGCAAATTTTGAAGGAGAAAGTGAACACAATAATAAAACCTCCACCAATGAAATGGAAGAGCAGCC
AGAACACATGACTGAGAAACAAAGTTATGACTACAAACATGAAGACTTTCCACCAGAGACCAGCAAACCACAAGAAGAAGAAGATAGCAACGTTAAG
ACTGGTCACATAGGGGTAGAACTTTTAACAGAGCAACAGTGGGTAGCTGAAGAGCAGTATGGTTCTGGTAATGAAGCTTCTCTGACAGAAGGACATT
TCACTGAACAGATGCAAGATGGCAACTCATTTAGACAGCTAGCTCCCACAGACGGTAGTGAAGAATGCCCTGAAGAATCATATGAAACAGATCAAAG
TGCATCGCTGAATGAGCCCTTCCACAGTATCCTGGATGTCAGTGCACAGAAAAGCCGCATTCTCCTCCTCAGAAAAACCTCAGTTCGCCGACGCCCA
GGTCAGCGTCTAGTGATGTTTCAAGAAGAGCTGGCTGATCCGTCAGTGATCCCACCACTAAATATGGGAGTAACACCAGATCCCGAATCATCTTATC
CCACTGAGGAAGCTACTGAGATGAGTAATACCTCAGAGCCGTTATTACATAGAAAGTCCTCTATTCGTCGACGGGGGCAGCATCAACCGACGTTTCA
GGAAGAGCTGGCTGGTTCATCAGCACTCCCACCACTAAATATGGGTATGTCACCAGCTCCTGAGTCCTCATATCCCAGCGAAGAAGCTACAGAGATG
AGTGATGCCTCAGAGCCGTTATTACGTAGAAAGTCCACTATTCGACGAAGGGGGCCACGTCCAGTGACATTTCAGGAGGAGCCATCATTGCCATTGA
TCACATCTGCGGAGTCACCACACCCCACCGAAGAACCTAGGAATGACAGTACCATTTCAGAGCAGATATTACTTGGAGAGTCCTCAATTCATCAACA
TCAGGGGCAGCATCGAGTGGCATTTGAAGATGAGCCAGTTAAATCAATACCACCAGTGATAATGCCACTAAAAATGGGAGTTCCACATTTTTTGGGG
GGGATACCCATACTTTCACCAGCTGTGGCCCCAAAGCCTGAATTATTGCACCCTGCTGAGGAACCCAGGGATGAGGGTACCACCTCAGAGCCAATGT
TACGCAGAAAGTCCTCTGTTCGTCGCCCCAAAGGGAAGCAGGAGCAGCCCATTGAGCCACCCCAAAGGGAAGCAGGAGCACATATGACCCCAGCTCC
TGCGCCATCGCACCATGAAGGGGAATCTAGGGAGGAGAAGAAGGCCTCAGAGGAACTGATCAAGCCAAAGAAGGGGTTCCTAAAGCATGCTGGTAGG
TGTGGAACCTCTGTGAGATACGTATTCAGTACTGTTAGAAGAATTTTCTTCCCTTTTGGTATGGTTAGTAAACTTCTGAGTATTGCAATGAGCTTGC
CAGCAAGGTGTAACGATATGGTGGCCTAG

Supplementary Figure 4A. Nucleotide sequence of unannotated transcript, *R. catesbeiana* genome contig ID: AB205_00398331-RC

AB205_00398331-RC was increased 5.8-fold in the cold temperature condition and 5.3-fold in the temperature shift condition. A BLASTn search found that the only annotation found for this 3,909 bp transcript was an uncharacterized *Rana temporaria* locus (Accession Number: XM_040335092.1)

.

> Contig ID: AB205_00398331-RC

MGCATWALLLDIVNDPPSDALEGQHPDYQGAEVTRSNEIKVIESTESKNIVVIPHNVQSIVNQEQVNPPDLLELKKKVLIGCEIKVSQYEEELTSRV
ENLEDNEPSGNSEHKVYKGGQHTGEPSSDGQYEESLFQPITLQSLSFEDQKQLVGTTGQEEEEKIKSLIEITTEKWEYSIATEQEAQVLEESIDSTV
TLEFDVDTILDVIENNKKLVTPVDEPESSSSQGGDSRKTLEDLLETANRLAKHCDLFQKVEDQKGSDNLRDLDETLGSMPASILSTDLGYTEENLTS
VDVSLTKSNFFLEQNENKQTNLEEETIKTQSLVFGQSNRNFEEEGKEVSAKDLSKPTNKEDVQGIEGHLTEKQEEKHQFKESERQPNISKKQKIKRR
VHFSPSTEDLFKKSERASRNTLQMVCDEILEGELQPGEDREQLGSSYIIKDLGESPSKEREGNYLGGTTCSYDSHYDGQSTSEEEETNGLNEGQTVW
YDEYPAQAEHGERCDSLGAVTDQNVHVDFKMEESFATATDSRSKEEHLDHIPSSEETLSFETESAGNRDKSNINNVNLEQTLFTENKNESHALRETV
NKSEKESLAASDGTEETVRKEDSFLEEEKYQVEYLLEDRKDLLECDPTHVKESIDDIRQSSDTLDTKNVGVPKDFTDEQKQTDILFLEQAILGQDYP
TEDTDNKQLQNIIHYSAHRDITETASAENDLTLVQCSILKTDKIIKSEQDGKEVQDETFLSDAKDVLKSFEEQTRSGIVQFEEDTLLRQPVSRNGDD
GYPENLHGTQLSTSVDEICMSLVGDVELRDGPPSEEHKEVFRDANFEGESEHNNKTSTNEMEEQPEHMTEKQSYDYKHEDFPPETSKPQEEEDSNVK
TGHIGVELLTEQQWVAEEQYGSGNEASLTEGHFTEQMQDGNSFRQLAPTDGSEECPEESYETDQSASLNEPFHSILDVSAQKSRILLLRKTSVRRRP
GQRLVMFQEELADPSVIPPLNMGVTPDPESSYPTEEATEMSNTSEPLLHRKSSIRRRGQHQPTFQEELAGSSALPPLNMGMSPAPESSYPSEEATEM
SDASEPLLRRKSTIRRRGPRPVTFQEEPSLPLITSAESPHPTEEPRNDSTISEQILLGESSIHQHQGQHRVAFEDEPVKSIPPVIMPLKMGVPHFLG
GIPILSPAVAPKPELLHPAEEPRDEGTTSEPMLRRKSSVRRPKGKQEQPIEPPQREAGAHMTPAPAPSHHEGESREEKKASEELIKPKKGFLKHAGR
CGTSVRYVFSTVRRIFFPFGMVSKLLSIAMSLPARCNDMVA

Supplementary Figure 4B. Protein sequence derived from unannotated transcript, *R. catesbeiana* genome contig ID: AB205_00398331-RC

Expasy was used to produce a putative protein for AB205_00398331-RC from reading frame 1 (5'→ 3').

```
AB205_00398508-RB       ATGCCCGGGATAATTCTAAACAAAGAAATGGAGAGCGGAGTCGGCAAGAATAAGAAATGC   60
AB205_00398508-RA       ATGCCCGGGATAATTCTAAACAAAGAAATGGAGAGCGGAGTCGGCAAGAATAAGAAATGC   60
                        ************************************************************

AB205_00398508-RB       TCTAAAACTCCCACACCCAAGAAGATCAAGAGGAAAATCCAAAATGGGGACACAGAAGAA   120
AB205_00398508-RA       TCTAAAACTCCCACACCCAAGAAGATCAAGAGGAAAATCCAAAATGGGGACACAGAAGAA   120
                        ************************************************************

AB205_00398508-RB       CTTGAGCAAGCAACCGAACTGAACGGCTTGGTGAACGAAGATTTAAATAACAATGATCAG   180
AB205_00398508-RA       CTTGAGCAAGCAACCGAACTGAACGGCTTGGTGAACGAAGATTTAAATAACAATGATCAG   180
                        ************************************************************

AB205_00398508-RB       AAGACACCGAAACTGAAGAAGAAAAAGAAGAAGCTTGTGGAAAATGAGAGTTCTTTTGAA   240
AB205_00398508-RA       AAGACACCGAAACTGAAGAAGAAAAAGAAGAAGCTTGTGGAAAATGAGAGTTCTTTTGAA   240
                        ************************************************************

AB205_00398508-RB       GCAGCTGAGCAGTGTAGTGAGGAGCCGGACAACTCGGACGCTCCAGCACCAAAGAAAAAA   300
AB205_00398508-RA       GCAGCTGAGCAGTGTAGTGAGGAGCCGGACAACTCGGACGCTCCAGCACCAAAGAAAAAA   300
                        ************************************************************

AB205_00398508-RB       AGAAAGATTGAGCCTGAAATAAATGGGCTGAATGAGGAACCTAAAACAGAGGAAGAGGAA   360
AB205_00398508-RA       AGAAAGATTGAGCCTGAAATAAATGGGCTGAATGAGGAACCTAAAACAGAGGAAGAGGAA   360
                        ************************************************************

AB205_00398508-RB       ATTAACTTGGAGAAAATTGAGGGTGATTTTTCTAAATTTCCAATTTCCCAAGAAACTATT   420
AB205_00398508-RA       ATTAACTTGGAGAAAATTGAGGGTGATTTTTCTAAATTTCCAATTTCCCAAGAAACTATT   420
                        ************************************************************

AB205_00398508-RB       GCAAACTTACAAGCCAAAGGAGTCGCTTACCTGTTCCCCATACAAACGAAAACCTTCCAC   480
AB205_00398508-RA       GCAAACTTACAAGCCAAAGGAGTCGCTTACCTGTTCCCCATACAAACGAAAACCTTCCAC   480
                        ************************************************************

AB205_00398508-RB       ACTGCCTACATTGGGAAAGATGTTGTTGTTCAGGCTCGTACTGGCACTGGAAAAACCTTC   540
AB205_00398508-RA       ACTGCCTACATTGGGAAAGATGTTGTTGTTCAGGCTCGTACTGGCACTGGAAAAACCTTC   540
                        ************************************************************

AB205_00398508-RB       TCATTTGCCATTCCTTTAATTGAGAAGCTAATCCAAGATAAAGCGCCACTGGCACAAGGA   600
AB205_00398508-RA       TCATTTGCCATTCCTTTAATTGAGAAGCTAATCCAAGATAAAGCGCCACTGGCACAAGGA   600
                        ************************************************************

AB205_00398508-RB       CGCCCACCAAGGGTGCTGATCCTAACTCCTACTAGAGAGCTGGCAATTCAGATTATGAAT   660
AB205_00398508-RA       CGCCCACCAAGGGTGCTGATCCTAACTCCTACTAGAGAGCTGGCAATTCAGATTATGAAT   660
                        ************************************************************

AB205_00398508-RB       GAAATTCGCAGCATATCTAAAAAGCTAAAGACTTGTTGCTTCTATGGTGGAAGTCCCTAT   720
AB205_00398508-RA       GAAATTCGCAGCATATCTAAAAAGCTAAAGACTTGTTGCTTCTATGGTGGAAGTCCCTAT   720
                        ************************************************************

AB205_00398508-RB       CAGCAGCAAGTATTTGCTATAAGAACTGGACTTGACATACTTGTTGGGACACCTGGTCGT   780
AB205_00398508-RA       CAGCAGCAAGTATTTGCTATAAGAACTGGACTTGACATACTTGTTGGGACACCTGGTCGT   780
                        ************************************************************

AB205_00398508-RB       ATACGGGACCTTGTCCAGAATTATAAATTGAACCTCACTGCACTGAAACATGTGGTGCTA   840
AB205_00398508-RA       ATACGGGACCTTGTCCAGAATTATAAATTGAACCTCACTGCACTGAAACATGTGGTGCTA   840
                        ************************************************************

AB205_00398508-RB       GACGAGGTGGATATGATGTTAGAAATGGGGGTTTGCTGAACAGGTGGAAGAAATTTTATCT   900
AB205_00398508-RA       GACGAGGTGGATATGATGTTAGAAATGGGGGTTTGCTGAACAGGTGGAAGAAATTTTATCT   900
                        ************************************************************

AB205_00398508-RB       GTCCGTTATACATCTGATCCTGAACAGAATCCACAAACTCTTCTATTCTCTGCAACATGT   960
AB205_00398508-RA       GTCCGTTATACATCTGATCCTGAACAGAATCCACAAACTCTTCTATTCTCTGCAACATGT   960
                        ************************************************************

AB205_00398508-RB       CCAGACTGGATGTACAACGTTGCCAAAAAATACATGCAAAAGGACTTCTCAAAGATCGAC  1020
AB205_00398508-RA       CCAGACTGGATGTACAACGTTGCCAAAAAATACATGCAAAAGGACTTCTCAAAGATCGAC  1020
                        ************************************************************

AB205_00398508-RB       CTTGTTGGACACCGTAGTCAGAGGGCTGCCATCACTGTTGAGGATTTGGCCATTGAGTGT  1080
AB205_00398508-RA       CTTGTTGGACACCGTAGTCAGAGGGCTGCCATCACTGTTGAGGATTTGGCCATTGAGTGT  1080
                        ************************************************************
```

```
AB205_00398508-RB      AACAGATTCCAGAAGCCAGCTGTCCTTGAAGCTCATGAATTGTCGACCAACTGCTCATTG   1140
AB205_00398508-RA      AACAGATTCCAGAAGCCAGCTGTCCTTGGTGACATTATCTAA------------------   1122
                       ***************************  *    *   *

AB205_00398508-RB      AAACAGTCTGCCAAAGCTCTACATGGTGACCTTCAACAAAAGGAGCGTGAAGTCATCTTG   1200
AB205_00398508-RA      ------------------------------------------------------------   1122


AB205_00398508-RB      AAAGGCTTTAGAAATGGATCATTTGAAATTCTTATTGCAACAAATGTTGCTGCTCGAGGT   1260
AB205_00398508-RA      ------------------------------------------------------------   1122


AB205_00398508-RB      CTAGATATCCCAGAAGTTGATCTAGTTGTGTTATATTCTGCACCAAGGGAAGCGGATGCA   1320
AB205_00398508-RA      ------------------------------------------------------------   1122


AB205_00398508-RB      TACGTCCATCGTTCAGGACGTACGGGTAGAGCTGGGCACACAGGAATTTGTATTTCTCTT   1380
AB205_00398508-RA      ------------------------------------------------------------   1122


AB205_00398508-RB      TATGAACCCAGAGACAGACATTGCCTTCCAATGGTGGAGAGGAGTACGGGTATTAAGTTC   1440
AB205_00398508-RA      ------------------------------------------------------------   1122


AB205_00398508-RB      AAGCGGGTTGGTATTCCATCCATACTTAATGTTGCTGAGTCCTCCAGTGCTGATGCAATA   1500
AB205_00398508-RA      ------------------------------------------------------------   1122


AB205_00398508-RB      AAGTCACTGGAATCCATCCCAGCTGATGTCATTGAACATTTTAAAGTATATGCAGAAGAA   1560
AB205_00398508-RA      ------------------------------------------------------------   1122


AB205_00398508-RB      CTTATTGAAAAGAAGGGAACATTAAATGCTCTTGCAGCAGCTTTAGCACATATTTCTGGA   1620
AB205_00398508-RA      ------------------------------------------------------------   1122


AB205_00398508-RB      GCTTCATCCTTGAAACAACGATCGCTTCTTAATATGGAAACTGGCTATATCACCGTTGTA   1680
AB205_00398508-RA      ------------------------------------------------------------   1122


AB205_00398508-RB      TTAAAGACTTCAGTTCCCATCCATACCTTGAGCTATGTTTGGCGTGCAATTAAAGAACAA   1740
AB205_00398508-RA      ------------------------------------------------------------   1122


AB205_00398508-RB      ATGGGAGAAGAAATTGATTCCCAAATTTACCGGATGTGCCTCCTAAAAGATGCCATGGGC   1800
AB205_00398508-RA      ------------------------------------------------------------   1122


AB205_00398508-RB      GTTTGTTTTGATGTTAAGGAAGACACTTTAAAGACTTTTCAAGATTCCTGGAAAGATTCA   1860
AB205_00398508-RA      ------------------------------------------------------------   1122


AB205_00398508-RB      AGGCGTTGGCAGTTTTCTGTGCCAACTGAGCTCCCAGCGCTTCAAGAATCAAGGAGAGAC   1920
AB205_00398508-RA      ------------------------------------------------------------   1122


AB205_00398508-RB      CAAGAAGGTTCACGTGGTAGAGGAGGCAGATCATTTGACAGACGCAACAACAGAAATTCA   1980
AB205_00398508-RA      ------------------------------------------------------------   1122


AB205_00398508-RB      TCACACAGAGGCGGAAATAGAGGAAGAGGCAGACAAGGAGGTTTTGGAAGGAGGAATTAG   2040
AB205_00398508-RA      ------------------------------------------------------------   1122
```

Supplementary Figure 5A. Nucleotide sequence alignment of the two DEAD-box helicase 21 (DDX21) transcripts

The nucleotide sequences of the two DEAD-box helicase 21 (DDX21) transcripts identified by their *R. catesbeiana* genome contig IDs AB205_00398508-RA and AB205_00398508-RB were aligned using ClustalOmega. "*" indicates a shared nucleotide sequence.

```
AB205_00398508-RB      MPGIILNKEMESGVGKNKKCSKTPTPKKIKRKIQNGDTEELEQATELNGLVNEDLNNNDQ       60
AB205_00398508-RA      MPGIILNKEMESGVGKNKKCSKTPTPKKIKRKIQNGDTEELEQATELNGLVNEDLNNNDQ       60
                       ************************************************************

AB205_00398508-RB      KTPKLKKKKKKLVENESSFEAAEQCSEEPDNSDAPAPKKKRKIEPEINGLNEEPKTEEEE       120
AB205_00398508-RA      KTPKLKKKKKKLVENESSFEAAEQCSEEPDNSDAPAPKKKRKIEPEINGLNEEPKTEEEE       120
                       ************************************************************

AB205_00398508-RB      INLEKIEGDFSKFPISQETIANLQAKGVAYLFPIQTKTFHTAYIGKDVVVQARTGTGKTF       180
AB205_00398508-RA      INLEKIEGDFSKFPISQETIANLQAKGVAYLFPIQTKTFHTAYIGKDVVVQARTGTGKTF       180
                       ************************************************************

AB205_00398508-RB      SFAIPLIEKLIQDKAPLAQGRPPRVLILTPTRELAIQIMNEIRSISKKLKTCCFYGGSPY       240
AB205_00398508-RA      SFAIPLIEKLIQDKAPLAQGRPPRVLILTPTRELAIQIMNEIRSISKKLKTCCFYGGSPY       240
                       ************************************************************

AB205_00398508-RB      QQQVFAIRTGLDILVGTPGRIRDLVQNYKLNLTALKHVVLDEVDMMLEMGFAEQVEEILS       300
AB205_00398508-RA      QQQVFAIRTGLDILVGTPGRIRDLVQNYKLNLTALKHVVLDEVDMMLEMGFAEQVEEILS       300
                       ************************************************************

AB205_00398508-RB      VRYTSDPEQNPQTLLFSATCPDWMYNVAKKYMQKDFSKIDLVGHRSQRAAITVEDLAIEC       360
AB205_00398508-RA      VRYTSDPEQNPQTLLFSATCPDWMYNVAKKYMQKDFSKIDLVGHRSQRAAITVEDLAIEC       360
                       ************************************************************

AB205_00398508-RB      NRFQKPAVLEAHELSTNCSLKQSAKALHGDLQQKEREVILKGFRNGSFEILIATNVAARG       420
AB205_00398508-RA      NRFQKPAVLGDII-----------------------------------------------       373
                       *********

AB205_00398508-RB      LDIPEVDLVVLYSAPREADAYVHRSGRTGRAGHTGICISLYEPRDRHCLPMVERSTGIKF       480
AB205_00398508-RA      ------------------------------------------------------------       373

AB205_00398508-RB      KRVGIPSILNVAESSSADAIKSLESIPADVIEHFKVYAEELIEKKGTLNALAAALAHISG       540
AB205_00398508-RA      ------------------------------------------------------------       373

AB205_00398508-RB      ASSLKQRSLLNMETGYITVVLKTSVPIHTLSYVWRAIKEQMGEEIDSQIYRMCLLKDAMG       600
AB205_00398508-RA      ------------------------------------------------------------       373

AB205_00398508-RB      VCFDVKEDTLKTFQDSWKDSRRWQFSVPTELPALQESRRDQEGSRGRGGRSFDRRNNRNS       660
AB205_00398508-RA      ------------------------------------------------------------       373

AB205_00398508-RB      SHRGGNRGRGRQGGFGRRN   679
AB205_00398508-RA      -------------------   373
```

Supplementary Figure 5B. Protein sequence alignment of the two DEAD-box helicase 21 (DDX21) transcripts

The protein sequences of the two DEAD-box helicase 21 (DDX21) transcripts identified by their *R. catesbeiana* genome contig IDs AB205_00398508-RA and AB205_00398508-RB were translated at reading frame 1 with Expasy. Protein sequences were aligned using ClustalOmega. "*" indicates a shared amino acid sequence.

7 Supplementary Tables

Supplementary Table 1. RNA-Seq read alignment.
75 bp paired end reads sequenced from the cultured back skin (C-Skin) of *R. catesbeiana* tadpoles (n = 5 tadpoles per temperature condition) exposed to 10 nM T_3 (TH) or a 400 nM NaOH control (Control). The reads were mapped to the *R. catesbeiana* genome (NCBI Genbank Accession No: LIAG00000000, BioProject PRJNA285814; Hammond et al., 2017). The mean and standard error of the mean (SEM) are shown.

		Warm			Cold			Temperature Shift		
Treatment	**Animal**	Input Reads	Mapped Reads	% Mapped Reads	Input Reads	Mapped Reads	% Mapped Reads	Input Reads	Mapped Reads	% Mapped Reads
Control	1	42,637,062	33,385,684	78.3	31,325,133	24,397,576	77.88	41,287,466	32,284,483	78.19
	2	32,631,109	25,885,893	79.33	31,452,619	24,442,676	77.71	30,069,556	23,820,651	79.22
	3	36,718,652	28,594,780	77.88	43,902,400	34,860,981	79.00	33,534,352	26,831,760	80.01
	4	40,380,014	31,218,506	77.31	29,750,605	23,725,840	79.00	33,969,332	26,615,874	78.35
	5	32,410,976	25,456,751	78.54	32,192,058	25,224,356	78.36	30,156,084	23,494,240	77.91
TH	1	50,978,108	40,284,750	79.02	37,714,445	29,611,276	78.51	31,393,601	24,310,892	77.44
	2	30,370,487	23,944,475	78.84	32,415,730	25,213,943	77.78	27,393,579	21,683,286	79.15
	3	35,365,167	27,596,138	78.03	43,296,066	34,367,789	79.38	30,036,608	23,482,858	78.18
	4	29,030,397	22,763,542	78.41	27,175,855	21,564,665	79.35	29,515,334	22,984,958	77.87
	5	34,452,099	27,300,816	79.24	29,178,484	23,143,486	79.32	33,483,814	26,464,561	79.04
	Mean	36,497,407	28,643,134	78.49	33,840,340	26,655,259	78.63	32,083,973	25,197,356	78.54
	SEM	1,982,215	1,555,488	0.19	1,747,319	1,401,787	0.20	1,154,828	907,090	0.24

Supplementary Table 2. Gene count and annotations
Total number of genes from C-Skin RNA libraries sequenced from *R. catesbeiana* tadpoles kept in one of three temperature conditions – cold, warm, and temperature shift. Total genes include those detected in any of the control or T_3 treatment animals for each respective temperature condition. Genes were annotated using BLASTx and BLASTn (version 2.6.0, National Centre for Biotechnology Information). A gene was considered differentially expressed (DE) if there was a statistically significant ($p_{adj} \leq 0.05$) difference in gene abundance between the paired control and treatment samples in the repeated measures design with a false discovery rate (FDR) of 0.05.

Condition	Total Genes	% Genes Annotated	DE Genes	% DE Genes Annotated
Warm	13,377	87.81	494	86.84
Cold	13,302	87.81	6	83
Temperature Shift	13,525	87.57	947	88.70

Supplementary Table 3. TH-responsive transcript counts
Transcript counts detected in each *R. catesbeiana* tadpole exposed to 10 nM T_3 (n=5 per temperature condition) and their paired 400 nM NaOH control for the indicated transcripts: *thyroid receptor alpha (thra), thyroid receptor beta (thrb), thyroid hormone-induced basic region leucine zipper-containing transcription factor (thibz), deiodinase 2 (dio2), deiodinase 3 (dio3) and heket (heket*). ND = Not detected.

		Transcript Counts																	
		Warm						Cold						Temperature Shift					
Treatment	**Animal**	*thra*	*thrb*	*thibz*	*dio2*	*dio3*	*heket*	*thra*	*thrb*	*thibz*	*dio2*	*dio3*	*heket*	*thra*	*thrb*	*thibz*	*dio2*	*dio3*	*heket*
400 nM NaOH control	1	220	342	40	21	3	34	161	450	18	33	ND	20	175	235	106	9	0	10
	2	183	756	31	19	1	27	94	639	17	27	ND	5	128	408	45	12	3	21
	3	242	723	60	10	6	57	133	841	9	55	ND	28	217	344	47	4	10	19
	4	227	452	69	17	19	33	138	254	17	86	ND	22	150	374	44	23	0	16
	5	172	1611	116	7	0	71	124	1125	233	57	ND	191	125	834	231	7	0	61
10 nM T_3 treatment	1	170	2360	6278	9	5	428	107	336	39	28	ND	6	173	2123	5586	23	17	209
	2	287	3974	9482	11	1	1276	140	750	26	17	ND	19	271	3760	7972	16	6	871
	3	174	1191	907	5	34	166	114	1099	19	37	ND	25	122	3211	6343	6	13	310
	4	182	2567	6679	10	23	570	120	530	18	53	ND	21	232	2846	10411	31	39	469
	5	203	3039	9601	5	10	1164	165	861	239	60	ND	227	157	2941	7514	19	10	822